

UNIVERSITA' DEGLI STUDI DELL'INSUBRIA



PhD COURSE IN BIOTECHNOLOGIES, BIOSCIENCES AND SURGICAL TECHNOLOGIES
(XXXII cycle)

Curriculum: Molecular and Food Biotechnologies

**Study of regulatory factors in Non Small Cell Lung Cancer: a role for Proline
Dehydrogenase?**

**Studio di fattori regolativi nel tumore al polmone non a piccole cellule: un ruolo
per la Prolina Deidrogenasi?**

Docente Guida: **Prof. Loredano Pollegioni**

Tutor: **Dott.ssa Paola Campomenosi**

Thesis of:
Sarah Grossi
Matr. 713421

Dip. Biotecnologie e Scienze della Vita - Università degli Studi dell'Insubria
Anno accademico 2019-2020

TABLE OF CONTENTS

SUMMARY	1
RIASSUNTO	5
INTRODUCTION	9
Proline dehydrogenase.....	9
Organization of the <i>PRODH</i> gene and involvement in human diseases	13
Role of proline dehydrogenase in cancer.....	16
Regulation of proline dehydrogenase expression.....	17
Proline dehydrogenase, stress response and its contribution to tumorigenesis.....	20
Lung cancer	25
Classification of lung cancer	27
Molecular genetics of lung cancer	29
Thyroid transcription factor-1	32
TTF-1 in lung cancer	34
AIM OF THE STUDY	37
RESULTS	39
1. Proline dehydrogenase is expressed in lung adenocarcinoma and modulates cell survival and 3D growth in a cell line-specific manner	40
ABSTRACT	41
INTRODUCTION	42
MATERIALS AND METHODS	44
Samples for immunohistochemical analysis	44
Immunohistochemical analyses	44
Cells culture and vectors	46
RNA extraction from FFPE tumours and qPCR analyses	48
RNA extraction from cell lines and digital PCR analyses	48
Immunoblotting.....	49
Colony formation assay	51

Cell proliferation assays	51
Wound healing assay.....	51
Soft agar assay.....	52
Statistical Analysis	52
RESULTS.....	53
PRODH expression in lung cancer samples	53
PRODH expression in adenocarcinoma cell lines	57
DISCUSSION	67
REFERENCES	71
AUTHOR CONTRIBUTION STATEMENTS	75
2. TTF-1 contributes to transcriptional regulation of the <i>PRODH</i> gene, encoding proline dehydrogenase, in lung adenocarcinoma cells	76
ABSTRACT	77
INTRODUCTION	78
MATERIALS AND METHODS	80
Cell culture.....	80
Immunoblotting.....	80
RNA extraction and gene expression	81
Plasmid constructs	82
Luciferase assays	84
Statistical Analysis	84
RESULTS.....	85
DISCUSSION	90
REFERENCES	94
AUTHOR CONTRIBUTION STATEMENTS	100
CONCLUSIONS AND FUTURE PERSPECTIVES.....	101
REFERENCES	105
Human Primary Dermal Fibroblasts Interacting with 3-Dimensional Matrices for Surgical Application Show Specific Growth and Gene Expression Programs	120

SUMMARY

Proline dehydrogenase (PRODH) is a mitochondrial inner-membrane and stress-inducible flavoenzyme catalysing the first step in the proline degradation pathway. Due to its distinctive chemical structure, in fact, proline is metabolized by a distinct set of enzymes, compared to the other aminoacids. Proline metabolizing enzymes constitute a “catalytic cycle”, transferring reducing potential into mitochondria and connecting proline to several metabolic pathways involved in basal metabolism, such as the tricarboxylic acids (TCA) cycle and the urea cycle. Thus, proline metabolism entails several regulatory pathways that are important in both redox regulation and bioenergetics.

Electrons deriving from PRODH activity can be transferred from the flavin adenine dinucleotide (FAD) cofactor to the oxidative phosphorylation pathway, thus inducing the formation of Reactive Oxygen Species or ATP. ROS generation by PRODH has been proposed as the mechanism by which this enzyme displays proapoptotic effects; nevertheless, PRODH was also described to induce cell protective autophagy and to potentially promote survival during some types of stress by inducing ATP production. Therefore, PRODH seems capable of influencing the balance between survival and apoptosis, likely depending on the cell type and on the type and severity of stress acting on those cells.

Mutations and alterations of PRODH activity are responsible for mendelian conditions or contribute to complex diseases. Indeed, absence or reduced PRODH activity (and proline accumulation) is responsible for “hyperprolinemia type 1” (HP1), an autosomal recessive disorder, but a role has also been proposed in behavioural disorders such as schizophrenia. Indeed, patients affected by HPI show increased susceptibility to schizoaffective disorders, further supporting the role of PRODH in these diseases. Noteworthy, at least 16 PRODH missense mutations have been identified with moderate to severe effect on PRODH activity.

PRODH was also proposed to play a role in cancer. Indeed, its involvement in tumour development and progression has been supported by studies concerning its expression and biological functions in different types of tumour. In particular, immunohistochemistry experiments have shown that the levels of proline dehydrogenase are lower in tumour tissues than the corresponding healthy tissues in different types of cancer, such as kidney, bladder, and digestive tract tissues including colon, rectum, stomach, liver and pancreas.

More recently, however, PRODH was shown to have a role in tumour promotion and progression in other types of tumours, favouring survival and invasion in breast and pancreatic cancer and in melanoma.

In this PhD project, we focused on the characterization of PRODH expression, regulation and functions in lung cancer, the most frequent and one of the deadliest cancer types.

Lung cancer is a highly heterogeneous disease, comprising Small Cell Lung Cancer (SCLC, comprising 15% of lung cancer cases) and Non Small Cell Lung Cancers (NSCLC, 85% of lung cancer cases), in turn comprising two subtypes, adenocarcinoma (ADC, ≈55% of cases) and squamous cell carcinoma (SCC, ≈ 45%).

Immunohistochemical characterization of PRODH expression in NSCLC cases showed that this protein is strongly expressed in a high proportion of early stage lung ADCs compared to lung SCC, whereas no expression was detected in SCLC cases. Moreover, PRODH expression seemed to correlate with a favourable prognosis.

Then, we aimed to investigate what cellular processes are influenced by PRODH in lung ADC. We tested the effect of modulation of PRODH expression in lung ADC tumor cell lines by performing a panel of phenotypic assays.

We found that in 5 out of 7 lung adenocarcinoma cell lines tested in this work, PRODH overexpression led to a decrease in cell survival, as determined by clonogenic assays. However, in 2 cell lines, namely A549 and NCI-H1437 lung ADC cell lines, modulation of PRODH expression suggested that PRODH favoured cell

survival; we hypothesized that the genetic background of these cell lines may influence the outcome.

Moreover, in NCI-H1650 and NCI-H1299, *PRODH* overexpression led to an increase in cell motility and a decrease in the ability of these cells to form spheroids when grown in soft agar, indicating reduced anchorage independence, that represents a hallmark of tumorigenesis.

In this project, we investigated if the *PRODH* gene is a target of TTF-1, also known as NKX2-1, a homeodomain containing transcriptional factor that regulates normal development and morphogenesis of the lung and adult lung physiology.

This hypothesis was formulated based on observations and analogies between these two proteins and the dual function they can exert on lung cancer cell growth. Indeed, they are expressed in the same cell types in normal lung tissue and in the majority of lung ADC cases, and both can have either promoting or inhibiting effects on tumours.

Transfection of a construct encoding TTF-1 in two adenocarcinoma cell lines (A549 and NCI-H1299) showed an increase in *PRODH* transcript compared to cells transfected with empty vector. Moreover, luciferase assays showed that one (RE1) of the four putative response elements (REs) for TTF-1 identified bioinformatically in the *PRODH* gene was able to increase luciferase activity and that mutagenesis of this RE abolished this induction, suggesting a direct binding of this sequence by TTF-1.

The results obtained support the hypothesis that TTF-1 may be a direct - albeit weak - transcriptional regulator of the *PRODH* gene and suggest that other cofactors may collaborate in *PRODH* transactivation.

In conclusion, the data obtained in this PhD project suggest that *PRODH* can influence several aspects of cell behaviour in lung cancer cell lines and identify TTF-1 as a novel regulator of *PRODH* gene expression in the lung.

The results presented here encourage further work to elucidate PRODH roles and regulation during lung tumorigenesis, aiming at a possible application of this protein as a biomarker for prognosis and differential diagnosis of lung adenocarcinoma.

RIASSUNTO

La prolina deidrogenasi (PRODH) è un flavoenzima localizzato sulla membrana mitocondriale interna, indotto da vari tipi di stress cellulare e che catalizza la prima reazione della degradazione della prolina. Infatti la prolina, a causa della sua peculiare struttura chimica rispetto agli altri aminoacidi, viene metabolizzata da enzimi specifici. Tali enzimi costituiscono un "ciclo", in grado di trasferire il potenziale riducente nei mitocondri e di convertire la prolina in altri composti, connettendola a diverse vie metaboliche coinvolte nel metabolismo basale, tra cui il ciclo degli acidi tricarbossilici (TCA) e il ciclo dell'urea. Pertanto, il metabolismo della prolina influenza vari processi cellulari tra cui il mantenimento di un corretto potenziale redox, il metabolismo bioenergetico, la crescita e il differenziamento cellulare.

Gli elettroni derivanti dall'attività della PRODH possono essere trasferiti dal cofattore flavina adenina dinucleotide (FAD) alla via della fosforilazione ossidativa, inducendo così la formazione di specie reattive dell'ossigeno o ATP. La generazione di ROS da parte di PRODH è stata proposta come un meccanismo attraverso il quale questo enzima esplica effetti pro-apoptotici; tuttavia, è stato anche descritto che PRODH possa indurre un'autofagia cellulare protettiva e potenzialmente promuovere la sopravvivenza cellulare durante alcuni tipi di stress, tramite la produzione di ATP. Pertanto, PRODH sembra in grado di influenzare l'equilibrio tra sopravvivenza e apoptosi, probabilmente a seconda del tipo cellulare e del tipo e gravità dello stress che agisce sulle cellule.

Mutazioni e conseguente alterazione dell'attività di PRODH causano patologie mendeliane o contribuiscono all'insorgenza di malattie complesse. Infatti, l'assente o ridotta attività di PRODH (e l'accumulo di prolina) sono responsabili dell'iperprolinemia di tipo 1 (HP1), un disturbo autosomico recessivo, ma è stato anche proposto un coinvolgimento nei disturbi comportamentali come la

schizofrenia. I pazienti affetti da HPI mostrano una maggiore suscettibilità ai disturbi schizoaffettivi, e ciò supporta ulteriormente il ruolo di PRODH in queste malattie. In particolare, sono state identificate almeno 16 mutazioni di senso per PRODH con un effetto da moderato a grave sull'attività di tale enzima.

Inoltre, è stato proposto un ruolo di PRODH nei tumori. Infatti, il suo coinvolgimento nello sviluppo e nella progressione tumorale è supportato da studi sulla sua espressione e sulle sue funzioni biologiche in diverse tipologie di tumore. In particolare, esperimenti di immunostochimica hanno dimostrato che i livelli di prolina deidrogenasi sono più bassi nei tessuti tumorali rispetto ai corrispettivi tessuti sani in diversi tipi di tumore, come quelli dei tessuti del tratto digerente inclusi colon, retto, stomaco, fegato e pancreas, oltre a rene e vescica.

Più recentemente, tuttavia, PRODH ha dimostrato di avere un ruolo promuovente nello sviluppo e nella progressione di altri tipi di tumore, favorendo la sopravvivenza cellulare, l'invasione e la metastatizzazione nel tumore alla mammella, al pancreas e nel melanoma.

In questo progetto di dottorato ci siamo concentrati sulla caratterizzazione dell'espressione, della regolazione e delle funzioni di PRODH nel tumore al polmone, che rappresenta uno dei tumori più frequenti e con la più alta mortalità in entrambi i sessi nel mondo.

Il cancro del polmone è molto eterogeneo clinicamente e viene suddiviso in tumore del polmone a piccole cellule (SCLC, che comprende il 15% dei casi di tumore del polmone) e tumore del polmone non a piccole cellule (NSCLC, 85% dei casi), che a sua volta comprende due istotipi principali: l'adenocarcinoma (ADC, ≈55% dei casi) e il carcinoma squamocellulare (SCC, ≈ 45%).

La caratterizzazione immunostochimica dell'espressione di PRODH nei casi di NSCLC ha mostrato che questa proteina è fortemente espressa in un'alta percentuale di ADC a stadi precoci rispetto agli SCC, mentre nei casi di SCLC non è stata rilevata alcuna espressione. Inoltre, l'espressione di PRODH sembra correlare con una prognosi favorevole.

Abbiamo quindi deciso di indagare quali processi cellulari fossero influenzati da *PRODH* negli ADC polmonari. Per tale motivo, abbiamo testato l'effetto della regolazione dell'espressione di *PRODH* nelle linee cellulari di adenocarcinoma del polmone, allestendo una serie di saggi fenotipici.

Su un totale di 7 linee cellulari analizzate, in 5 abbiamo riscontrato che l'iperespressione di *PRODH* porta ad una diminuzione della sopravvivenza cellulare. Tuttavia, in 2 linee cellulari, le A549 e le NCI-H1437, la modulazione dell'espressione di *PRODH* ha favorito la sopravvivenza cellulare; abbiamo ipotizzato che il background genetico delle cellule ne potesse influenzare l'esito.

Inoltre, nelle NCI-H1650 e NCI-H1299, l'iperespressione di *PRODH* ha portato ad un aumento della motilità cellulare e ad una diminuzione della capacità di queste cellule di formare sferoidi durante la crescita su soft agar, indicando una ridotta capacità di crescita cellulare indipendente dall'ancoraggio al substrato, che rappresenta un segno distintivo della tumorigenesi.

In questo progetto di dottorato, è stato inoltre indagato se il gene *PRODH* possa essere un target di TTF-1, noto anche come NKX2-1, fattore di trascrizione con omeodominio che regola il normale sviluppo e la morfogenesi del polmone e la sua fisiologia nel tessuto adulto.

L'ipotesi di una possibile interazione tra questi due fattori è stata formulata sulla base di osservazioni e analogie riscontrate tra queste due proteine e sulla duplice funzione che possono svolgere nella crescita delle cellule tumorali. Infatti, entrambi questi fattori sono espressi negli stessi tipi di cellule nel tessuto polmonare sano e nella maggior parte dei casi di ADC polmonari, inoltre entrambi possono svolgere un ruolo come promotori o inibitori sulla crescita tumorale.

La trasfezione di un costrutto codificante per TTF-1 in due linee cellulari di adenocarcinoma (A549 e NCI-H1299) ha portato ad un aumento del trascritto di *PRODH* rispetto alle cellule trasfettate con il vettore vuoto di controllo. Inoltre, tramite saggi di luciferasi, è stato osservato come in presenza di uno dei quattro putativi response elements (RE) per TTF-1 (chiamato RE1) identificati

bioinformaticamente nel gene *PRODH*, l'attività della luciferasi aumentasse; la mutagenesi di RE1 aboliva l'induzione, suggerendo così un legame diretto di TTF-1 a tale sequenza.

I risultati ottenuti supportano l'ipotesi che TTF-1 possa essere un regolatore trascrizionale diretto, anche se debole, del gene di *PRODH* e suggeriscono che altri cofattori possano collaborare alla sua transattivazione.

In conclusione, i dati ottenuti in questo progetto di dottorato suggeriscono che *PRODH* possa influenzare diversi aspetti della crescita cellulare nelle linee cellulari tumorali del polmone, e identificano TTF-1 come un nuovo regolatore dell'espressione genica di *PRODH* nel tumore al polmone.

I risultati qui presentati incoraggiano ulteriori studi volti a chiarire i ruoli e la regolazione di *PRODH* durante la tumorigenesi del polmone, mirando a una possibile applicazione di questa proteina come biomarcatore per la prognosi e la diagnosi differenziale dell'adenocarcinoma polmonare.

INTRODUCTION

Proline dehydrogenase

Since the description of the so called “Warburg effect”, an altered metabolism has been increasingly recognised to play an important role in tumour promotion and progression (Cairns et al., 2011; Galluzzi et al., 2013). Metabolism of nonessential amino acids (NEAA), such as glutamine, has been shown to be important for cancer cell survival in almost all types of cancer (Liu et al, 2015; Phang, 2019).

Also the non-essential aminoacid proline has been proposed to play a role in tumorigenesis (Liu et al, 2015; Phang, 2019). L-proline is one of the most abundant amino acids in the extracellular matrix, as it accounts, together with hydroxyproline, for 25% of the aminoacids in collagen, its main component (Pandhare et al., 2009). Proline is the only proteinogenic secondary amino acid with its α -amino group within a pyrrolidine ring (Adams, 1980; Phang 2019). Because of its particular structure, proline is not subjected to the activity of amino acid processing enzymes such as aminotransferases, decarboxylases, and racemases (Adams, 1970; Phang, 1985). Instead, the initial step of proline catabolism is unique and occurs exclusively through the activity of proline dehydrogenase (PRODH or POX, EC 1.5.5.2, formerly EC 1.5.99.8), a mitochondrial inner membrane and stress-inducible enzyme, containing a flavin adenine dinucleotide (FAD) cofactor (Phang et al., 2010; Liu and Phang, 2012).

This enzyme is widely distributed in living organisms, and participates to a variety of regulatory functions, such as redox homeostasis, osmotic adjustment and protection against metabolic stress (Phang et al., 1982; Peng et al., 1996). It is also involved in peculiar functions such as the use of proline as a fuel for initiation of flight in several insect species (Sacktor, 1976; Scaraffia and Wells, 2003).

To date, PRODH structures from eukaryotes are not available yet, whereas the structures of various bacterial orthologs have been widely characterized, allowing to obtain a reliable template for modelling of human PRODH (Figure 1) (Tanner et al., 2018).

Human PRODH is composed of 600 aminoacids and has a molecular mass of approximately 68 kDa. Homology modelling, performed by Tanner et al., predicts a $(\beta\alpha)_8$ -barrel fold within residues 121-579 (Figure 1). Two large inserts of uncertain structure corresponding to residues 150-205 and 241-349 and two important α -helices ($\alpha 5a$ and $\alpha 8$) were predicted by the modelling. Moreover, the L447 residue is predicted as an important residue that packs against the adenine of the FAD, which is presumed to be important for establishing the correct cofactor conformation (Figure 1) (Tanner et al., 2018).

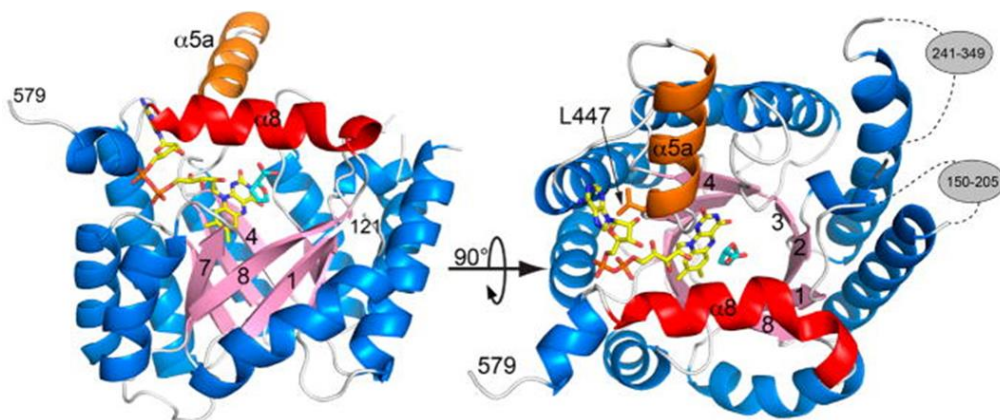


Figure 1. PRODH $(\beta\alpha)_8$ -barrel fold was predicted by homology model of residues 121–579 of human PRODH1 made with SWISS-MODEL (modified from Tanner et al., 2018). The template chosen by SWISS-MODEL was PDB ID 5KF6.42. FAD (yellow); proline analogue L-THFA (cyan); $\alpha 5a$ helix (orange); $\alpha 8$ helix (red).

In order to elucidate the structure-function relationships of this enzyme, a crucial step is the purification of a soluble, active human PRODH protein. The catalytic domain of human PRODH, named PO-barrel N-His (residues 176–578) was first identified by comparison with bacterial proteins and then successfully expressed in

E. coli and purified in a work by Tallarita et al. (Tallarita et al., 2012) (Figure 2). This variant (with a theoretical mass of 46,276 Da) possesses the typical properties and flavin reactivity of flavoprotein oxidases and its specific activity is 3-fold lower than the value previously estimated for the full length PRODH (0.032 and 0.1 U/mg, respectively, in which one unit is defined as the amount of enzyme which transfer electrons from 1 μ mol of L-Pro to DCPIP in 1 min at 25 °C) (Krishnan et al., 2008; Tallarita et al., 2012).

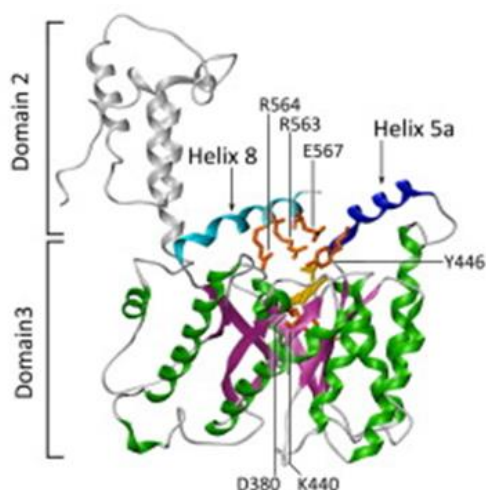


Figure 2. Model of the three-dimensional structure of PO Barrel_N-His variant (modified from Tallarita et al., 2012). The ($\alpha\beta$)8-barrel region of the protein (catalytic domain, domain 3) is represented in green and purple; α -helix 5a is in blue and α -helix 8 in cyan. Helices are named according to the *E. coli* PutA numbering. Conserved residues proposed to be important for catalysis are indicated (orange).

From the biochemical point of view, PRODH catalyses L-proline oxidation, transferring two electrons from proline to FAD, thus generating 1-Pyrroline-5-carboxylic acid (P5C) and reduced FAD (FADH₂). Also thanks to the subcellular localization, the electrons produced during proline oxidation can be transferred from the FAD cofactor to the electron transport chain to produce either reactive oxygen species (ROS) or adenosine triphosphate (ATP) (Figure 3).

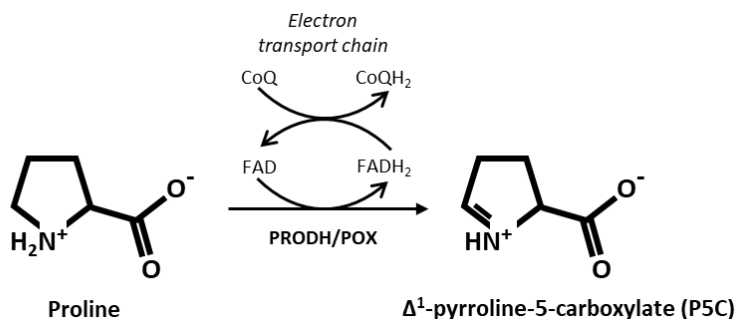


Figure 3. Reaction catalysed by proline dehydrogenase. Proline is oxidized to Δ^1 -pyrroline-5-carboxylate (P5C) by proline dehydrogenase (PRODH/POX) in the mitochondrion. PRODH couples proline oxidation to the reduction of coenzyme Q (CoQ) in the electron transport chain.

P5C undergoes spontaneous conversion into γ -glutamyl semialdehyde (GSA), that is oxidized to L-glutamate by P5C dehydrogenase (P5CDH, EC 1.5.1.12). Glutamate generated by proline oxidation can be deaminated to α -ketoglutarate by glutamate dehydrogenase and enter the tricarboxylic acid cycle, or -in some organs- it can enter the urea cycle after conversion into ornithine by ornithine- δ -aminotransferase (OAT) (Figure 4).

Moreover, P5C can be exported from mitochondria to the cytosol, where it is converted back to proline by the cytosolic enzyme P5C reductase (PYCR, EC 1.5.1.2), using NADPH or NADH as a cofactor (Figure 4). At this level, proline metabolism is interconnected with the pentose phosphate pathway, as the reducing potential of NADPH, produced by the pentose phosphate pathway, can be transferred to the mitochondrial electron transport chain for ATP generation by a new proline oxidation reaction (Liu and Phang, 2012; Phang et al., 2015) (Figure 4). PRODH and PYCR, together, form the so called “proline cycle”, shuttling proline and P5C in and out of the mitochondrion (Liu et al., 2012).

As mentioned before, the electrons deriving from oxidation of L-proline can be used to produce ATP, a process that becomes particularly important for cell survival during nutrient stress (Liang et al., 2013). In alternative, the oxidation of proline can

lead to the formation of reactive oxygen species (ROS), capable of activating downstream events such as programmed cell death, but also pro-survival autophagy, contributing to tumorigenesis and tumour progression (Liu and Phang, 2012; Phang et al., 2015). Thus, PRODH can represent a key protein in regulation of tumour metabolism (Liu and Phang, 2012).

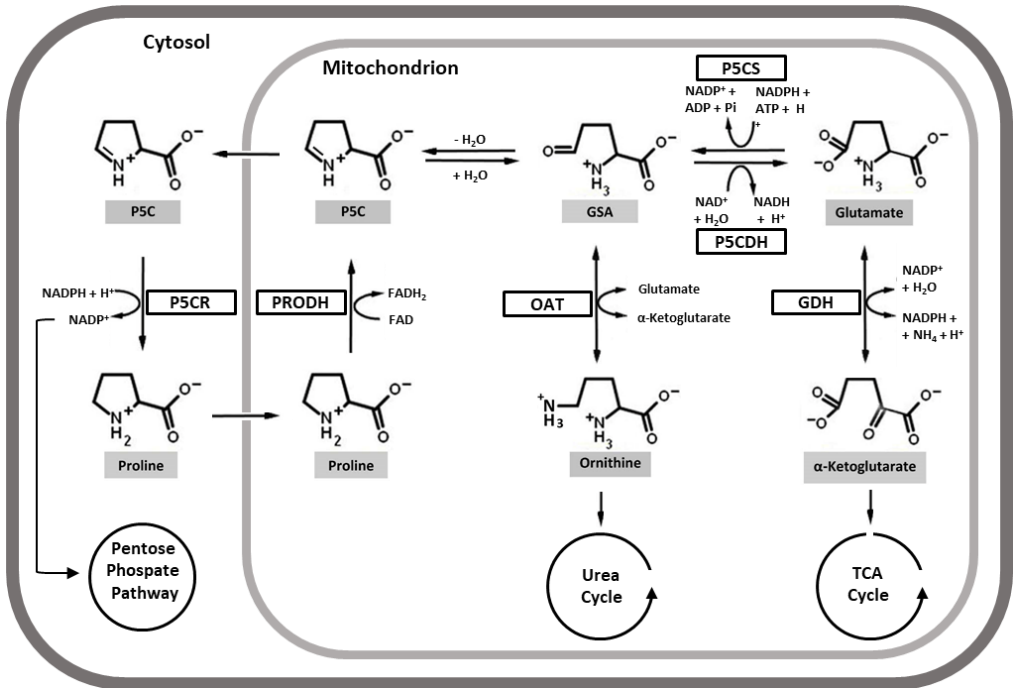


Figure 4. Reaction and enzymes involved in proline metabolism (modified from Zhang and Becker, 2015). The abbreviations are: P5C, Δ¹-pyrroline-5-carboxylate; GSA, glutamic-γ-semialdehyde; PRODH, proline dehydrogenase; P5CR, P5C reductase; P5CS, P5C synthetase; P5CDH, P5C dehydrogenase; OAT, ornithine-δ-aminotransferase; GDH, glutamate dehydrogenase; TCA cycle, tricarboxylic acid cycle.

Organization of the *PRODH* gene and involvement in human diseases

The *PRODH* gene, encoding for proline dehydrogenase, is evolutionarily conserved starting from prokaryotes, confirming the importance of its biochemical, if not biological, role (Liu et al., 2009).

This gene is composed of 15 exons and encompasses 23.8 kb; it is located on chromosome 22q11.2, in a region that frequently undergoes chromosomal rearrangements, in particular microdeletions and microduplications (Figure 5). A possible reason for these rearrangements is the presence of a Low Copy Repeat (LCR) in this region, including a *PRODH* pseudogene (Ψ -*PRODH*).

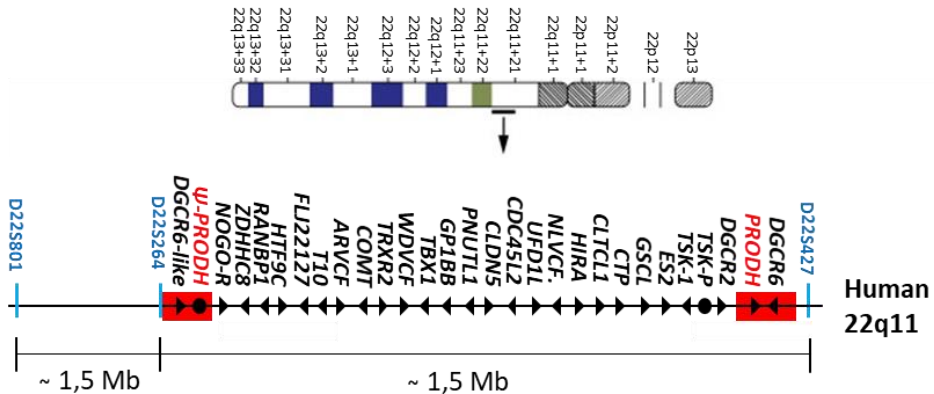


Figure 5. Organisation of the 22q11 chromosomal region, where *PRODH* is located (modified from Karayiorgou and Gogos, 2004). The red rectangles indicate the low copy repeat (LCR) sequences. Microsatellite markers are reported in blue, the *PRODH* gene and Ψ -*PRODH* pseudogene are written in red. Triangles indicate the transcriptional direction of the known genes.

The LCRs have a significant pathogenetic role, as they can give rise to unequal crossing-over events, causing microdeletions and microduplications in the 22q11.2 genomic region (Bender et al., 2005; Willis et al., 2008).

In particular, these microdeletions are the cause of DiGeorge syndrome, a condition characterized by multiple malformations, heart diseases, mental retardation, epilepsy and neuropsychiatric disorders, such as schizophrenia (McDermid et al., 2002). Patients suffering from DiGeorge syndrome frequently show hyperprolinemia, attributable to the reduced *PRODH* levels, due to the microdeletion.

The high prevalence of schizophrenia among DiGeorge syndrome patients supports the hypothesis that in this genomic region lie one or more susceptibility genes for schizophrenia, a complex and debilitating psychiatric disorder, which has an incidence of about 1% in the world population (Baron, 2001; Jacquet et al., 2002). *PRODH* could be involved in this disorder as proline dehydrogenase activity can affect glutamatergic neurotransmission. However, data about the involvement of the *PRODH* gene in schizophrenia are conflicting (Jacquet et al., 2002).

There are also two autosomal recessive Mendelian conditions related to proline metabolism, namely hyperprolinemia type 1 (HP1), and hyperprolinemia type 2 (HP2), that are due to single nucleotide variants in the genes encoding proline dehydrogenase and P5C dehydrogenase, respectively. They generally lead to a mild increase in levels of plasmatic proline (3-10% for HP1; 10-15% for HP2) (Bender et al., 2005; Mitsubuchi et al., 2008; Willis et al., 2008). Single nucleotide variants in the *PRODH* gene cause partial or total loss of function and are present in patients with type 1 hyperprolinemia and schizophrenia (Jacquet et al., 2002; Liu et al., 2002). At least ten of the described variants have polymorphic frequencies that may be due to gene conversion mechanisms caused by the presence of the *PRODH* pseudogene.

In a work by Bender et al, *PRODH* variants were tested in order to understand the functional effects they exerted on proline dehydrogenase activity. In particular, it was shown that among the 16 different missense substitutions identified, four (R185Q, L289M, A455S, A472T) resulted in a slight reduction (<30%) of the proline dehydrogenase activity, six (Q19P, A167V, R185W, D426N, V427M and R431H) were associated with a moderate reduction (30-70%) and, finally, five (P406L, L441P, R453C, T466M and Q521E) were associated with a severe reduction in *PRODH* activity (>70%), while only one of the mutations in question (Q521R) increased its activity (Bender et al., 2005). Notably, the authors used as reference sequence one of the first versions of NM_016335 RefSeq, that they deposited in

GenBank themselves, and in which Q521 was present. In recent versions, R521 is considered the wild-type sequence.

Analyses of plasma proline levels and PRODH genotypes showed that the most serious cases of hyperprolinemia occurred in individuals with PRODH deletions and/or missense mutations leading to high reduction in the catalytic activity of proline dehydrogenase (such as L441P and R453C), while a modest hyperprolinemia was associated with an equally modest reduction in PRODH activity. Of considerable importance is the fact that three of the four allelic variants found in schizophrenic subjects (V427M, L441P and R453C) result in a severe reduction in proline dehydrogenase activity and in hyperprolinemia. These observations, overall, support the hypothesis that a reduction in proline dehydrogenase activity represents a risk factor for schizophrenia (Bender et al., 2005).

Finally, the 22q11.2 region may be also involved in cancer, as copy number variations (CNV) in this region recur in various types of cancer (McDonald-Mc Ginn et al., 2006). It has been suggested that patients with the 22q11.2 microdeletion syndrome have a higher risk of developing neoplasms (McDonald-Mc Ginn et al., 2006; Liu et al., 2009).

Role of proline dehydrogenase in cancer

Metabolism influences several aspects of tumour cell growth, including proliferation, maintenance of redox homeostasis, epigenetic reprogramming of the cell and also invasion and metastatisation (Pandhare et al., 2009).

The first pionieristic studies on the changes of metabolism in cancer focused on the main metabolic pathways and in particular on glycolysis since cancer cells use glucose and glutamine as primary source of energy for proliferation and growth and as components for biosynthetic pathways (Warburg, 1956; Gottlieb et al., 2005; Ristow et al., 2006; Hagland et al., 2007; DeBerardinis and Chandel, 2020). During rapid growth, however, cancer cells can spatially or temporally find themselves in a

condition of inadequate blood supply and a consequent exhaustion of oxygen and paucity of nutrients (Liu and Phang, 2012). As a result, they are in a hostile microenvironment due to hypoxia or glucose deficiency or both. Under these conditions, cancer cells will need to find alternative energy sources to guarantee their survival and proliferation (Liu and Phang, 2012).

In this context, the catabolism of proline represents an excellent alternative source of energy for the cell, for at least two reasons: first, proline is abundant in the cellular microenvironment; second, proline is metabolized by a specific group of enzymes, thus it represents an independent pathway for energy provision during the reprogramming of metabolic pathways by oncogenes or by dysfunctional or non-functional tumour suppressor genes (Phang et al., 2015).

These considerations led scientists to investigate the role and significance of proline catabolism in cancer cells. Many of these studies analysed the consequences of expression of proline dehydrogenase, as it catalyses the first, limiting, step of proline catabolism. These studies showed how this enzyme can fulfil different roles in the fate of cancer cells, in some instances promoting their growth and in others mediating their death, according to the mechanisms that will be described later on (Liang et al., 2013).

Regulation of proline dehydrogenase expression

In normal tissues, PRODH expression occurs mainly in the liver, kidney, brain, intestine and lung (Kazberuk et al., 2020). Expression can also vary throughout the different stages of life and in the same cell and tissue type in presence of several types of cellular stress (Rivera & Maxwell, 2005).

Several studies showed that PRODH expression is tightly regulated by various transcription factors whose alteration plays an important role during tumour development (Figure 6) (Phang et al., 2012).

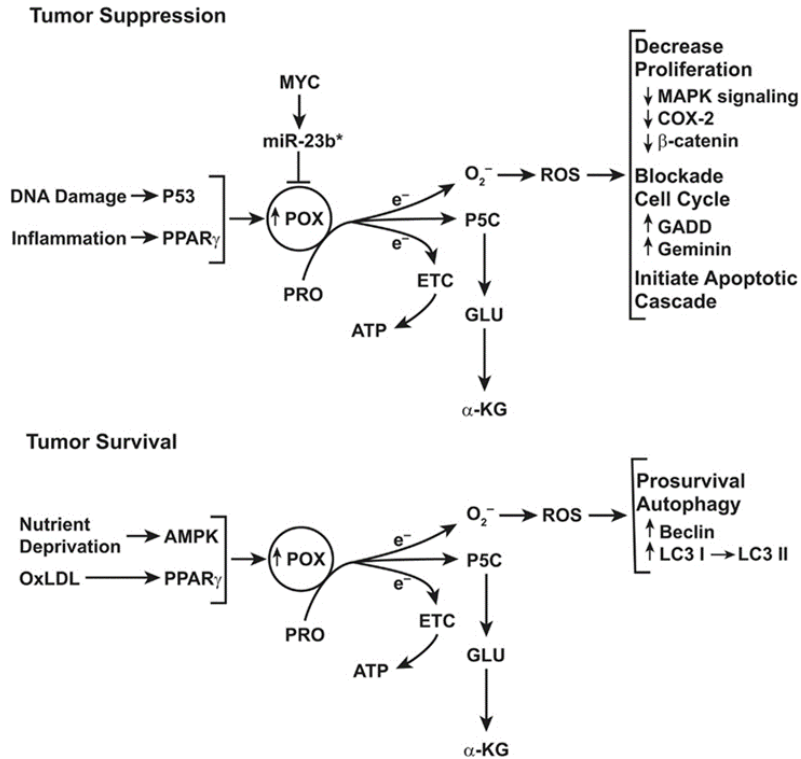


Figure 6. Schematic representation of the functions of *PRODH* in tumour suppression (top) and survival (down) (from Phang et al., 2012).

One of the first transcription factors shown to regulate the expression of the *PRODH* gene was p53, which is defined as the “guardian of the genome” (Levine et al., 2006). In response to various stimuli or types of stress, p53 regulates a number of pathways involved in cell cycle arrest, DNA repair, apoptosis, autophagy and others, mainly by transcriptional regulation of target genes (Lane 1992; Vousden and Lu, 2002; Kruse and Gu, 2009; Vousden and Prives, 2009). The importance of p53 as “guardian of the genome” is underlined by the fact that it is mutated in more than half of human tumours (Rivlin et al., 2011). p53 protects the organism from tumour development by allowing the repair of DNA damage or by eliminating too heavily damaged cells (Liu and Phang, 2012; Moxley & Reisman, 2020).

Among the target genes of this transcription factor *PRODH* was one of the most strongly induced by p53 during apoptosis induction in response to the chemotherapeutic agent doxorubicin and was therefore named as *PIG6* (P53 inducible gene 6) (Polyak et al., 1997).

Subsequent studies investigating *PRODH* gene regulation by p53 showed the presence of different p53 response elements in the *PRODH* gene sequence, among which an intronic element was the most efficiently responding not only to p53 but also to other members of the p53 family (Raimondi et al., 2013). Functional studies have confirmed the contribution of *PRODH* in p53-mediated apoptosis (Liu and Phang, 2012).

Another transcription factor that controls the expression of the *PRODH* gene is PPAR- γ (peroxisome proliferator activated receptor gamma), a nuclear hormone receptor that regulates lipid and glucose metabolism. Following its activation, PPAR- γ transactivates target genes, including *PRODH*, with the consequent production of intracellular ROS and therefore with the activation of apoptosis mechanisms (Pandhare et al., 2006; Kazberuk et al., 2020).

The c-MYC transcription factor, a proto-oncogene whose expression is deregulated in various types of cancer, instead, decreases *PRODH* expression through the induction of a microRNA, miR23b*, that targets the 3'UTR of the *PRODH* transcript. In fact, when c-MYC activity is suppressed, the levels of *PRODH* increase, inducing the generation of ROS and the triggering of apoptosis, thus leading to a decrease in growth and proliferation of cancer cells. This result suggested that c-MYC-induced *PRODH* inhibition likely results in reduced apoptosis as well as metabolic reprogramming. Overall, these elements would contribute to tumorigenesis and tumour progression (Liu et al., 2012).

Proline dehydrogenase, stress response and its contribution to tumorigenesis

Given the importance of proline and its possible involvement in tumour formation and progression, several research groups have investigated the expression of proline dehydrogenase, the key enzyme of this metabolic pathway, and its regulation under stress conditions. Several lines of evidence show that PRODH expression, activity and cellular outcome may vary according to the type of tissue but also the type of stress to which cells are exposed.

In response to specific types of stress, such as genotoxic stress, PRODH has been shown to play a role in apoptosis induction. Apoptosis is a process that allows the removal of damaged or obsolete cells and plays a fundamental role in various physiological processes and its dysregulation is involved in the development of various pathologies, including tumour development. Several studies have shown that expression of PRODH triggers apoptosis by activating both intrinsic (or mitochondrial) and extrinsic (or mediated by death-receptor) pathways (Figure 7) (Liu et al., 2006; Liu et al., 2012; Zareba and Palka, 2016). The intrinsic pathway is activated by PRODH when the electrons produced during proline oxidation are used for production of ROS species. ROS act at several levels: at the mitochondrial membrane they induce an increase in permeability and cause the release of cytochrome c, a fundamental event that triggers the activation of the effector molecules of this process; regarding the extrinsic pathway, on the other hand, ROS production by PRODH induces two important components of this pathway, namely DR5 (Death Receptor 5) and TRAIL (TNF-related apoptosis-inducing ligand) which, in turn, will activate the initiating components of this branch of the apoptotic process (Liu et al., 2006).

The ability to activate the apoptotic process suggests a tumour suppressor role for PRODH. However, the oncosuppressor role of PRODH also occurs by its modulation of different regulatory pathways in the cell (Liu and Phang, 2012).

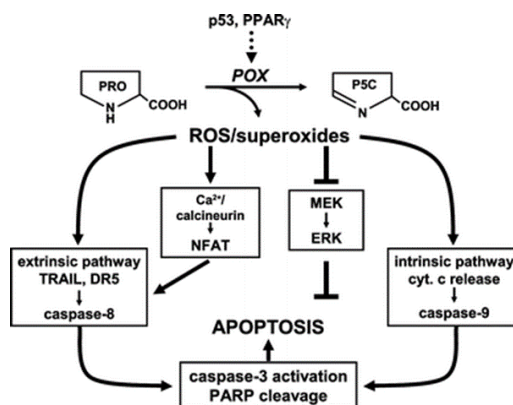


FIGURE 7. Schematic of POX-mediated induction of apoptosis by both intrinsic (mitochondrial) and extrinsic (death receptor) pathways (from Phang et al., 2008).

For example, PRODH was shown to modulate HIF-1 (hypoxia inducible factor 1) function (Liu and Phang, 2012). HIF-1 transcription factor regulates the expression of different genes in response to hypoxic condition, and its stabilisation plays an important role in tumour development by stimulating angiogenesis, growth and tumour invasion. It was shown that PRODH activity, by stimulating the production of α -ketoglutarate, increases the activity of prolyl hydroxylases. These enzymes mediate the O_2 dependent degradation of HIF-1 in presence of oxygen, inducing proteasomal degradation of the HIF-1 α regulatory subunit (Liu and Phang, 2012). Thus, PRODH can suppress HIF-1 function in those tumours that have this pathway activated in spite of the presence of oxygen in the microenvironment (Liu and Phang, 2012).

However, PRODH can also induce autophagy and survival in response to specific conditions. Autophagy is a physiological process during which various cytoplasmic components and intracellular organelles are degraded within the lysosomes thus allowing the recycling of basic components, including amino acids. It can represent a temporary survival process during nutrient stress, that is exploited by cancer cells (Mizushima and Komatsu, 2011; Liu and Phang, 2012; Liu et al., 2012).

In conditions of either low glucose alone, or concomitant glucose deficiency and hypoxia, a rather common situation during tumour development, an induction in the expression of PRODH was observed, due to the activation of the AMPK (protein kinase AMP-activated) protein, that functions as a "sensor" of the cellular metabolic state. AMPK represents a metabolic checkpoint and can block anabolic processes that determine energy consumption in the cell, such as protein synthesis, simultaneously stimulating catabolic pathways that allow the production of energy (Pandhare et al., 2009).

The consequence of PRODH induction by AMPK in condition of concomitant glucose deficiency and hypoxia is an increase in tumour cell survival. The degradation of proline can represent one of the mechanisms used by cancer cells to maintain an adequate level of ATP (Liu and Phang, 2012; Liu et al., 2015).

The condition of hypoxia alone, if associated with an adequate glucose level, also induces an increase in PRODH expression within the cancer cell. However, despite being mediated by the AMPK protein, in this condition PRODH does not induce ATP production, but the generation of ROS species and the induction of protective autophagy (Liu et al., 2012).

The proline necessary for promotion of cell survival by PRODH can be obtained by increased degradation of the extracellular matrix, in particular collagen fibres that are rich in this amino acid. This process is mediated by activated metalloproteinases (MMPs), followed by the action of prolydase, that will release proline from proline containing di- or tri-peptides, to fuel energy production (Pandhare et al., 2009; Zareba and Palka, 2016; Karna et al., 2020).

Aminoacids derived from intracellular and extracellular protein degradation can be used for protein synthesis or for ATP production, by entering the tricarboxylic acid cycle (TCA cycle).

PRODH involvement in tumour development and progression has also been supported by studies concerning its expression in tumour tissues. Immunohistochemistry experiments have shown that the levels of proline

dehydrogenase are lower in tumour tissues than the corresponding healthy tissues in different types of cancer, such as kidney, bladder, and digestive tract tissues including colon, rectum, stomach, liver and pancreas (Figure 8) (Liu et al., 2009; Liu et al., 2010).

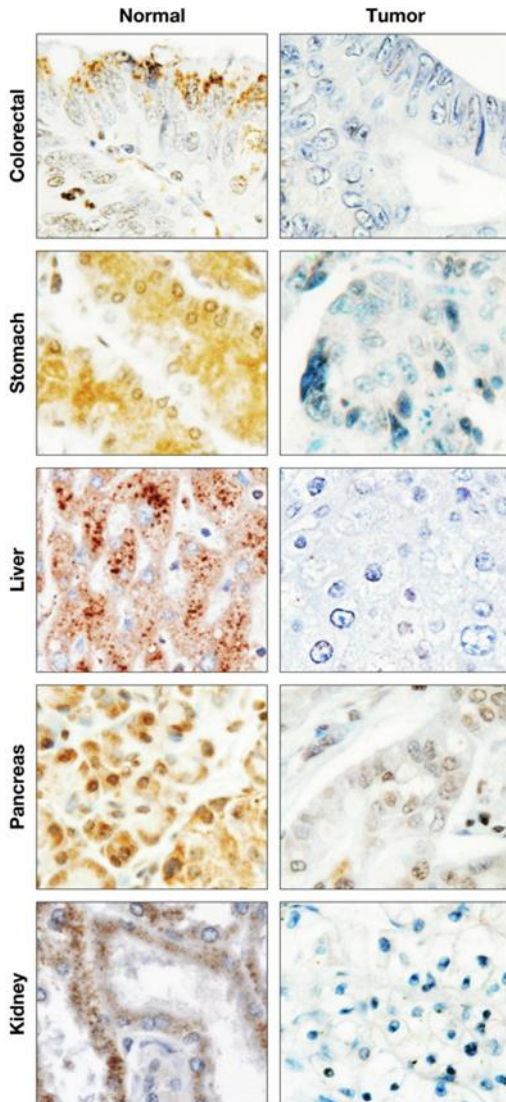


Figure 8. The reduced expression of PRODH in human tumor tissues (modified from Liu et al., 2009). Pairs of human cancer and normal tissues from same patient were immunohistochemically stained for PRODH. The representative images were shown from paired tissue of colon, stomach, liver, pancreas and kidney. Magnification 100X.

In some of these tumour tissues, such as colorectal and renal cancer, PRODH was shown to behave as a tumour suppressor, mainly by modulating the apoptotic process (Maxwell and Rivera, 2003; Liu et al., 2009).

In colon cancer cell lines it was also shown that, by its ability to increase ROS, PRODH can down-regulate some cellular signalling pathways, including MAPK, COX-2 and EGFR (Liu et al., 2006; Liu et al., 2008; Liu et al., 2009).

More recently, however, PRODH was shown to have a role in tumour promotion and progression in other tissues, favouring survival and invasion in breast and pancreatic cancer and in melanoma (Maxwell & Rivera, 2003; Liu et al., 2012; Elia et al., 2017; Olivares et al., 2017; Liu et al., 2020).

In a study carried out in the MCF7 breast cancer cell line, Zareba et al. showed that PRODH down-regulation may promote autophagy whereas its up-regulation would promote apoptosis. The switch between survival and apoptotic mode seems to be dependent on PRODH activity and the availability of proline, in particular connected with the collagen biosynthetic pathway (Zareba et al., 2017; Zareba et al., 2018).

Moreover, PRODH expression can contribute to the metastatic process in breast cancer. In particular, it was found that its expression was higher in metastases compared to primary breast cancer in patients, and when its expression was inhibited in MCF10A breast epithelial cell line transduced with H-Ras^{V12} or in a mouse model, the formation of breast cancer-derived lung metastases was impaired (Elia et al., 2017).

In pancreatic ductal adenocarcinoma cell lines, under nutrient deprivation, PRODH activity promotes survival by inducing autophagy and/or ATP production (Olivares et al., 2017).

In oral cancer tissues, PRODH expression is decreased compared to control tissues, but celecoxib can still activate the apoptotic pathway via induction of PRODH in cell lines derived from squamous cell carcinoma of the tongue (Toloczko-Iwaniuk et al., 2020).

Recently, in a metabolomic study, it was shown that during lung tumorigenesis, proline levels are significantly decreased by the chromatin remodelling factor LSH; the Authors showed that an increase in PRODH expression by LSH and increased proline catabolism promote epithelial to mesenchymal transition in PC9 and A549

lung cancer cells and the activation of IKK α -dependent inflammatory genes, such as *CXCL1*, *LCN2* and *IL17C* (Liu et al., 2020).

These results, together with other evidence described above, suggests that in specific types of tumour, PRODH may represent a target for cancer therapy.

Our interest focused on the study of PRODH expression and functions in lung cancer, one of the deadliest cancer types in the world.

Lung cancer

With 1.8 million new cases and more than 1.5 million deaths annually worldwide in both sexes (Figure 9), lung cancer is the most frequent and one of the deadliest cancer types (Torre et al., 2016; Islami et al., 2015). In particular, it is the most commonly diagnosed cancer (11.6% of the total cases) and the leading cause of cancer death (18.4% of the total cancer deaths) (Bray et al., 2018).

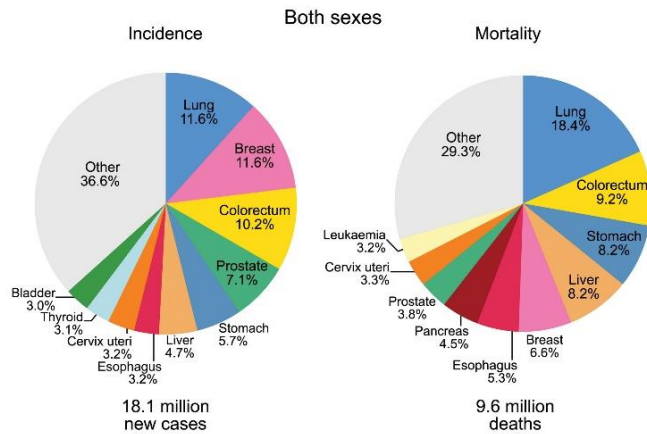


Figure 9. Pie charts represent the Distribution of Cases and Deaths for the 10 Most Common Cancers in 2018 (modified from Bray et al, 2018).

If diagnosis occurs when the tumour is still at early stages, either surgical resection or platinum-based doublet chemotherapy and radiation alone or in combination can be effective, leading to an increase in survival of 50-70% in Non-Small Cell Lung

Cancer (NSCLC); on the contrary, the survival rate drops to 2-5% for patients that are diagnosed with lung tumours at advanced stages (Goldstraw et al., 2007), because no therapy is effective for stage III-IV tumours.

The main problem is that diagnosis is mainly based on symptoms (e.g., cough, chest pain, haemoptysis, shortness of breath) often when surgery or chemotherapy are no more feasible. Accepted screening methods, such as low-dose computed tomography are not devoid of drawbacks such as costs and rate of false positives, so that they are not applied in large scale (The National Lung Screening Trial Research Team, 2011)

It is now well-established that lung cancer is the result of multiple and complex combinations of morphological, molecular and genetic alterations. The deregulation of onco-suppressor genes and oncogenes provides the cell with the potential to become malignant, altering a number of characteristics of the normal cell and determining the acquisition of cancer "hallmarks" (Hanahan and Weinberg, 2011; Davidson et al, 2013).

Cigarette smoking is undoubtedly the most significant risk factor for the onset of lung cancer: in fact, 85-90% of all lung tumours are attributable to smoking (Humphrey et al., 1995). More than 60 carcinogens are contained in cigarette smoke, among which more than 20 appear strongly associated with the development of lung cancer. Although it is generally accepted that cigarette smoking causes lung cancer, not all smokers develop this condition. Following this reasoning, a series of epidemiological studies were conducted which led to suggest the possibility that some genetic factors may also predispose an individual to the development of a pulmonary neoplasm (Hecht, 2012).

Moreover, environmental exposure to radon, asbestos and heavy metals such as chromium, cadmium and arsenic also significantly increase the risk of developing lung cancer (Yokota et al., 2010).

Further risk factors are represented by chronic inflammatory processes such as tuberculosis or Chronic Obstructive Pulmonary Disease (COPD) (Amos et al., 1999; Sato et al., 2007).

Classification of lung cancer

Primary lung tumours are traditionally divided into two main types, namely Non-Small-Cell Lung Cancer (NSCLC) and Small-Cell Lung Cancer (SCLC). The first represents about 85% of all lung cancers while the latter makes up to about 12-15% (AJCC Cancer Staging Manual, Seventh Edition; Davidson et al, 2013).

Small cell lung carcinomas are malignant tumours characterized by small epithelial cells displaying neuro-endocrine features, with small diameter and distinct cytological features: ill-defined cell borders, scant cytoplasm and finely granular nuclear chromatin without obvious nucleoli (Davidson et al., 2013; Travis et al., 2015).

Non-small cell lung carcinomas can be divided into three main histological subtypes: squamous cell carcinoma (SCC), adenocarcinoma (ADC) and large cell carcinoma (LCC).

Lung cancer can originate either from the main bronchi, and in this case it is defined as central cancer, or from the small bronchi, from the bronchioles or from the alveoli located in the distal airways, and therefore it is defined as peripheral cancer. In general, ADCs originate at the distal airways while SCCs occur in proximal airways and are more strongly associated with smoking and chronic inflammation than ADCs; indeed, adenocarcinomas are the most common type in patients who have never smoked (Figure 10) (Wistuba et al., 2006; Herbst et al., 2008; Chen et al., 2014).

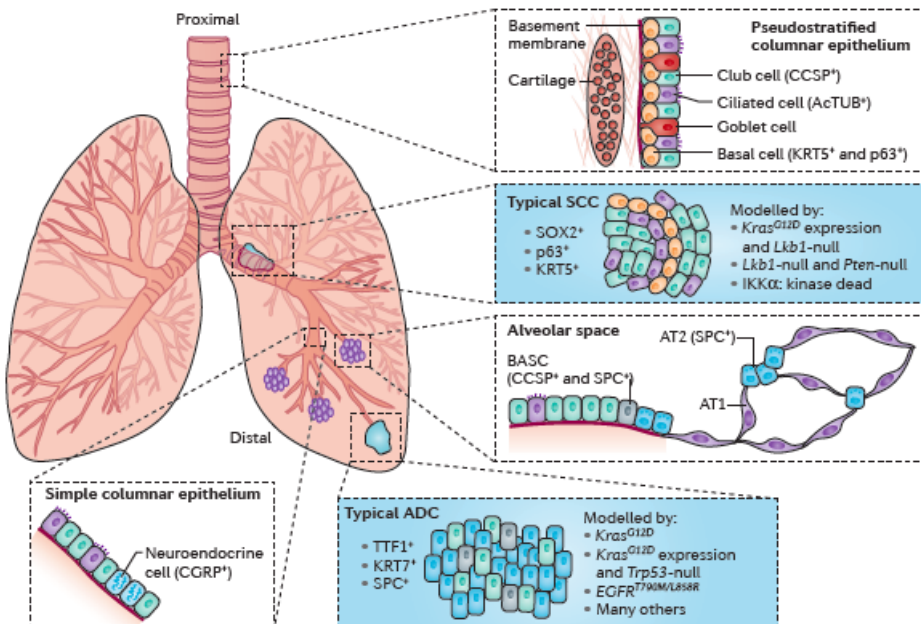


Figure 10. Representation of distal and proximal lung cells, putative lung ADC and SCC cells of origin and their biomarkers. Lung ADCs seem to arise from two different bronchiolar cell populations: the bronchiolar progenitor cells and the bronchioalveolar stem cells (BASCs). The theory is supported by the expression of typical biomarkers, namely Surfactant Protein C (SPC), Thyroid Transcription Factor 1 (TTF1) and Cytokeratin 7 (KRT7). Lung SCCs, instead seem to arise from pseudostratified columnar epithelial cells, typical of the lining of trachea, characterized by the expression of p63, SRY-box 2 (SOX2) and Cytokeratin 5 (KRT5) biomarkers (from Chen et al., 2014).

In addition to the different localization at the lung level, ADCs and SCCs also differ in the types of cell from which they originate: ADCs essentially derive from cells with glandular or secretory properties, such as type II pneumocytes and Clara cells, while SCCs originate from cells of the multilayered squamous epithelium that are not normally present but likely originate from metaplastic cells that develop as a result of exposure to tobacco products, inflammation or irritation (Chen et al., 2014). This different cell derivation is exploited for differential diagnosis, by evaluating the

expression of biomarkers that are characteristic of one or the other population of cells.

ADC biomarkers are TTF1 (Thyroid Transcription Factor 1) and CK7 (Cytokeratin 7), while SCCs are identified in the clinical field using CK5/6 (Cytokeratin 5 and Cytokeratin 6), p63 (in particular the p40 isoform, devoid of the transactivation domain) and the transcription factor SOX2. Additional biomarkers can be studied, which are however used to a lesser extent as they have a lower sensitivity than those previously listed (Sun et al., 2007; Davidson et al., 2013; Chen et al., 2014).

Other differences between the two main NSCLC subtypes are found upon histological analysis. Indeed, SCCs can be defined as malignant epithelial tumours that present keratinization and/or the presence of intercellular bridges at the bronchial epithelium level; ADCs, on the other hand, are also malignant epithelial tumours, but histologically characterized by the presence of glandular differentiation and/or mucus production (Travis et al., 2015).

Finally, comprised in NSCLCs are large cell carcinomas (LCC), which represent approximately 3% of all lung tumours. LCCs are traditionally diagnosed by exclusion when cancer cells neither show either the common morphological characteristics nor express the characteristic biomarkers of the other two subtypes. LCCs tend to be large and partially necrotic tumours formed by groups of cells with vesicular nuclei and prominent nucleoli (Davidson et al., 2013; Chen et al., 2014; Travis et al., 2015).

Molecular genetics of lung cancer

Lung cancer develops through a multi-stage process by which a normal lung epithelial cell turns into a malignant cells.

Molecular genetic studies demonstrate the presence of multiple genetic and epigenetic abnormalities - more than 20 per tumour - affecting lung tumours (Figure 11). These abnormalities include the alteration of specific DNA sequences, copy

number variations, or an aberrant hypermethylation of promoter sequences and, in general, lead to activation of oncogenes and inactivation of tumour suppressor genes.

Overall, these alterations are fundamental to contribute to the initiation, development and maintenance of lung cancer (Sato et al., 2007).

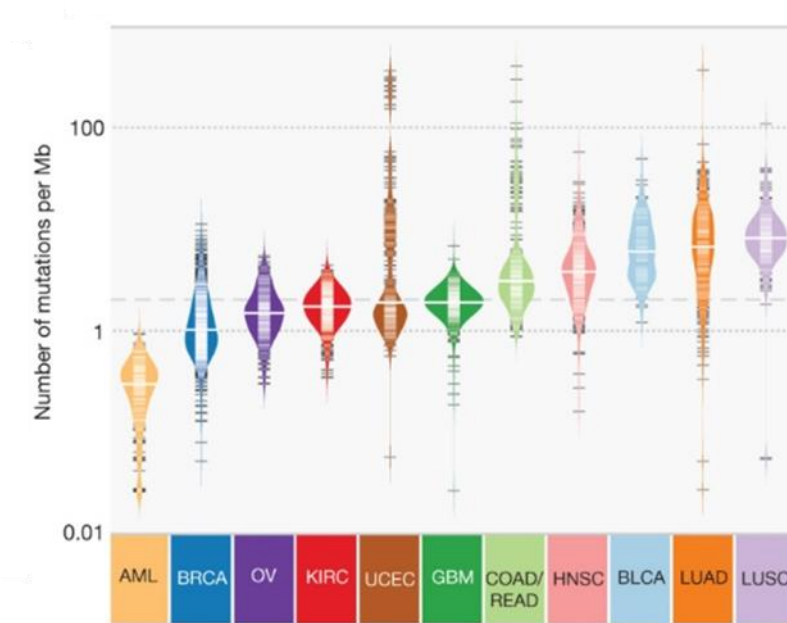


Figure 11. Distribution of mutation frequencies across 12 cancer types (modified from Kandoth et al., 2013). AML, acute myeloid leukaemia; BRCA, breast adenocarcinoma; OV, ovarian serous carcinoma; KIRC, kidney renal clear cell carcinoma; UCED, uterine corpus endometrial carcinoma; GMB, glioblastoma multiforme; COAD/READ, colon and rectal carcinoma; HNSC, head and neck squamous cell carcinoma; BLCA, bladder urothelial carcinoma; LUAD, lung adenocarcinoma; LUSC, lung squamous cell carcinoma.

Dashed grey and solid white lines denote average across cancer types and median for each type, respectively.

Among the oncogenes that contribute most to the development of lung cancer there are, for example, c-MYC (myelocitomatosis oncogene), KRAS (kirsten rat sarcoma viral oncogene homolog), BCL2 (B-cell CLL/ lymphoma 2) or EGFR

(epidermal growth factor), whose sequences can be mutated or changed in the number of copies, as well as oncosuppressor genes, including *TP53* (tumour protein p53), *RB* (retinoblastoma), *CDKN2A* (encoding p16INK4a). Products of these genes (or their lack) act at different levels within the tumour cell in order to promote the development and acquisition of malignant features: some allow uncontrolled growth of the cell or its escape from the apoptosis process, others induce higher telomerase activity, which contributes to make the cancer cell immortal, even at early stages (Wistuba et al., 2006; Sato et al., 2007).

The two main categories of lung carcinomas, namely SCLC and NSCLC, as well as the two major histological subtypes of NSCLCs, show molecular patterns that are different from each other; however, there is also a high heterogeneity within the same lung cancer subtype.

For ADCs, recurrent mutations have been observed in *HER2* (human epidermal growth factor receptor 2), *EGFR*, *MET* (receptor tyrosine kinase), *FGFR1/2* (fibroblast growth factor receptor 1 and 2), *ALK* (anaplastic lymphoma kinase), *ROS1* (receptor tyrosine kinase 1), *NRG1* (neuregulin 1), *NTRK1* (neurotrophic tyrosine kinase receptor type 1) and *RET* genes. As for the SCCs, there are less recurrent mutations but some have been identified, for example in *DDR2* (discoidin domain-containing receptor 2), *FGFR1*, *FGFR2*, *FGFR3* and genes of the PI3K pathway (Wistuba et al., 2006; Chen et al., 2014).

Lung cancer heterogeneity very often represents the cause of the poor success in the treatment of these pathologies. Not only genetic and epigenetic factors (as seen above) but also the type of microenvironment with which the tumour interacts contribute to this heterogeneity. Cancer cells, in fact, are closely associated with the extracellular matrix, mesenchymal cells such as fibroblasts, macrophages and other immune cells and the vascular components. In some cases, this microenvironment is essential for initiation and progression of the tumour, while in other cases it can prevent tumorigenesis or even promote the disappearance of the tumour itself (Chen et al., 2014).

Thyroid transcription factor-1

TTF-1 (Thyroid Transcription factor-1), also known as Nkx2.1 or T/EBP (thyroid-specific-enhancer-binding protein), is a transcription factor that activates the expression of a number of target genes in the thyroid, the lung and part of the brain (Bingle, 1997). Transcription factors play a very important role in the early stages of embryonic development and in subsequent differentiation (Gehring, 1987; Scott et al., 1989). TTF-1 is strongly expressed both in the early stages of thyroid, lung and brain formation, and during adulthood for the maintenance of tissue homeostasis (Lazzaro et al., 1991; Stahlman et al., 1996; Zhou et al., 1996). Thyroid organogenesis is in fact marked by the coexpression of TTF-1 and PAX8, while that of the lungs by TTF-1 and FOXA2 (Bohinski et al., 1994; Di Palma et al., 2003): the lack of these homeotic transcription factors, which normally act in cascade, causes the failure or incorrect development of the organs in which they should be expressed. For example, it has been observed that in mice the deletion of TTF-1 elicits malformations of the organs previously mentioned (Kimura et al., 1996) and that mutations in the human gene for Nkx2.1 are associated with hypothyroidism and respiratory disease in children (Devriendt et al., 1998).

TTF-1 is a protein with a homeodomain, a sequence of 60 amino acids, encoded by 180 bp of DNA, which is capable of binding to a specific sequence in the DNA of target genes. TTF-1 is a protein of about 38-42 kDa and the homeodomain sequence contained therein is found only in the mammalian kingdom, although homology (82% identity) is present with *Drosophila* NK-2 homeodomain (Guazzi et al., 1990). The protein has 98% similarity between man (Ikeda et al., 1995), rat (Mizuno et al., 1991) and mouse (Oguchi et al., 1995), while the homeodomain sequence of 60 amino acids is perfectly preserved, underlining the importance of the functions performed by the transcription factor.

The *NKX2-1* gene is present in a single copy per haploid genome and maps to chromosome 14 in humans (Guazzi et al., 1990); it is organized in 3 exons and 2

introns (Hamdan et al., 1998). The encoded protein is composed of 372 amino acids and contains two transactivating domains, one located at the N-terminus and one at the C-terminus of the protein (De Felice et al., 1995). The protein undergoes several post-translational modifications, such as the phosphorylation of 7 serines (S4, S12, S18, S23, S254, S327, S336) and the oxidation of Cys87, which is associated to a reduction in the ability to bind its DNA consensus sequences (Figure 12) (Tell et al., 2002).

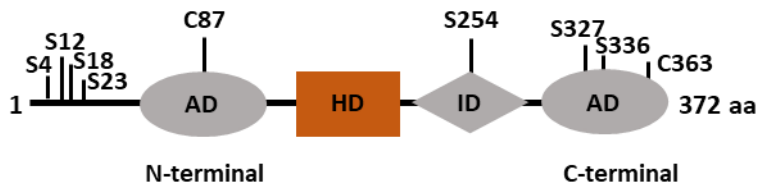


Figure 12. TTF-1 protein organization (modified from Boggaram, 2009). The abbreviations are: AD, activation domain; HD, homeodomain; ID, inhibitor Domain; S, serine-phosphorylation sites; C, redox-sensitive cysteine residues.

Moreover, an induction of the TTF-1 gene by glucocorticoids, cAMP (cyclic AMP) and TGF β (Transforming Growth Factor β) has been demonstrated (Boggaram, 2009). The transcriptional activity of TTF-1 is maintained by cooperation with other transcription factors, such as HNF-3 (Hepatocyte Nuclear Factor-3, also known as FOXA (Forkhead box A), Sp1, Sp3 (specificity protein), GATA-6 and HOXB3 (homeobox B3).

The fine regulation of the transcription factor activity is in agreement with the pleiotropic functions controlled by TTF-1: embryogenesis, morphogenesis and organogenesis.

In fact, in the thyroid, TTF-1 regulates the expression of genes encoding for thyroglobulin, thyroperoxidase and the thyrotropin receptor, thus playing an important role in its functionality (Boggaram, 2009).

In the lung, on the other hand, TTF-1 regulates the expression of the genes encoding SP-A (surfactant protein-A), SP-B, SP-C, CCSP (Clara Cell Secretory Protein), ABCA3 (ATP Binding-Cassette transporter A3). It has also been recently observed that TTF-1 is fundamental for regulating the expression of some genes at the level of type II pneumocytes, including LAMP3 (Lysosomal-Associated Membrane Protein 3) and CEACAM6 (Carcino Embryonic Antigen related Cell Adhesion Molecule 6). TTF-1 is therefore essential for lung physiology and alterations in its expression and activity are reflected in respiratory dysfunctions and a greater tendency to lung infections: surfactant proteins, in particular, play a fundamental role in maintaining lung stability and in protection from external agents (Boggaram, 2009).

During the post-natal phase, the expression of TTF-1 is found only in type II alveolar cells and non-ciliated bronchial epithelial cells. Alterations in TTF-1 levels are found in type II alveolar cells involved in inflammatory processes or in the case of edema.

TTF-1 in lung cancer

The expression of TTF-1 is also maintained in 85-90% of lung adenocarcinomas, the most frequent NSCLC subtype, allowing it to be used as a specific marker for diagnosis. The availability of such specific marker allows diagnosis not only of primary tumours but also to identify metastases of lung cancer to other organs (Ordóñez, 2000; Zamecnik et al., 2002; Moldvay et al., 2004). Its expression is usually investigated by immunohistochemistry (Myong, 2003; Tan et al., 2003). Many studies have also shown that TTF-1 staining can be used as a prognostic indicator, as a high expression of the transcription factor correlates to a favourable prognosis (Puglisi et al., 1999; Haque et al., 2002; Myong, 2003; Tan et al., 2003; Saad et al., 2004; Anagnostou et al., 2009).

The characteristics of TTF-1 during lung tumorigenesis and progression suggest that it can be considered a potential "lineage survival oncogene" in this tissue (Figure 13), because, albeit on one hand it is able to favour the survival and growth of the

primary tumour, on the other hand it is able to suppress the metastatization process (Tanaka et al., 2007; Boggaram 2009; Mu 2013; Yamaguchi et al., 2013).

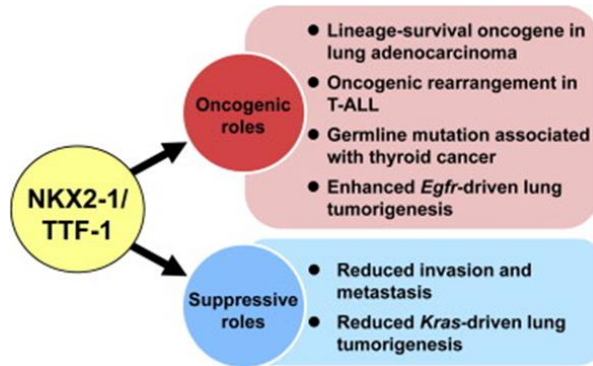


Figure 13. Double-edged characteristic of NKX2-1/TTF-1 in cancer development and progression (modified from Yamaguchi et al., 2013)

In some instances, increased levels of TTF-1 protein are associated with gene amplification (Tanaka et al., 2007; Kwei et al., 2008). In addition, RNAi (RNA-interference) experiments in different cell lines derived from lung cancer have shown that a decrease in TTF-1 levels leads to a reduction in cell proliferation. Moreover, low levels of TTF-1 can lead to alterations in the cell cycle and apoptosis (Tanaka et al., 2007; Kwei et al., 2008). It is also interesting to see how, in situations of haploinsufficiency or in mice knockout for TTF-1, an increase in invasiveness of mucinous pulmonary adenocarcinomas, under the control of k-Ras, was observed (Maeda et al., 2012; Snyder et al., 2013); finally, the expression of TTF-1 is significantly associated with EGFR mutations (Yatabe et al., 2005; Takeuchi et al., 2006).

However, TTF-1 can also play an oncosuppressive role (Figure 6), by activating the expression of occludin (OCLN) and claudins 1 and 18 (CLDN1 and CLDN18), epithelial tight-junction proteins and other TTF-1 targets that encode for cytoskeletal regulatory proteins (Niimi et al., 2001; Runkle et al., 2012). In summary, many TTF-1 targets negatively affect cell motility and invasion, thus preventing the metastatization of lung tumours (Yamaguchi et al., 2013).

However, TTF-1 cannot be used as a specific molecular target for the treatment of lung cancer because it is indispensable for the normal physiology of the organ, for example for the production of surfactant proteins (Yamaguchi et al., 2013). One of more of its target genes may be use as therapeutic targets instead. In this thesis we investigated if proline dehydrogenase could be one of its targets, based on several analogies in their behaviour.

AIM OF THE STUDY

Proline dehydrogenase (PRODH) is a mitochondrial inner-membrane and stress-inducible flavoenzyme catalyzing the first step in the proline degradation pathway (Phang et al., 2010), that is involved in the regulation of cell survival, autophagy and apoptosis (Phang et al., 2015).

Indeed, proline oxidation produces electrons, that can be transferred from the flavine adenine dinucleotide (FAD) cofactor to the electron transport chain to either produce reactive oxygen species (ROS) or ATP. These molecules mediate PRODH-dependent apoptosis (ROS) or autophagy (ROS or ATP) (Phang et al., 2015).

In line with these different biological functions, PRODH has a role as a tumour suppressor in renal and colorectal cancer (Maxwell et al., 2003; Liu et al., 2009); however, in breast and pancreatic cancers expression of this protein favours invasion and metastatization (Elia et al., 2017).

This PhD project aims to investigate PRODH function in the context of lung tumorigenesis and to obtain some hints into its regulation by lung specific transcription factors. Lung tumours show high genetic and cellular heterogeneity and ongoing research aims to find markers to improve diagnosis and tumour classification, to predict prognosis and/or to find novel targets for therapy.

According to our preliminary results, PRODH may represent a new marker for discriminating lung adenocarcinomas from other subtypes of lung cancer or metastases from other organs. However, to envisage an application as diagnostic or prognostic marker, a thorough understanding of the significance of PRODH expression in lung cancer and its possible regulation by factors involved in lung tumorigenesis.

This project is aimed to identify molecular factors associated with PRODH expression in lung cancer. Then, in order to characterize the cellular processes

affected by PRODH in lung cancer, appropriate cellular models to carry out stable transfection or silencing experiments were selected.

Upon completion of this project, a more detailed comprehension of the role played by PRODH in lung tumorigenesis will be obtained.

RESULTS

The results of my PhD work are included in the following manuscript drafts:

1. Proline dehydrogenase is expressed in lung adenocarcinoma and modulates cell survival and 3D growth in a cell line-specific manner.
2. TTF-1 contributes to transcriptional regulation of the *PRODH* gene in lung adenocarcinoma cells.

Moreover, during my PhD I contributed to the following papers:

- **Grossi S**, Grimaldi A, Congiu T, Parnigoni A, Campanelli G, Campomenosi P. Human Primary Dermal Fibroblasts Interacting with 3-Dimensional Matrices for Surgical Application Show Specific Growth and Gene Expression Programs. *Int J Mol Sci*. 2021 Jan 7;22(2):E526. doi: 10.3390/ijms22020526. PMID: 33430241.
- Claudio Procaccini, Silvia Garavelli, Fortunata Carbone, Dario Di Silvestre, Dario Greco, Alessandra Colamatteo, Maria Teresa Lepore, Deriggio Faicchia, Francesco Prattichizzo, **Sarah Grossi**, Paola Campomenosi, Fabio Buttari, Pierluigi Mauri, Antonio Uccelli, Marco Salvetti, Vincenzo Brescia Morra, Mario Galgani, Roberta Lanzillo, Giorgia Teresa Maniscalco, Diego Centonze, Paola de Candia and Giuseppe Matarese. "Signals of Pseudo-Starvation Unveil SLC7A11 as Key Molecular Determinant in the Control of Human Treg Cell Proliferative Potential" Submitted to "Immunity" (IMMUNITY-D-20-00820).
Preparation of the revised manuscript is ongoing.

1. Proline dehydrogenase is expressed in lung adenocarcinoma and modulates cell survival and 3D growth in a cell line-specific manner

Sarah Grossi¹, Arianna Parnigoni¹, Raffaella Cinquetti¹, Anna Maria Chiaravalli², Fausto Sessa^{2,3} and Paola Campomenosi^{1,*}

¹ University of Insubria, Department of Biotechnology and Life Sciences, DBSV, Via J.H. Dunant 3, 21100 Varese, Italy;

²Ospedale di Circolo e Fondazione Macchi, Laboratorio di Anatomia Patologica, Via O. Rossi 9, 21100 Varese, Italy;

³University of Insubria, Department of Medicine and Surgery, DMC, Via Guicciardini 9, 21100 Varese, Italy;

*Correspondence: paola.campomenosi@uninsubria.it

Keywords

Proline dehydrogenase; Lung cancer; Immunohistochemical analysis; Adenocarcinoma cell lines; cell-based assays.

ABSTRACT

Non-Small Cell Lung Cancer (NSCLC) ranks second among tumours for incidence and first for mortality, regardless of gender and comprises two main histotypes, adenocarcinoma (ADC) and squamocellular carcinoma (SCC). Identification of markers for early diagnosis, to predict prognosis and improve therapeutic options of NSCLC is key to increase survival. This work aims to investigate whether proline dehydrogenase (PRODH), a mitochondrial flavoenzyme catalyzing the key step in proline degradation which is involved in the regulation of cell survival, autophagy and apoptosis, may play a role in lung cancer. PRODH expression was investigated in NSCLCs by immunohistochemistry and it was found to be present in the majority of lung ADCs. Patients with PRODH positive tumours had better cancer-free specific survival and overall survival compared to those with negative tumours. Protein staining correlated with transcript levels, suggesting that regulation occurs at the transcript level. Moreover, PRODH expression correlated with presence of EGFR activating mutations.

In NCI-H1650 and other four lung ADC cell lines tested in this work, ectopic modulation of PRODH expression seemed to decrease cell survival assayed by clonogenic assay; conversely, in A549 and NCI-H1437 cell lines, PRODH overexpression led instead to an increase in cell survival. Moreover, in NCI-H1650 cells PRODH overexpression also induced an increase in cell motility and a reduction in the ability of these cells to grow in soft agar. These results were confirmed in the NCI-H1299 adenocarcinoma cell line. This study supports a possible role of PRODH in the pathogenesis of lung cancer and as a prognostic marker in lung adenocarcinoma.

INTRODUCTION

Lung cancer is the leading cause of cancer death worldwide (Siegel et al, 2019). This is mainly due to the fact that diagnosis occurs at late stages, when tumours are metastasized and surgery is no longer an option, nor is therapy effective (Jantus-Lewintre et al, 2012). Lung cancer is clinically heterogeneous, comprising Small Cell Lung Cancer (SCLC, accounting for about 15% of lung cancer cases) and Non-Small Cell Lung Cancer (NSCLC, 85% of lung cancer cases), that in turn includes two major histotypes, adenocarcinoma (ADC, ≈55% of cases) and squamous cell carcinoma (SCC, ≈ 45%) (Chen et al, 2014).

Given the poor survival rate of lung cancer at advanced stages, early diagnosis, prognosis and therapy of NSCLC would greatly benefit from the identification of novel biomarkers.

Since the description of the so called “Warburg effect” (Warburg, 1956), an altered metabolism has been increasingly recognised to play an important role in tumour promotion and progression. Metabolism of nonessential amino acids (NEAA), such as glutamine, has been shown to be important for cancer cell survival in almost all types of cancer (Pandhare et al., 2009; Possemato et al; 2011; Liu et al, 2015; Yang and Vousden, 2016; Phang 2019).

Recently, proline has been proposed to play a role in tumorigenesis (Liu et al, 2015; Phang 2019). Proline can be synthesized in two steps from glutamate by the activity of Δ -1-pyrroline-5-carboxylate synthase (P5CS) and P5C reductase (PYCR, EC 1.5.1.2). This amino acid can also be obtained from ornithine by the sequential action of ornithine- δ -aminotransferase (OAT) and P5C reductase (Liang, 2013).

The catabolism of proline occurs exclusively through proline dehydrogenase (PRODH, EC 1.5.5.2, formerly EC 1.5.99.8), a mitochondrial inner-membrane and stress-inducible enzyme, containing a flavin adenine dinucleotide cofactor (FAD). Proline dehydrogenase catalyses the first step in the proline degradation pathway (Phang et al., 2010; Liu and Phang, 2012). The regulation of this enzyme is complex

and involves several transcription factors with an important role in cancer development and microRNAs (Phang et al, 2010).

PRODH can play a dual role in the tumorigenic process, either promoting cell survival through the production of ATP or by inducing ROS-dependent protective autophagy, as well as by inducing ROS-mediated apoptosis (Pandhare et al, 2006; Circu et al., 2010; Liu and Phang, 2012; Phang et al., 2015; Zareba and Palka, 2016). Indeed, PRODH is one of the main proapoptotic effectors of p53, when induced by genotoxic stress (Polyak et al, 1997). PRODH plays also a role in response to other types of stress, including nutrient stress (Pandhare et al., 2009; Olivares et al., 2017). In this context, it must be underlined that its substrate, proline, can be easily retrieved by degradation of the extracellular matrix, in particular collagen, where it accounts, together with hydroxyproline, for 25% of the aminoacids (Pandhare et al., 2009).

Therefore, PRODH seems capable of influencing the balance between survival and apoptosis, likely depending on the cell type and on the type and severity of stress acting on those cells (Raimondi et al, 2013).

Several studies document that this protein is dysregulated in several types of cancer. In particular, PRODH expression has been studied in kidney, bladder, stomach, colon and rectum and liver, where it was shown to be down-regulated compared to normal tissue (Maxwell and Rivera, 2003; Liu et al., 2009). This, together with evidence that PRODH is a known p53 target gene involved in apoptosis (Maxwell and Rivera, 2003; Raimondi et al., 2013; Monti et al., 2014) and can suppress tumorigenesis in mouse models, led scientists to conclude that in these tumours PRODH behaves as a tumour suppressor (Liu et al., 2009). More recently, however, PRODH expression was shown to favour invasion and metastatization in breast cancer (Elia et al., 2017) and to promote pancreatic tumour growth (Olivares et al, 2017). On the other hand, in the MCF7 breast cancer cell line, PRODH downregulation was shown to promote autophagy whereas its up-regulation would promote apoptosis (Zareba et al., 2017; Zareba et al., 2018).

The aim of this study was to investigate if PRODH could play a role in lung tumorigenesis.

To do so, PRODH expression in lung cancer was characterized by immunohistochemistry; we tested if there was a correlation between the expression of this protein and expression of known lung cancer markers. Moreover, to elucidate the functions exerted by PRODH in lung cancer, we performed proliferation, invasion and 3D growth experiments in adenocarcinoma cell lines, after modulating its expression.

MATERIALS AND METHODS

Samples for immunohistochemical analysis

The study was performed on formalin-fixed paraffin-embedded samples of lung cancer collected by the Pathology Department of the “Ospedale di Circolo” in Varese from 1996 to 2015.

Hematoxylin-eosin staining of tumour sections were revised and all tumours were classified according to the criteria of the WHO classification system (4th edition, Travis et al, 2015). The tumour stage was assessed using the tumour node metastases system (TNM 7th edition) defined by the International Union Against (AJCC CANCER STAGING MANUAL seventh edition, 2010).

135 Non-small cell lung carcinomas (NSCLC) and 13 small-cell lung carcinomas (SCLC) were included in this study. Among NSCLC, 70 were adenocarcinomas and 65 squamocellular lung carcinomas. Healthy lung tissue was used as control. The study was carried out in accordance with the Declaration of Helsinki (1975).

Immunohistochemical analyses

Immunohistochemical analyses were performed on 3 µm formalin-fixed, paraffin-embedded sections, deparaffinised and rehydrated through Bioclear incubation and

alcohol series to water. After washing in Tris buffered saline (TBS) pH 7,4, endogenous peroxidase activity was blocked with 3% aqueous hydrogen peroxide for 15 min, followed by washes in TBS+ 0,2% Triton (v/v). Antigen retrieval was performed incubating slides in a solution of trypsin at a final concentration of 0,5 mg/mL (starting from a 50 mg/mL stock) in TBS for 20 minutes at 37°C. For detection of immunohistochemical expression of PRODH protein, we initially tested a commercial antibody anti-PRODH raised in rabbit (Prestige anti-PRODH antibody, code HPA020361, Sigma-Aldrich, Milan, Italy) in parallel with a custom antibody, raised in rabbit using PRODH recombinant protein encompassing aminoacids 176-572 as immunogen (Tallarita et al., 2012) (Davids Biotechnologie, Dabio, Regensburg, Germany, kind gift from Prof. Pollegioni). Subsequently, all the immunohistochemical analyses were performed with the custom rabbit polyclonal antibody (Davids Biotechnologie, Dabio, Regensburg, Germany), at a 1:100 dilution in 1% normal goat serum in TBS, incubating overnight at 4°C. Negative controls were performed by substituting primary antibody with non-immune serum or by preabsorption of antibody with 20 nmol of the recombinant protein used for raising the antibody (kind gift from Prof. Pollegioni). Sections were then washed in TBS + 0,2% Triton (v/v) and the signal was detected with the UltraVision Quanto detection system HRP DAB (ThermoFisher Scientific, Milan, Italy) according to manufacturer's protocol. Nuclei were counterstained with Harris hematoxylin and after rinse in running water, sections were dehydrated and embedded in Pertex (Kaltex Srl, Padua, Italy).

A case was considered as positive for PRODH staining when at least 25% of tumour cells showed cytoplasmic immunoreactivity.

Cells culture and vectors

The cell lines used in this study and their culture conditions are described in Table 1. All media and reagents for cell culture were from Carlo Erba Reagents, Milan Italy, unless otherwise specified.

Table 1. Cell lines used in this work

Cell line	Histology	Growth medium
A549	NSCLC, adenocarcinoma	RPMI1640 + 10% FBS + 2 mM L-Gln
NCI-H1299	NSCLC, derived from lymph node metastatic site	RPMI1640 + 10% FBS + 2 mM L-Gln
NCI-H1650	NSCLC, broncho-alveolar adenocarcinoma, pleural Effusion	RPMI1640 + 10% FBS + 2 mM L-Gln
NCI-H1975	NSCLC, adenocarcinoma	RPMI1640 + 10% FBS + 2 mM L-Gln + Sodium Pyruvate
NCI-H2228	NSCLC, adenocarcinoma	RPMI1640 + 10% FBS + 2 mM L-Gln + Sodium Pyruvate
SK LU-1	NSCLC, adenocarcinoma	DMEM + 10% FBS + 2 mM L-Gln + Sodium Pyruvate + MEM non-essential amino acids (NEAA)
NCI-H441	NSCLC, papillary adenocarcinoma	RPMI1640 + 10% FBS + 2 mM L-Gln + 10 mM Hepes + Sodium Pyruvate + Glucose (final 4500 mg/L)
LX1	NSCLC, squamous-cell carcinoma	DMEM + 10% FBS + 2 mM L-Gln
SKMES-1	NSCLC, squamous-cell carcinoma (derived from metastatic site: pleural effusion)	DMEM + 10% FBS + 2 mM L-Gln
HCC827	NSCLC, adenocarcinoma	RPMI 1640 + FBS 10% + 2 mM L-Gln
HCC827-GR5	NSCLC, adenocarcinoma (derived from HCC827)	RPMI 1640 + FBS 10% + 2 mM L-Gln + 1 μ M Gefitinib
NCI-H2342	NSCLC, adenocarcinoma	DMEM:F12 Medium + heat inactivated FBS 5% + 4,5 mM L-Gln + 0,0005 mg/ml Insulin + 0,01 mg/ml Transferrin + 30 nM Sodium selenite + 10 nM Hydrocortisone + 10 nM beta-estradiol
NCI-H1437	NSCLC, adenocarcinoma (derived from metastatic site: pleural effusion)	RPMI 1640 + FBS 10% + 2 mM L-Gln
NCI-H727	Bronchial carcinoid	RPMI 1640 + FBS 10% + 2 mM L-Gln
IGROV-1	Ovarian endometrioid adenocarcinoma (positive control for PRODH expression)	RPMI 1640 + FBS 10% + 2 mM L-Gln + MEM non-essential amino acids (NEAA)

Cultures were incubated at 37°C in 95% humidity and 5% CO₂ atmosphere. At confluence, cells were removed from culture flasks by trypsinisation. A new batch

of frozen cells was thawed on average 2 weeks before each experiment to have sufficient numbers of cells.

To evaluate the presence of mycoplasma, cells were routinely checked by using the nested PCR method described in Tang et al. (Tang et al., 2000).

The PRODH overexpressing construct, carrying the wild-type PRODH coding sequence under the early CMV promoter was created by cloning PRODH cDNA into pcDNA3.1 vector. The silencing constructs were obtained by identifying suitable PRODH specific and control (“scrambled”) shRNAs with the program pSicoligomaker 3.0 and cloning them into the pSico vector. Two different shRNA producing constructs were prepared, targeting two different regions of the PRODH transcript (named 505 and 1828 after the position targeted on the transcript).

For stable transfection, 4×10^4 cells (NCI-H1650), 8×10^4 cells (NCI-H1975), 9×10^4 cells (NCI-H2228 and SK LU-1), $3,5 \times 10^4$ cells (NCI-H1299) or 5×10^4 cells (NCI-H1437) were seeded in a 24-well multiwell plate, or $1,8 \times 10^5$ cells (A549) were seeded in a 6-well multiwell plate, to be 70% confluent on the following day, when transfection was performed using 0,4 μg (24-well) or 1,2 μg (6-well) of DNA and Fugene HD transfection Reagent (Promega, Milan, Italy), according to manufacturer’s instructions. 24 hours later, cells were split into one or more petri dishes and after further 24 hours the appropriate concentration of G418 (Aurogene, Rome, Italy) or puromycin (Aurogene, Rome, Italy) was added for selection of cell clones integrating pcDNA3.1 and pSico constructs, respectively. In particular, for G418 selection, 320 $\mu\text{g}/\text{mL}$ (A549), 270 $\mu\text{g}/\text{mL}$ (NCI-H1650), 250 $\mu\text{g}/\text{mL}$ (NCI-H1299), 900 $\mu\text{g}/\text{mL}$ (NCI-H1975), 750 $\mu\text{g}/\text{mL}$ (NCI-H2228) and 1000 $\mu\text{g}/\text{mL}$ (SK-LU-1) were used, as determined by preliminary cytotoxicity curves; for puromycin, 0,75 $\mu\text{g}/\mu\text{l}$ were used for selection of NCI-H1437 resistant clones. Selective growth medium was substituted every 3-4 days, until clones were sufficiently grown to be isolated and expanded. Single or pooled clones were frozen in liquid nitrogen and expression of the transgene was checked by immunoblot analysis.

RNA extraction from FFPE tumours and qPCR analyses

Total RNA from formalin-fixed and paraffin embedded tissues was extracted using the RecoverAll Total Nucleic Acid Isolation Kit (Ambion by Life Technologies, Milan, Italy) following manufacturer's instructions. RNA samples were quantified with a Qubit RNA assay kit (Life Technologies Italia, Milan, Italy) on a Qubit instrument (Life Technologies Italia, Milan, Italy) and run on agarose gel for quality control.

cDNA was prepared from 500 ng of RNA using the iScript select cDNA synthesis kit (Biorad, Milan, Italy), and a reverse primer specific for *PRODH* (5'-TGGTATTGCTTGTCCTCCGCTT-3') and for beta-2-Microglobulin (β 2M) (5'-GTCCCGGCCAGCCAGGTCC-3').

For real-time quantitative PCR (qPCR) primer pairs specific for *PRODH* (forward: 5'-GCAGAGCACAAGGAGATGGA-3', reverse: 5'-TGGTATTGCTTGTCCTCCGCTT-3') and beta-2-Microglobulin (β 2M) (forward: 5'-AGGCTATCCAGCGTACTCCA-3' and reverse: 5'-ATGGATGAAACCCAGACACA-3') were used.

Gene expression analysis was performed in triplicate using a CFX96 thermal cycler (Biorad, Milan, Italy) and the iTAQ Universal Sybr Green Supermix (Biorad, Milan, Italy). No template controls (NTC), in which distilled water was used instead of cDNA, were included in each analysis. Melting curve analysis was performed to ensure that single amplicons were obtained for each target.

The difference (ΔC_q) between the C_q obtained for *PRODH* (GOI) and that for *B2M* (REF) was calculated for each sample. The smaller the value of the ΔC_q the higher the expression levels of *PRODH*.

RNA extraction from cell lines and digital PCR analyses

Total RNA was extracted from cell lines with TriReagent (Sigma-Aldrich, Milan, Italy), according to manufacturer's instructions. RNA samples were quantified with a

NanoDrop 2000c (ThermoFisher, Life Technologies Italia, Milan, Italy) and run on an agarose gel for quality control.

cDNA was obtained from 500 ng of RNA by using the iScript cDNA synthesis kit (Biorad, Milan, Italy).

For droplet digital PCR (ddPCR), 15 ng cDNA were used in a 20 μ L reaction, adding 10 μ L of QX200 EvaGreen ddPCR Supermix (Biorad, Milan, Italy), primer pairs specific for PRODH (forward: 5'-GCAGAGCACAAGGAGATGGA-3', reverse: 5'-TGGTATTGCTTGTCCCCTT-3') and beta-2-Microglobulin (B2M; forward: 5'-AGGCTATCCAGCGTACTCCA-3', reverse: 5'-ATGGATGAAACCCAGACACA-3') and nuclease-free water to volume. Two no template controls (NTC), in which distilled water was used instead of cDNA, were included in each analysis.

Each 20 μ L reaction was loaded into a well of a droplet generation cartridge (Biorad, Milan, Italy) and 70 μ L of QX200 Droplet generation oil (Biorad, Milan, Italy) were added into the appropriate wells. The cartridge was loaded into the QX200 Droplet Generator (Biorad, Milan, Italy) to generate the droplets, that were transferred to a 96-well plate with a Rainin multichannel pipette. The plate was sealed with Pierceable foil (Biorad Milan, Italy) and put in a T100 thermal cycler (Biorad, Milan, Italy).

Cycling conditions were: 95 °C for 5 min, followed by 40 cycles of 95 °C for 30 s and 60 °C for 1 min, then signal stabilization steps (4 °C for 5 min, 90 °C for 5 min) and final hold at 4 °C. The ramp rate was 2 °C/s. After PCR, plates were loaded into the QX200™ Droplet Reader (Biorad, Milan, Italy) for detection.

Immunoblotting

Protein extracts were obtained by mechanically scraping the cells from 100 mm plates in PBS supplemented with 5 mM EDTA (Euroclone, Milan, Italy). Cells were counted and resuspended in RIPA Buffer (150 mM NaCl, 50 mM Tris-HCl pH 7.5, 1% Igepal CA630, 0,1% SDS, 0,5% Sodium deoxycholate) supplemented with protease

inhibitors (PMSF, benzamidine, aprotinin and leupeptin). Samples were incubated on a rotating wheel at 4°C for 50 min, then the insoluble fraction was removed by centrifugation. Protein concentration was evaluated using the Quick Start Bradford 1X Dye Reagent (Biorad, Milan, Italy) following manufacturer's instructions, using bovine serum albumin to build a standard curve.

Alternatively, cells lysates were obtained after cell detachment from cell culture vessels. Cells were counted and resuspended in Laemmli Sample Buffer 2X, using 1µl of buffer every 2×10^4 cells. The samples were lysed by incubation at 95°C for 3 min followed by vortexing, repeating these steps for three times.

For SDS-PAGE 50 µg of extract or 12 µl of cell lysate were used. Proteins were transferred onto nitrocellulose membranes (Amersham Hybond ECL, GE Healthcare Life Sciences, by Euroclone, Milan, Italy) using the Mini-PROTEAN Tetra System (Biorad, Milan, Italy) and, after blocking in 4% non-fat milk in PBS-T (0.1% Tween20 in PBS) and incubation with the appropriate primary and secondary antibodies, signals were detected with the Amersham ECL Prime Western Blotting Detection Reagent (GE Healthcare, Milan, Italy), using an Odyssey LI-COR FC imaging system (Carlo Erba Reagents, Milan, Italy).

Primary antibodies were rabbit polyclonal anti-PRODH (1:550, SAB1303113, Sigma-Aldrich, Milan, Italy), and mouse monoclonal anti alpha-tubulin (1:1500, MAB-94264, Immunological Sciences, Rome, Italy) for normalization.

Secondary antibodies were: stabilized goat anti-rabbit HRP-conjugated monoclonal antibody (1:900, ThermoFisher Scientific, Milan, Italy) or IR-Blot 800 Goat anti-Rabbit (1:25000, Cyanagen, Bologna, Italy) and stabilized goat anti-mouse HRP-conjugated monoclonal antibody (1:900, ThermoFisher Scientific, Milan, Italy) or IR-Blot 700 Goat anti-Mouse (1:25000, Cyanagen, Bologna, Italy). All antibodies were diluted in 2% non-fat milk in PBS-T.

Colony formation assay

Transfection was performed as described above. After 15 days of selection, clones were stained with 0,1% crystal violet (Sigma, Milan, Italy) in 35% ethanol solution for 30 minutes directly in the culture dishes. Alternatively, clones were stained with 1% methylene blue (Sigma, Milan, Italy) in 50% ethanol solution for 30 minutes. Three replicates were prepared for each cell line.

Cell proliferation assays

Cells from single PRODH or control transfected NCI-H1650 clones were plated onto 96-well plates at a density of 2×10^3 cells/well. MTT assay was used to monitor cell proliferation in different growth conditions (Table 2). Briefly, the medium was discarded and cells were washed with PBS. 100 μ L MTT (0,5 mg/mL in PBS; Across Organics, Carlo Erba, Milan, Italy) was added and incubated for 2 hrs at 37°C. After a wash with PBS, 80 μ L of DMSO (dimethyl sulfoxide; Euroclone, Milan, Italy) were added in each well. After 30 minutes of incubation with gentle shaking at room temperature to dissolve MTT crystals, the absorbance at 590 nm was read with an Infinite 200 plate reader (Tecan, Cernusco sul Naviglio, Italy).

Table 2. Composition of media used for proliferation assays.

Conditions	Medium	FBS	L-Glutamine	L-Proline	G418
Standard	RPMI 1640	10%	1%	-	270 μ g/mL
Serum starvation	RPMI 1640	0,1%	1%	-	270 μ g/mL
L-glutamine starvation	RPMI 1640	10%	-	-	270 μ g/mL
L-glutamine starvation + L-proline	RPMI 1640	10%	-	50 mg/L	270 μ g/mL

Wound healing assay

Cells from single PRODH or control transfected clones or pools were plated at high density [150000 cell/well (NCI-H1650), 160000 cell/well (NCI-H1975) and 60000

cell/well (NCI-H1299)] in a 12-well multiwell plate and cultured overnight. The following day, a “wound” was created with a 200 μ L pipette tip; closure of the wounds by surrounding cells was monitored 0, 1, 2, 4, 6 and 24 hrs after performing the scratch. The results are presented as percentage of wound closure obtained with TScratch software (CSElab, Computational Science & Engineering Laboratory, version 1.0).

Soft agar assay

Cells from single PRODH or control transfected clones were suspended in 0.3% agar (stock solution 2% agar in H₂O, sterilised by autoclaving) in RPMI 1640 cell culture medium containing 20% FBS at a density of 1×10^2 cells/well, and plated on solidified agar (0.6% agar in RPMI 1640 culture medium containing 20% FBS) in 12-well dishes. Three replicates were prepared for each condition and each cell line. The plates were incubated for 16 days at 37°C in 5% CO₂. Growth of colonies was monitored using a light microscope (TIEsseLab, Milan, Italy) and their number and size was evaluated. Results presented are the average of 3 independent experiments.

Statistical Analysis

The difference in PRODH staining in the samples analysed by immunohistochemistry was evaluated by Fisher’s exact test; the difference in PRODH expression among ADC and SCC samples was compared using t-test. The correlation between PRODH expression levels and the presence of EGFR activating mutations or p53 mutations was evaluated using t-test.

The failure time according to PRODH in ADC Kaplan Maier curves was evaluated by chi-squared test.

The difference in the distribution of Δ Ct (GOI-REF) values between IHC positive and negative cases was evaluated by Anova test.

The difference in % of wound healing and the results obtained by soft agar assays were compared using t-test. All statistical analyses were done with GraphPad Prism statistical software, 4.02 version.

RESULTS

PRODH expression in lung cancer samples

To investigate PRODH expression in lung cancer, we performed immunohistochemical analyses on 135 lung cancer samples. The clinico-pathological data of the analysed tumors and the results of PRODH expression are presented in Table 3. PRODH was observed as granular immunoreactive deposits in the cytoplasm of tumour cells, with an intensity and a percentage of immunoreactive cells variable from case to case. Representative images of PRODH expression are reported in Figure 1. No immunoreactivity was observed when primary antibody was substituted with non-immune serum or after preabsorption of antibody with 20 nmol of the recombinant protein used to raise the antibody (not shown).

Considering a threshold at $\geq 25\%$ stained cancer cells, PRODH expression was elevated in NSCLC (36,3%) and was never observed in SCLC. In particular, an intense and diffuse staining was frequently observed in ADC (57,14%) and in a small proportion of SCCs (13,85%) (Table 3). The difference in PRODH staining between ADC and SCC cases was statistically significant ($p < 0,0001$, Fisher's exact Test) (Table 3). Moreover, the staining was significantly stronger and involved a higher percentage of cells in ADC, compared to SCC. In fact, the mean percentage of immunoreactive cells was 35% (range 0-90%) in ADC and 9% (range 0-75) in SCC ($p < 0.0001$, t-test) (Table 3).

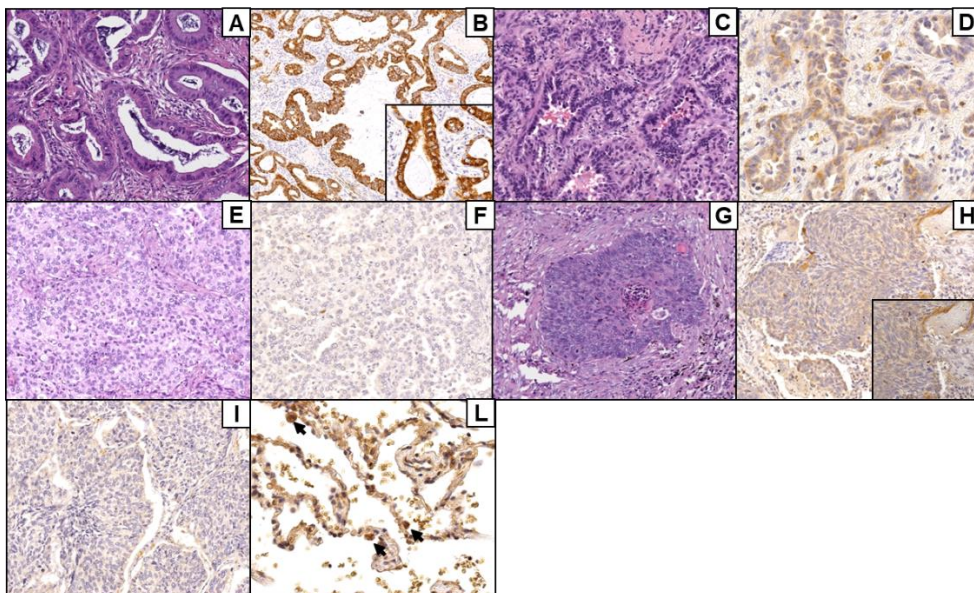


Figure 1. Representative results of PRODH immunostaining. Lung adenocarcinoma (ADC): A) Acinar ADC (hematoxylin-eosin, 200X) with B) abundant and intense cytoplasmic granular PRODH immunoreactivity (DAB-hematoxylin 100X, particular 400X); C) Acinar ADC (hematoxylin-eosin, 200X) with D) weak cytoplasmic PRODH immunoreactivity (DAB-hematoxylin, 400X); E) Predominantly solid lung ADC (hematoxylin-eosin, 200X) with F) no PRODH immunoreactivity (DAB-hematoxylin, 200X). Lung squamocellular carcinoma (SCC): G) SCC (hematoxylin-eosin, 200X) displaying H) showing weak, diffuse cytoplasmic PRODH staining (DAB-hematoxylin, 200X, inset 400X); I) SCC devoid of PRODH immunoreactivity (DAB-hematoxylin, 200X). L) Healthy lung parenchyma, showing rare PRODH positive cells, corresponding to type II pneumocytes and Clara cells, (DAB-hematoxylin, 400X).

Table 3. Correlation between PRODH expression and clinico-pathological data in adenocarcinomas and squamous cell carcinomas.

		ADC (70 cases)	SCC (65 cases)	Total cases (135)
		PRODH+ cs/tot (%)	PRODH+ cs/tot (%)	Total cases (135)
N. of cases		40/70 (57,14)	9/65 (13,85)	49/135 (36,3)
Grade	1	5/6 (83,33)	0/2 (0)	5/8 (62,5)
	2	24/50 (48)	8/40 (20)	32/90 (35,56)
	3	10/14 (71,43)	1/23 (4,35)	11/37 (29,73)
pT	1	22/32 (66,67)	5/26 (19,23)	27/59 (45,76)
	2	18/31 (58,06)	3/31 (9,68)	21/62 (33,87)
	3	0/5 (0)	1/4 (25)	1/9 (11,11)
	4	0/1 (0)	0/2 (0)	0/3 (0)
	x	0	0/2 (0)	0/2 (0)
pN	0	35/53 (66,04)	8/54 (14,81)	43/107 (40,19)
	1	0/2 (0)	1/2 (50)	1/4 (25)
	2	3/8 (37)	0/3 (0)	3/11 (27,27)
	x	2/7 (28,57)	0/6 (0)	2/13 (15,38)
Stage	I	37/55 (67,27)	8/55 (14,55)	45/110 (40,9)
	II	0/1 (0)	0/1 (0)	0/2 (0)
	III	3/8 (37,5)	1/6 (16,67)	4/14 (28,57)
	IV	0/5 (0)	0/3 (0)	0/8 (0)
	x	0/1 (0)	0	0/1 (0)

In addition, PRODH expression in adenocarcinoma samples correlated with the stage of the tumours. In particular, PRODH was more expressed in tumours at early stages (pTNM I and II; 66%), compare to tumours at late stages (pTNM III and IV; 23%) ($p=0,0104$, Fisher's exact Test) and it was also more expressed in small tumours (pT1 and pT2; 63,5%) compared to tumours bigger than 7 cm or tumours invading other tissues (pT3 and pT4; 0%) ($p=0,0040$, Fisher's exact Test). Moreover, the positivity for PRODH was higher in cases without metastasis (pN0; 66%), compared to metastatic cases (pN1 and pN2; 30%) ($p=0,0420$, Fisher's exact Test) (Table 3).

Data on a relatively small number of cancer-specific survival of patients bearing PRODH positive tumours suggested that PRODH is a favourable prognostic factor in lung adenocarcinoma, although statistical significance was not achieved (Figure 2A). Our results were confirmed by Kaplan-Meier overall survival curves obtained from KMplotter database (<https://kmplot.com/>), based on a larger cohort (719 Cases), where we observed a significant difference in survival of patients bearing high or low levels of PRODH expression ($p=0.0004$) (Figure 2B).

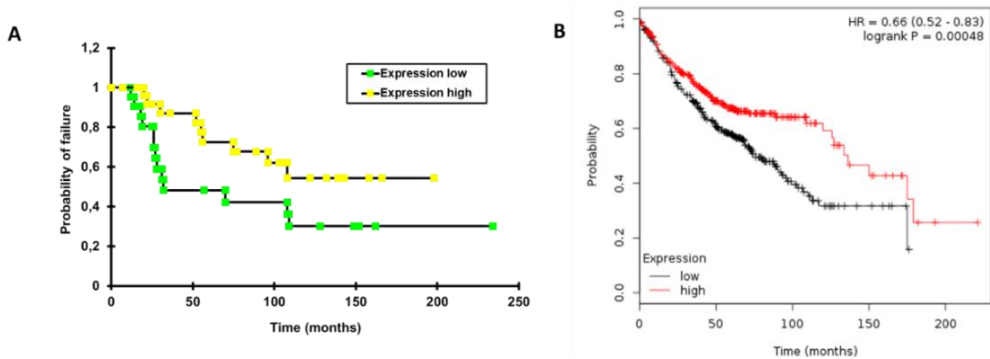


Figure 2. Kaplan-Meier curves. **A.** cancer-specific survival for adenocarcinoma samples with high or low PRODH expression levels from this study (cutoff value was 25%) ($p=0,0595$, chi-squared test); **B.** Overall survival curves obtained from KMplotter database for adenocarcinoma samples ($p=0.00048$, chi-squared test) (Gyórfy et al., 2013).

RT-qPCR analyses on a subset of samples showed that high levels of protein expression in positive cases was accompanied by an increase in transcript levels. The difference in ΔCt (CtGOI-CtREF) median values between PRODH protein positive and negative cases was highly significant ($p= 0.0099$, Anova test), suggesting concordance between protein and transcript levels (Figure 3).

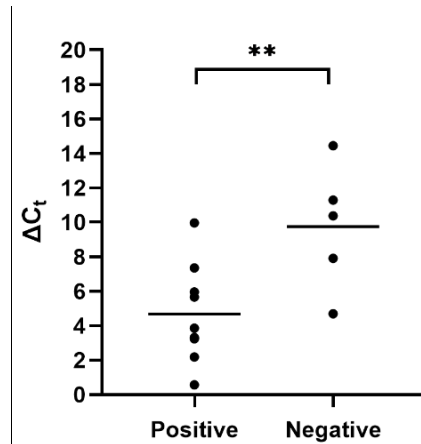


Figure 3. The increase in PRODH protein levels in IHC is paralleled by an increase in transcript levels in qPCR. Positive: lung adenocarcinomas with elevated expression of PRODH protein; negative: lung adenocarcinomas with low or no expression of PRODH protein. A small ΔC_t value indicates high transcript levels (C_t for PRODH similar to that of the reference gene). Horizontal lines indicate the mean value. Asterisks indicate that there is a significant difference (** $p=0.0099$, Anova test).

The association of PRODH expression with EGFR and p53 mutations was also evaluated. In 103 cases, we found that PRODH expression correlated with the presence of EGFR activating mutations ($p=0,0044$, t-test) but not with p53 mutations ($p=0.2707$ t-test, $n=108$).

PRODH expression in adenocarcinoma cell lines

As we found high level of PRODH expression in adenocarcinoma samples during immunohistochemical characterisation, we then focused on the effects of its expression in adenocarcinoma cell lines.

First, by bioinformatic analysis (Cancer Cell Line Encyclopedia: <https://portals.broadinstitute.org/ccle>) we identified some lung cancer cell lines with low (A549, NCI-H1299, NCI-H1650, NCI-H1975, NCI-H2228, NCI-H441, LX-1,

SKMES and SK LU-1) or relatively high (including HCC827, its derivative HCC 827-GR5, NCI-H1437, H727 and NCI-H2342) endogenous expression of PRODH.

Actual PRODH expression levels in the cell lines were measured by droplet digital PCR and western blot analyses (Figure 4) and overall confirmed bioinformatic data, meaning that cell lines with higher levels in CCLE were also positive to our analyses.

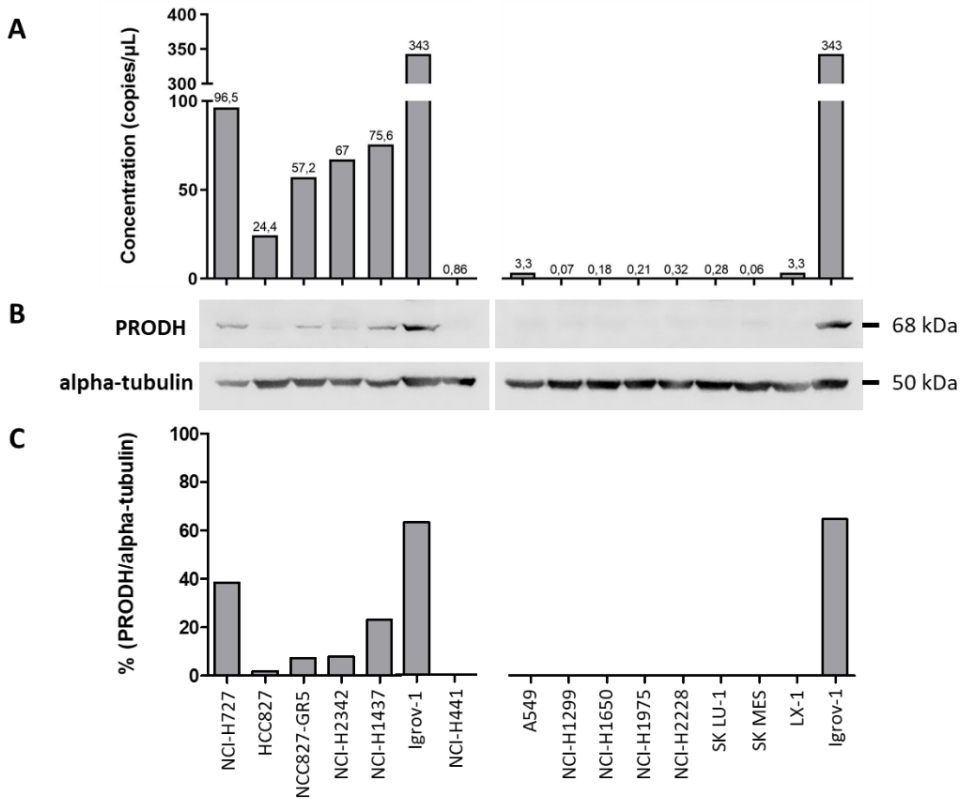


Figure 4. PRODH expression in the cell lines under investigation, as measured by ddPCR (A) and Western blot (B). **A.** Expression analyses by ddPCR was done on with the QuantaSoft software and yielded absolute expression as copies of transcript/ microliter of PCR reaction. As we used the same RNA and cDNA volumes for all cell lines, these data are directly comparable. **B.** Western blot analyses of extracts from the indicated cell lines, detected for PRODH; alpha-tubulin was detected for normalization purposes. **C.** The graph represents the relative expression in percentage of PRODH protein after normalisation (ratio of PRODH and alpha-tubulin x 100).

As a first test, clonogenic assays, testing the ability of cells to survive under stressful conditions, were performed on selected cell lines. Cell lines that showed low endogenous levels of PRODH were transfected with an expression construct encoding wild-type PRODH, as well as with the empty vector as control. The NCI-H1437 cell line, where endogenous PRODH expression was observed, was transfected two PRODH silencing constructs and a scrambled construct used as a control condition.

In 5 of the 7 cell lines tested, namely NCI-H1650, NCI-H1975, NCI-H2228, SKLU-1 and NCI-H1299, PRODH overexpression led to a decrease in cell viability (Figure 5). In contrast, in the A549 cell line, PRODH overexpression led to an increase of cells viability. A decrease in cell viability was observed in the NCI-H1437 cell line silenced for PRODH expression, confirming the data obtained in A549 cells (Figure 5).

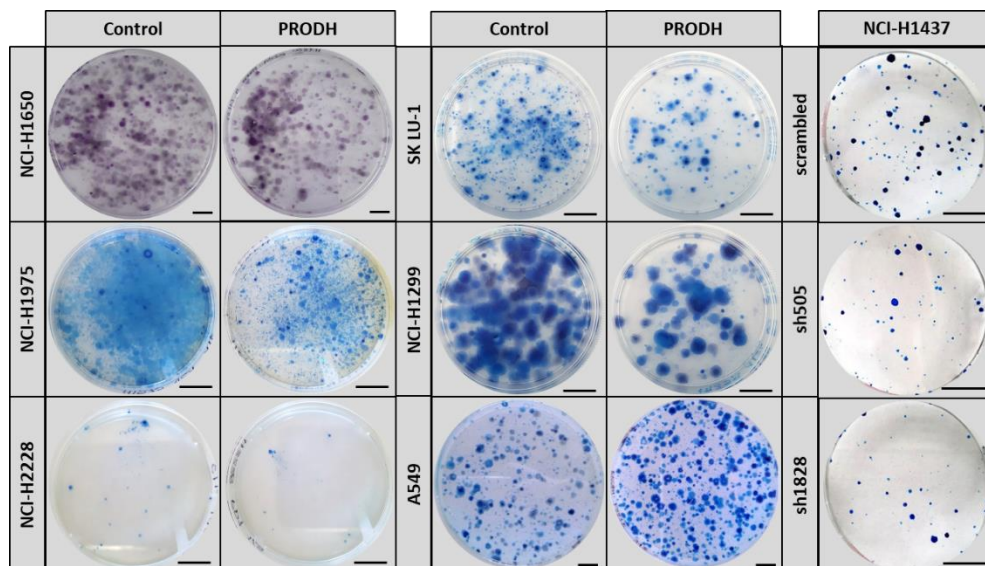


Figure 5. Representative clonogenic assays in NCI-H1650, NCI-H1975, NCI-H2228, NCI-H2228, SK LU-1, NCI-H1299, A549 and NCI-H1437 cell lines. Control: cells were transfected with pcDNA3.1 vector (control condition); PRODH: pcDNA3.1-PRODH (PRODH overexpression); Scrambled: pSico-scrambled sequence (control condition); sh505 and sh1828: pSico-PRODH constructs expressing two short hairpins directed towards two different PRODH transcript sequences. Bars indicate 1 cm.

Then the effects of PRODH ectopic expression on proliferation of the NCI-H1650 cell line was evaluated, using 7 control clones and 7 PRODH expressing clones, as assessed by western blot analysis (Figure 6).

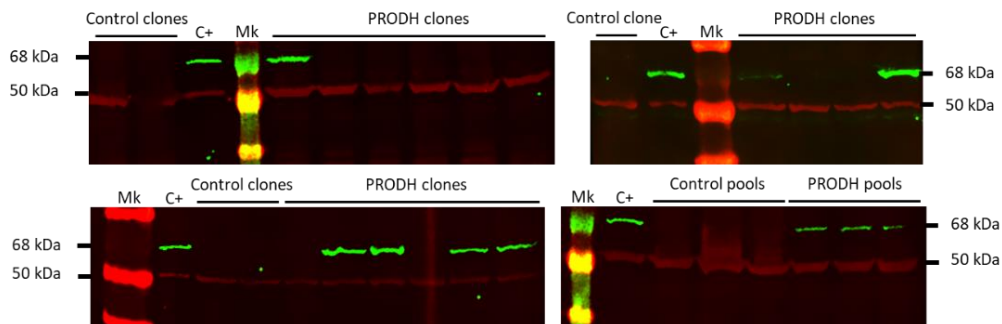


Figure 6. PRODH expression in NCI-H1650 transfected clones. Immunoblot of lysates from single NCI-H1650 clones or pools stably transfected with empty pcDNA3.1 vector or pcDNA3.1-PRODH construct was detected with anti-PRODH polyclonal antibody (green signal); a monoclonal against alpha-tubulin was used for normalization (red signal). Mk indicates the protein ladder; C+ indicates the Igrov-1 lysate used as positive control.

Proliferation assays were performed in standard growth conditions and in presence of stressful conditions, such as serum starvation, L-glutamine starvation, L-glutamine starvation + L-proline supplementation, by means of the MTT assay. A high variability within each type of clones (PRODH expressing or control clones) was observed. Consequently, although PRODH expressing clones showed on average a lower absorbance at 590 nm compared to control clones, the difference was not significant. Moreover, the same trend was apparent in all the tested conditions (Figure 7). We conclude that PRODH does not significantly affect proliferation in the NCI-H1650 lung ADC cell line.

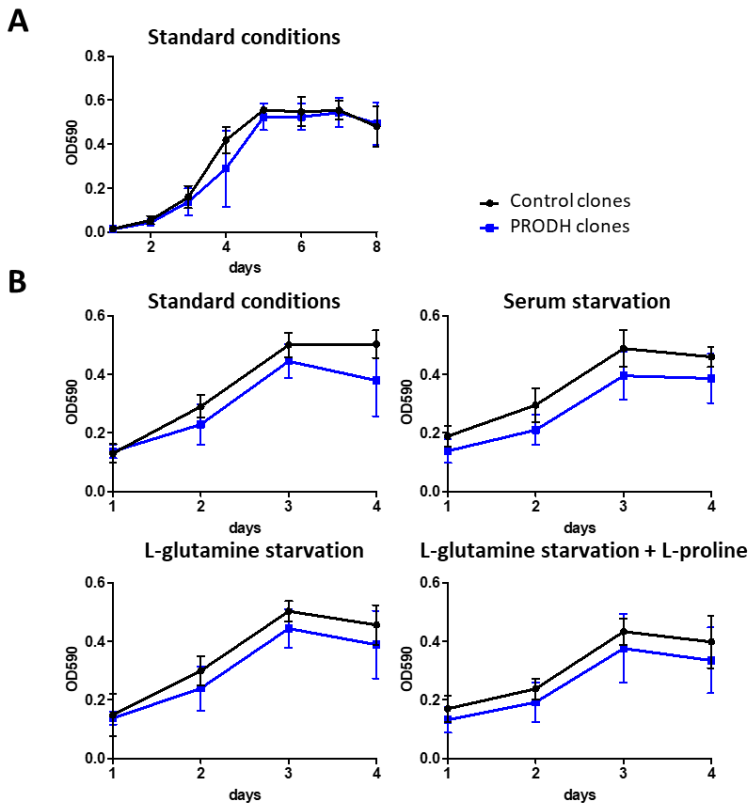


Figure 7. Effects of PRODH overexpression on NCI-H1650 cell proliferation. A. The graph reports the mean of the growth curves of control (black) or PRODH expressing clones (blue), evaluated by the MTT assay. B. Mean of the growth curves of control (black line) or PRODH expressing clones (blue) in four different conditions: standard culture conditions, serum starvation (0.1% FBS), L-glutamine starvation (no L-glutamine), L-glutamine starvation + supplementation with 50 mg/L L-proline (no L-glutamine + L-proline).

The migratory ability of NCI-H1650 cells in presence or absence of PRODH expression, was evaluated by wound healing experiments. Notably, all 7 tested PRODH expressing clones closed the wound faster than the 7 control clones and, at 24 hours, 6 out of 7 (85,7%) analysed PRODH expressing clones showed complete closure of the wound (Figure 8A). The difference of the means of all control and PRODH expressing clones was significant at both 6 and 24 hours after the wound (two-tailed t-test).

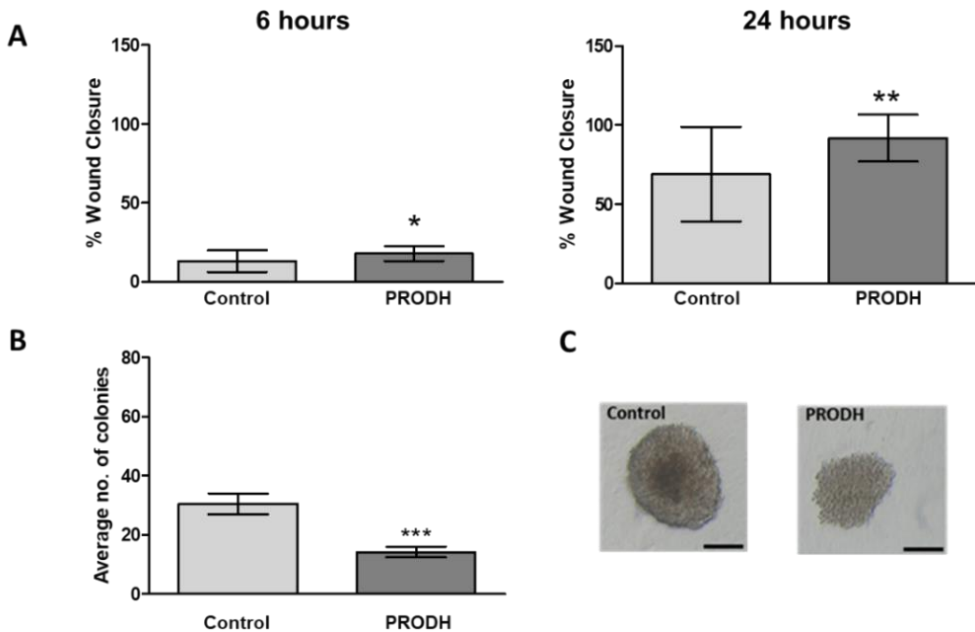


Figure 8. Effects of PRODH overexpression in the NCI-H1650 cell line. **A.** Wound healing assay. The graphs indicate the percentage of wound healing in clones transfected with a PRODH expressing construct or empty vector 6 and 24 hours after wound. 7 control clones and 7 PRODH expressing clones were used for this experiment. Results are the mean of three replicates \pm SD. Asterisks indicate significant differences (* $p < 0.05$; ** $p < 0,01$; two-tailed t -test). **B.** Soft agar assay. For each clone tested, cells were plated at very low seeding density (5×10^2 cells/ml) and grown in soft agar for 16 days. The colonies were counted and the average number obtained for the mean of all clones was plotted. The data represent the mean of triplicates \pm SE of two independent experiments, using 7 PRODH expressing clones and 7 control clones. Results were analysed by two-tailed t -test. Asterisks indicate significant differences (***) $p < 0,001$). **C.** Representative colonies formed by empty vector or PRODH vector. Bar indicates 150 μ m.

Finally, we performed the soft agar colony formation assay to assess the ability of NCI-H1650 cells to grow independently by the presence of a solid surface, which represents a hallmark of tumorigenesis. PRODH expressing clones formed less colonies in soft agar compared to control cells (Figure 8B). Moreover, the colonies formed by PRODH expressing clones were smaller than control clones (Figure 8C).

In order to confirm the results obtained with the NCI-H1650 cell line, we tested the effects of PRODH overexpression in other lung adenocarcinoma cell lines. To this purpose, the following cell lines, all showing low endogenous PRODH levels were stably transfected: A549, NCI-H1975, NCI-H2228, NCI-H1299 and SK LU-1.

Very few of the clones expressed the transgene: none of 20 isolated clones and none of six clone pools from the A549 cell line maintained PRODH expression, in spite of G418 resistance. Also from the NCI-H2228 none of 16 isolated clones and none of three clone pools was positive for PRODH expression. For the SK LU-1 cell line, only one pool out of 18 clones and 2 pools were weakly positive for PRODH expression. In the NCI-H1975 cell line, only one out of 18 clones and three out of 3 pools expressed the PRODH transgene. Finally, only 2 clone pools from NCI-H1299 were positive for PRODH expression. In the NCI-H1437 cell line, in which silencing was performed, 11 clones stably transfected with pSicoR-Oligo505 construct and 11 clones for pSicoR-Oligo1828 initially showed a reduction in PRODH expression, but for all clones silencing was lost after repeated freezing and thawing cycles. Moreover, sequencing of PRODH cDNA revealed a heterozygous mutation, giving rise to the amino acid substitution p.Val427Met, that has been shown to reduce PRODH activity by 60% (Bender et al., 2005).

The clone pools from NCI-H1975 and NCI-H1299 cell lines stably transfected with PRODH expression construct that initially screened positive for PRODH expression, continued to express the transgene after repeated freezing and thawing cycles (Figure 9), so these clone pools were used to confirm the results obtained with the NCI-H1650 cell line.

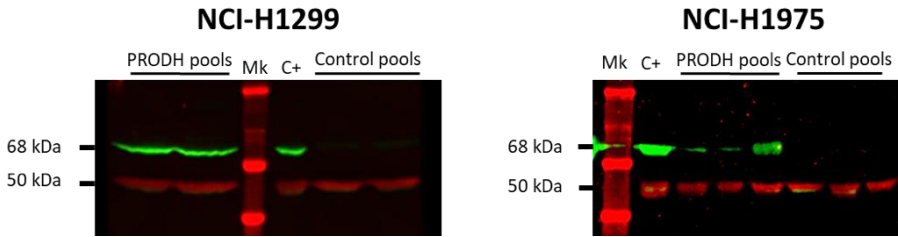


Figure 9. PRODH expression in NCI-H1299 and NCI-H1975 transfected pools. Immunoblot of lysates from NCI-H1299 and NCI-H1975 pools stably transfected with empty pcDNA3.1 vector or pcDNA3.1-PRODH construct was detected with anti-PRODH polyclonal antibody (green signal); a monoclonal against alpha-tubulin was used for normalization (red signal). Mk indicates the protein ladder; C+ indicates the Igrov-1 lysate used as positive control.

In the wound healing assay, NCI-H1299 PRODH expressing pools showed a complete closure of the wound at 24 hours (Figure 10) that was instead slower in control pools; the difference between the mean of control and PRODH expressing pools was significant.

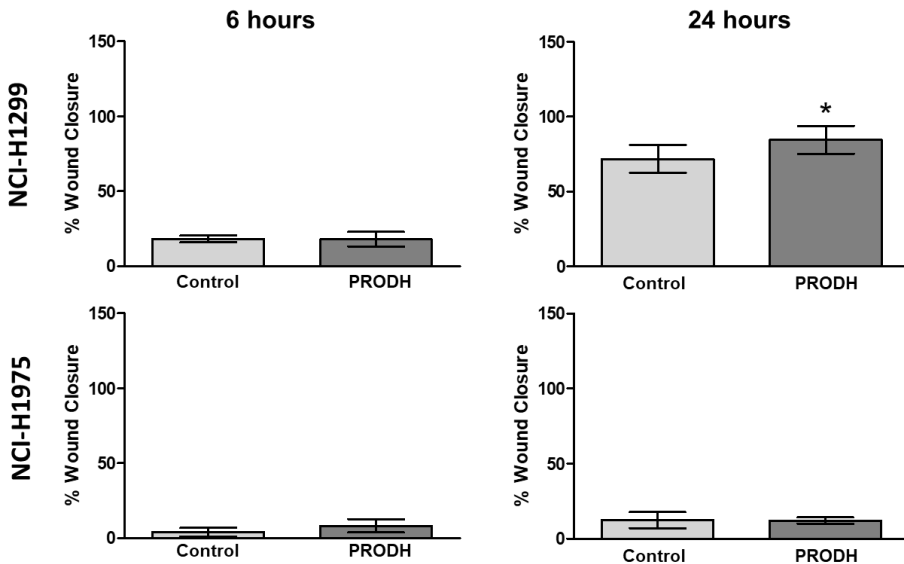


Figure 10. Wound healing assay. The graphs indicate the percentage of wound healing of control or PRODH expressing clone pools 6 hours and 24 hours after wound. Results are the average of three replicates \pm SD. Results were analysed by two-tailed t test. Asterisks indicate significant differences (* $p < 0.05$).

In general, the NCI-H1975 cell line did not show an elevated migratory ability. Moreover, a difference in wound healing in control versus PRODH expressing clone pools was not observed (Figure 10).

In the soft agar colony formation assay, PRODH expressing clones formed smaller colonies than control clones in both cell lines (Figure 11, A). Moreover, NCI-H1299 PRODH expressing clone pools formed significantly less colonies in soft agar compared to control clone pools (Figure 11, B), confirming the results obtained with the NCI-H1650 cell line. In the NCI-H1975 cell line, no difference was found in the number of clones formed by PRODH expressing clone pools compared to control clone pools.

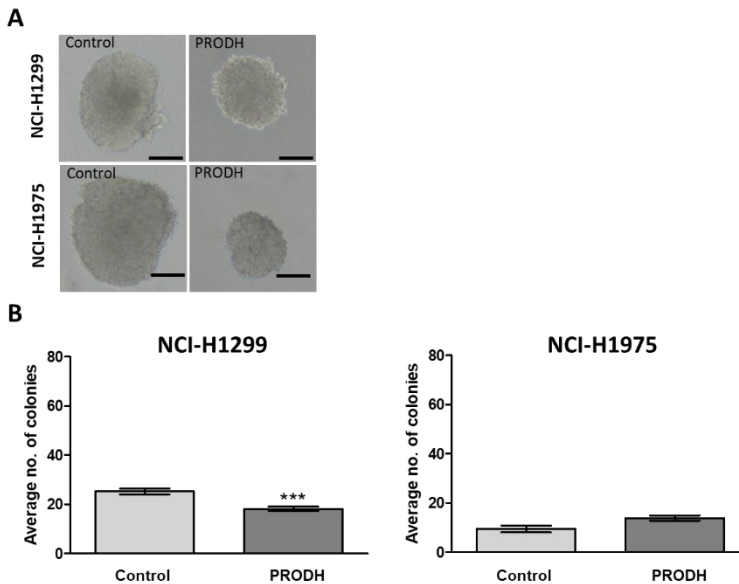


Figure 11. Soft agar assay. Cells were plated at very low seeding density (5×10^2 cells/ml) and grown in soft agar for 16 days. **A.** Representative colonies formed by NCI-H1299 and NCI-H1975 cell lines transfected with empty vector or a PRODH expression construct. Bar indicates 150 μ m. **B.** The colonies were counted and the mean of all clones was plotted. The data represent the mean of triplicates \pm SE of two independent experiments, performed with 2 PRODH expressing and 2 control pools from NCI-H1299 cells and 2 PRODH expressing and 2 control pools from NCI-H1975 cells. Results were analysed by two-tailed t test. Asterisks indicate significant differences (***) $p < 0,001$.

In conclusion, these results suggest that PRODH can influence several aspects of cell behaviour in lung adenocarcinoma cell lines. Table 4 summarizes the findings in the investigated cell lines.

Table 4. Summary of the results obtained from PRODH expressing clones compared to control clones for different cell lines in different tests.

	Clonogenic assay (survival)	Wound healing assay (motility)	Colony formation assay (anchorage independence)
NCI-H1650	↓ survival	↑ motility	↓ n° and size of colonies
NCI-H1299	↓ survival	↑ motility	↓ n° and size of colonies
NCI-H1975	↓ survival	No difference	↓ size, no difference in n° of colonies
NCI-H2228	↓ survival		
SK LU-1	↓ survival		
A549	↑ survival		
NCI-H1437	↑ survival		

DISCUSSION

Investigating the molecular bases of lung cancer, the leading cause of cancer death worldwide (Siegel et al., 2019), is key to find useful markers for different applications, such as early diagnosis, differential diagnosis, prognosis and to guide therapeutic options. This work focused on proline dehydrogenase (PRODH), a mitochondrial enzyme, key to proline metabolism, that plays an important role in induction of apoptosis and autophagy, influencing cellular outcomes. PRODH expression is dysregulated in several types of cancer, including colorectal, renal, mammary and pancreatic carcinomas (Maxwell & Rivera, 2003; Liu et al., 2009; Liu et al., 2012; Elia et al., 2017; Olivares et al., 2017; Zareba et al., 2017; Zareba et al., 2018; Liu et al., 2020; Toloczko-Iwaniuk et al., 2020).

Immunohistochemistry data suggest that PRODH plays a role in lung tumorigenesis, in particular in the ADC subtype, where it seems to improve prognosis in terms of cancer-specific survival and overall survival (Figures 1 and 2), and that there is a correlation between PRODH expression and EGFR mutations.

In this work, several lung ADC cell lines were analysed for PRODH expression, in order to find suitable cellular models to study the effects of PRODH expression modulation.

Comparison of the transcript levels described *in silico* (Cancer Cell Line Encyclopedia) with experimental data showed good correlation, but, most importantly, we found a correlation between protein and transcript levels, suggesting that PRODH is mainly regulated at the transcriptional level.

Some ADC cell lines with low endogenous PRODH expression levels were used to test the clonogenic ability after transfection with an expression construct encoding wild-type PRODH or empty vector as control. In A549 cells, PRODH overexpression favoured survival, observed as an increase in clonogenic ability in PRODH transfected compared to control cells, whereas in all the other cell lines the transfection with PRODH expression construct led to a decrease in clonogenic

ability. NCI-H1437 cell line, with relatively high PRODH expression levels, showed a decrease in clonogenic ability after silencing, thus showing a behaviour similar to the A549 cell line. This suggests that PRODH affects survival of lung cancer cells, but the outcome depends on additional and specific features of the cell lines. A possible explanation is that the difference in the observed behaviour among the tested cell lines may be caused by differences in their genetic background (Table 5).

Table 5. Characterized mutations of cells under study.

Cell lines	Characterized mutations
A549	wt <i>TP53</i> and <i>EGFR</i> , mutations in <i>KRAS</i> (p.G12S), <i>CDKN2A</i> , <i>STK11</i> and <i>SMARCA4</i>
NCI-H1650	Deletion in the <i>PTEN</i> gene (c.1027-?_1213+?del), mutations in <i>CDKN2A</i> , <i>EGFR</i> and <i>TP53</i>
NCI-H1437	wt <i>EGFR</i> ; mutations in <i>TP53</i> and <i>CDKN2A</i>
NCI-H1975	mutations in <i>EGFR</i>
NCI-H2228	<i>ALK-PTPN3</i> and <i>EML4-ALK</i> gene fusion
SK LU-1	mutations in <i>KRAS</i>
NCI-H1299	Deletion of the <i>TP53</i> gene

The attempt to obtain single clones stably expressing PRODH from the same cell lines tested in clonogenic assays was unsuccessful, since most of the clones that were resistant to the selective agent (G418) lost expression of the transgene. In the vector where PRODH was cloned (pcDNA3.1), transgene expression is under control of the strong Citomegalovirus (CMV) early promoter, that has been shown to often lead to unstable transgene expression (Wang et al., 2017). Other vectors with a different promoter will be tested.

Several PRODH expressing clones from the NCI-H1650 cell line were obtained. These clones were used for a panel of assays, such as proliferation curves, wound healing and colony formation assays. No significant difference in growth was observed in proliferation curves, neither when performed at standard culture conditions nor under specific stress conditions, between PRODH expressing and control clones.

The wound healing assay represents a simple way to analyse cell migrating abilities. The reason for performing this assay was that recently an association was found between PRODH expression and metastatization in breast cancer cells (Elia et al., 2017). However, it must be stressed that, in spite of the fact that in both lung adenocarcinoma and ductal infiltrating breast adenocarcinoma PRODH is highly expressed, the consequences of this expression may be different. In NCI-H1650 cells, PRODH expressing clones showed a greater motility than control clones. The results of the soft agar assay showed that PRODH expression decreases the ability of cells to form spheroids. This aspect, needs to further investigation focusing on 3D cells growth, for example using hydrogel coated plates.

The results with the NCI-H1650 cell line were confirmed in the NCI-H1299 cell line. A significant increase in motility and a reduced ability to grow in soft agar in PRODH expressing compared to control clones was found, while the NCI-H1975 cell line did not show cell migrating abilities neither in control and PRODH expressing clones, and also did not show differences in the ability to form spheroids. Thus, although PRODH is expressed both in lung adenocarcinoma and in ductal infiltrating breast adenocarcinoma, the outcomes of this expression appear to be different (Elia et al., 2017). In a recent work, lung adenocarcinoma cell lines were shown to recapitulate what was found in breast cancer cell lines (Liu et al., 2020). However, only the A549 cell lines was tested both in their work and in the present study and we show here that it behaved differently from other lung adenocarcinoma cell lines.

In conclusion, these results in lung adenocarcinoma cell lines suggest that PRODH can play a role in several aspects of tumour initiation and progression in lung cancer tumorigenesis. These results are supported by the results obtained by immunohistochemistry analysis. Actually, in the tumour samples analysed, we observed that PRODH expression diminishes with increasing stage or grading of the adenocarcinoma samples, suggesting that the function of PRODH in these cancer cells may be related to maintenance of differentiation and normal physiology of tumour cells. To further elucidate PRODH function in lung tumorigenesis, additional

cellular models in which PRODH expression is modulated by using an inducible promoter will be generated. These models could also be used for in vivo experiments in mice. Moreover, we aim to identify possible genetic modifiers of PRODH expression and/or function, starting with the most likely candidate, EGFR, taking into account the correlation that we found between PRODH expression and the presence of EGFR mutations in our samples.

REFERENCES

- Bender HU, Almashanu S, Steel G, Hu CA, Lin WW, Willis A, Pulver A, Valle D. Functional consequences of PRODH missense mutations. *Am J Hum Genet.* 2005 Mar;76(3):409-20.
- Chen Z, Fillmore CM, Hammerman PS, Kim CF, Wong KK. Non-small-cell lung cancers: a heterogeneous set of diseases. *Nat Rev Cancer.* 2014 Aug;14(8):535-46. doi: 10.1038/nrc3775. Erratum in: *Nat Rev Cancer.* 2015 Apr;15(4):247.
- Circu ML, Aw TY. Reactive oxygen species, cellular redox systems, and apoptosis. *Free Radic Biol Med.* 2010 Mar 15;48(6):749-62.
- Elia I, Broekaert D, Christen S, Boon R, Radaelli E, Orth MF, Verfaillie C, Grünewald TGP, Fendt SM. Proline metabolism supports metastasis formation and could be inhibited to selectively target metastasizing cancer cells. *Nat Commun.* 2017 May 11;8:15267.
- Gyórfy B, Surowiak P, Budczies J, Lánczky A. Online survival analysis software to assess the prognostic value of biomarkers using transcriptomic data in non-small-cell lung cancer. *PLoS One.* 2013 Dec 18;8(12):e82241.
- Jantus-Lewintre E, Usó M, Sanmartín E, Camps C. Update on biomarkers for the detection of lung cancer. *Lung Cancer (Auckl).* 2012 Jun 11;3:21-29.
- Liang X, Zhang L, Natarajan SK, Becker DF. Proline mechanisms of stress survival. *Antioxid Redox Signal.* 2013 Sep 20;19(9):998-1011.
- Liu Y, Borchert GL, Donald SP, Diwan BA, Anver M, Phang JM. Proline oxidase functions as a mitochondrial tumor suppressor in human cancers. *Cancer Res.* 2009 Aug 15;69(16):6414-22.
- Liu W, Le A, Hancock C, Lane AN, Dang CV, Fan TW, Phang JM. Reprogramming of proline and glutamine metabolism contributes to the proliferative and metabolic responses regulated by oncogenic transcription factor c-MYC. *Proc Natl Acad Sci U S A.* 2012 Jun 5;109(23):8983-8.

- Liu W, Phang JM. Proline dehydrogenase (oxidase), a mitochondrial tumor suppressor, and autophagy under the hypoxia microenvironment. *Autophagy*. 2012 Sep;8(9):1407-9.
- Liu W, Hancock CN, Fischer JW, Harman M, Phang JM. Proline biosynthesis augments tumor cell growth and aerobic glycolysis: involvement of pyridine nucleotides. *Sci Rep*. 2015 Nov 24;5:17206.
- Liu Y, Mao C, Wang M, Liu N, Ouyang L, Liu S, Tang H, Cao Y, Liu S, Wang X, Xiao D, Chen C, Shi Y, Yan Q, Tao Y. Cancer progression is mediated by proline catabolism in non-small cell lung cancer. *Oncogene*. 2020 Mar;39(11):2358-2376.
- Maxwell SA, Rivera A. Proline oxidase induces apoptosis in tumor cells, and its expression is frequently absent or reduced in renal carcinomas. *J Biol Chem*. 2003 Mar 14;278(11):9784-9.
- Monti P, Ciribilli Y, Bisio A, Foggetti G, Raimondi I, Campomenosi P, Menichini P, Fronza G, Inga A. Δ N-P63 α and TA-P63 α exhibit intrinsic differences in transactivation specificities that depend on distinct features of DNA target sites. *Oncotarget*. 2014 Apr 30;5(8):2116-30.
- Olivares O, Mayers JR, Gouirand V, Torrence ME, Gicquel T, Borge L, Lac S, Roques J, Lavaut MN, Berthezène P, Rubis M, Secq V, Garcia S, Moutardier V, Lombardo D, Iovanna JL, Tomasini R, Guillaumond F, Vander Heiden MG, Vasseur S. Collagen-derived proline promotes pancreatic ductal adenocarcinoma cell survival under nutrient limited conditions. *Nat Commun*. 2017 Jul 7;8:16031.
- Pandhare J, Cooper SK, Phang JM. Proline oxidase, a proapoptotic gene, is induced by troglitazone: evidence for both peroxisome proliferator-activated receptor gamma-dependent and -independent mechanisms. *J Biol Chem*. 2006 Jan 27;281(4):2044-52.

- Pandhare J, Donald SP, Cooper SK, Phang JM. Regulation and function of proline oxidase under nutrient stress. *J Cell Biochem.* 2009 Jul 1;107(4):759-68.
- Phang JM, Liu W, Zabirnyk O. Proline metabolism and microenvironmental stress. *Annu Rev Nutr.* 2010 Aug 21;30:441-63.
- Phang JM, Liu W, Hancock CN, Fischer JW. Proline metabolism and cancer: emerging links to glutamine and collagen. *Curr Opin Clin Nutr Metab Care.* 2015 Jan;18(1):71-7.
- Phang JM. Proline Metabolism in Cell Regulation and Cancer Biology: Recent Advances and Hypotheses. *Antioxid Redox Signal.* 2019 Feb 1;30(4):635-649.
- Polyak K, Xia Y, Zweier JL, Kinzler KW, Vogelstein B. A model for p53-induced apoptosis. *Nature.* 1997 Sep 18;389(6648):300-5.
- Possemato R, Marks KM, Shaul YD, Pacold ME, Kim D, Birsoy K, Sethumadhavan S, Woo HK, Jang HG, Jha AK, Chen WW, Barrett FG, Stransky N, Tsun ZY, Cowley GS, Barretina J, Kalaany NY, Hsu PP, Ottina K, Chan AM, Yuan B, Garraway LA, Root DE, Mino-Kenudson M, Brachtel EF, Driggers EM, Sabatini DM. Functional genomics reveal that the serine synthesis pathway is essential in breast cancer. *Nature.* 2011 Aug 18;476(7360):346-50.
- Raimondi I, Ciribilli Y, Monti P, Bisio A, Pollegioni L, Fronza G, Inga A, Campomenosi P. P53 family members modulate the expression of PRODH, but not PRODH2, via intronic p53 response elements. *PLoS One.* 2013 Jul 8;8(7):e69152.
- Siegel RL, Miller KD, Jemal A. Cancer statistics, 2019. *CA Cancer J Clin.* 2019 Jan;69(1):7-34.
- Tallarita E, Pollegioni L, Servi S, Molla G. Expression in *Escherichia coli* of the catalytic domain of human proline oxidase. *Protein Expr Purif.* 2012 Apr;82(2):345-51.

- Tang J, Hu M, Lee S, Roblin R. A polymerase chain reaction based method for detecting Mycoplasma/Acholeplasma contaminants in cell culture. *J Microbiol Methods*. 2000 Jan;39(2):121-6.
- Tołoczko-Iwaniuk N, Dziemiańczyk-Pakieła D, Celińska-Janowicz K, Zaręba I, Klupczyńska A, Kokot ZJ, Nowaszewska BK, Reszeć J, Borys J, Miltyk W. Proline-Dependent Induction of Apoptosis in Oral Squamous Cell Carcinoma (OSCC)-The Effect of Celecoxib. *Cancers (Basel)*. 2020 Jan 6;12(1):136
- Wang X, Xu Z, Tian Z, Zhang X, Xu D, Li Q, Zhang J, Wang T. The EF-1 α promoter maintains high-level transgene expression from episomal vectors in transfected CHO-K1 cells. *J Cell Mol Med*. 2017 Nov;21(11):3044-3054.
- Warburg O. On the origin of cancer cells. *Science*. 1956 Feb 24;123(3191):309-14.
- Yang M, Vousden KH. Serine and one-carbon metabolism in cancer. *Nat Rev Cancer*. 2016 Oct;16(10):650-62.
- Zareba I, Palka J. Prolidase-proline dehydrogenase/proline oxidase-collagen biosynthesis axis as a potential interface of apoptosis/autophagy. *Biofactors*. 2016 Jul 8;42(4):341-8.
- Zareba I, Surazynski A, Chrusciel M, Miltyk W, Doroszko M, Rahman N, Palka J. Functional Consequences of Intracellular Proline Levels Manipulation Affecting PRODH/POX-Dependent Pro-Apoptotic Pathways in a Novel in Vitro Cell Culture Model. *Cell Physiol Biochem*. 2017;43(2):670-684.
- Zareba I, Celinska-Janowicz K, Surazynski A, Miltyk W, Palka J. Proline oxidase silencing induces proline-dependent pro-survival pathways in MCF-7 cells. *Oncotarget*. 2018 Feb 9;9(17):13748-13757.
- AJCC Cancer Staging Manual, Seventh Edition 2010 American Joint Committee on Cancer.
- Travis WD, Brambilla E, Burke AP, Marx A, Nicholson AG. WHO Classification of Tumours of the lung, pleura, thymus and heart (4th edition), Lyon 2015.

AUTHOR CONTRIBUTION STATEMENTS

S.G. carried out the experiments and wrote the draft of the manuscript.

A.P. and R.C. contributed to cell maintenance, and preparation and transfection of the silencing construct.

A.M.C. and F.S. selected the cases for immunohistochemical analyses and contributed to the interpretation of the immunohistochemical results.

P.C. supervised the project.

2. TTF-1 contributes to transcriptional regulation of the *PRODH* gene, encoding proline dehydrogenase, in lung adenocarcinoma cells

Sarah Grossi, Arianna Parnigoni, Raffaella Cinquetti and Paola Campomenosi*

University of Insubria, Department of Biotechnology and Life Sciences, DBSV, Via J.H. Dunant 3, 21100 Varese, Italy;

* Correspondence: paola.campomenosi@uninsubria.it

Keywords

PRODH; Thyroid Transcription factor-1; Lung cancer; adenocarcinoma cell lines; gene expression.

ABSTRACT

Lung cancer is one of the most frequent and deadly cancers worldwide. It is a highly heterogeneous disease, comprising Small Cell Lung Cancer (SCLC) and Non-Small Cell Lung Cancer (NSCLC), which in turn is composed of two main histotypes, adenocarcinoma (ADC) and squamous cell carcinoma (SCC). Hence, identification of markers to improve diagnosis, prognosis and to guide therapeutic options for NSCLC is needed. Proline dehydrogenase (PRODH) is a mitochondrial inner-membrane and stress-inducible flavoenzyme catalyzing the first step in the proline degradation pathway, that is involved in the regulation of cell survival, autophagy and apoptosis. In line with these different biological functions, PRODH also showed different roles in tumorigenesis, as it behaves as a tumour suppressor in renal and colorectal cancer and as an oncogene, promoting invasion and metastatization, in breast and pancreatic cancer. In lung cancer, immunohistochemical analyses showed that PRODH is expressed in a high proportion of early stage lung ADCs but is rarely (SCC) or not expressed (SCLC) in other types of lung cancer. Expression decreases in high grade tumours and at high stages, suggesting it behaves as a differentiation marker. PRODH expression recapitulated expression of the main ADC marker, TTF-1, in normal lung tissues and in NSCLCs. Based on similar expression, involvement in the same tumours or genetic pathologies, and the presence of putative TTF-1 response elements in PRODH promoter, we hypothesized that the *PRODH* gene may be a transcriptional target of TTF-1.

Transfection of a TTF-1 expression construct into two lung ADC cell lines (A549 and NCI-H1299) led to an increase in PRODH transcript in both cell lines, suggesting that we may have identified a novel regulator of the PRODH gene. One of the predicted response element indeed was shown to be specifically activated by TTF-1. In conclusion, our data support a possible application of PRODH immunostaining as a marker to differentiate between lung ADC and SCC and opens up new research perspectives aimed to investigate the role of PRODH in NSCLC biology.

INTRODUCTION

Proline Dehydrogenase (PRODH) is the enzyme key to proline metabolism, that interconnects it with fundamental metabolic pathways, such as the tricarboxylic acid cycle or the urea cycle. Moreover, electrons derived from proline oxidation can be transferred from the FAD cofactor to the electron transport chain to produce ATP, favouring survival during nutrient stress. Alternatively, electrons are used to generate reactive oxygen species (ROS) that can regulate important processes, such as autophagy or apoptosis (Liang et al., 2013; Phang et al., 2015). Thus, PRODH has the potential to induce both cell survival and apoptosis. PRODH has been linked to several pathological conditions, such as type I hyperprolinemia, neuropsychiatric disorders (schizophrenia and schizoaffective disorders), epilepsy, mental retardation and cancer (Jacquet et al., 2002; Bender et al., 2005; Jacquet et al., 2005; Di Rosa et al., 2008; Mitsubuchi et al., 2008; Guilmatre et al., 2010; Clelland et al., 2011; Liu & Phang, 2012). PRODH expression and function has been studied in breast, renal, liver, colon, pancreas and stomach cancers (Maxwell and Rivera, 2003; Liu et al., 2012; Elia et al., 2017; Olivares et al., 2017; Liu et al., 2020) and, although initially described as a tumour suppressor, it is actually a dual role protein, capable on one side to suppress tumorigenesis by induction of apoptosis, but also to promote survival of cancer cells, invasion and metastatization (Maxwell et al., 2008; Liu et al., 2009; Liu and Phang, 2012; Raimondi et al., 2013; Monti et al., 2014).

Moreover, previous studies by Angulo et al. showed that PRODH is expressed in a subset of lung adenocarcinomas as part of a 13 gene signature that they suggested was due to EGFR mutations (Angulo et al., 2008). In our previous experiments, we confirmed that ADCs express PRODH and that expression correlates with the presence of EGFR mutations (Grossi et al., manuscript in preparation).

Indeed, immunohistochemical analyses on NSCLC and SCLC samples showed that the expression of PRODH is elevated in about 60% of adenocarcinomas (considering as positive tumours showing staining in more than 25% of tumour cells), whereas

expression is present in a significantly lower percentage of SCC cases, where staining is also less intense, and totally absent in SCLC. We also showed that in adenocarcinomas *PRODH* expression is elevated not only at the protein level but also at the transcript level, suggesting a transcriptional or post-transcriptional regulation.

Furthermore, in normal lung tissue, used as a control, *PRODH* is expressed in type II pneumocytes and Clara cells, that are considered the cells of origin of ADC (Chen et al., 2014). The expression pattern overlaps quite well with that of TTF-1, which is expressed in the same *PRODH* positive cells in normal lung tissue and is a marker of lung adenocarcinoma.

TTF-1 (Thyroid Transcription factor-1), also known as Nkx2.1 or T/EBP (thyroid-specific-enhancer-binding protein), is a homeodomain-containing transcription factor, involved in the development and differentiation of the lung, thyroid and part of the brain (Bingle, 1997; Boggaram, 2009). In the lung it is expressed in particular in Clara cells and type II pneumocytes, where it transcriptionally regulates the expression of target genes, including those encoding for surfactant proteins and proteins involved in cell adhesion, such as occludin and claudins (Runkle et al., 2012). It is used as a molecular marker for adenocarcinomas, aiding differential diagnosis. Unfortunately, TTF-1 cannot be used as a target for therapy of such tumours, as its function is also essential for normal lung physiology.

The observations described above led us to hypothesize that there could be a correlation between *PRODH* and TTF-1 expression. In particular, we aimed to test the hypothesis that TTF-1 could transcriptionally regulate *PRODH* gene expression.

MATERIALS AND METHODS

Cell culture

A549 and NCI-H1299 human lung adenocarcinoma cell lines were used in this work. Cells were maintained in RPMI 1640 supplemented with 10% FBS and 1% glutamine. All cell culture media and supplements were from CARLO ERBA Reagents (Milan, Italy).

Cultures were incubated at 37°C in 95% humidity and 5% CO₂ atmosphere. At confluence, cells were detached from culture flasks by trypsinisation. A new batch of frozen cells was thawed on average 1-2 weeks before each experiment to have sufficient numbers of cells.

To evaluate the presence of mycoplasma, cells were routinely checked by using the nested PCR method described in Tang et al. (Tang et al., 2000).

For transient transfections, $1,8 \times 10^5$ cells were seeded in a 6-well multiwell plate, to be 70% confluent on the following day, when transfection was performed using 2 µg of DNA/well and Fugene HD transfection Reagent (Promega, Milan, Italy), according to manufacturer's instructions. A pRcCMV construct carrying the wild-type TTF1 coding sequence and pcDNA3.1 empty vector as control condition were transfected into cells. 48 hours later, cells were collected for total RNA extraction and preparation of cells lysates.

Immunoblotting

Cell lysates were obtained after manual scraping of cells from cell culture vessels using PBS. Cells were counted and, after centrifugation, they were resuspended in Laemmli Sample Buffer 2X (125 mM Tris-HCl, 4% SDS, 20% glycerol, 10% β-mercaptoethanol, 2mM EDTA, pH 6.8), using 1 µl every 2×10^4 cells. The samples were lysed by incubation at 95°C for 3 min followed by vortexing, repeating these

steps for three times and stored at -80°C until use. For SDS-PAGE 17 µl of cell lysate were used.

Proteins were transferred onto a nitrocellulose membrane (Amersham Hybond ECL, GE Healthcare Life Sciences, by Euroclone, Milan, Italy) using the Mini-PROTEAN Tetra System (Biorad, Milan, Italy); after blocking in 4% non-fat milk in PBS-T (0.1% Tween20 in PBS) and incubation with the appropriate primary and secondary antibodies, signals were detected with the Amersham ECL Prime Western Blotting Detection Reagent (GE Healthcare Life Sciences by Euroclone, Milan, Italy), using an Odyssey LI-COR FC imaging system (Carlo Erba Reagents, Milan, Italy).

Primary antibodies were a mouse monoclonal antibody against Anti-TTF-1, clone 8G7G3/1 (790-4398, Roche diagnostics, Monza, Italy, working dilution 1:10) and a mouse monoclonal antibody against α -tubulin, clone B-5-1-2 (T6074, Merck, Milan, Italy, working dilution 1:8000) for normalization. Stabilized HRP-conjugated goat anti-mouse Ig was used as secondary antibody (1:900, ThermoFisher Scientific, Milan, Italy). Antibodies were diluted in 2% non-fat milk in PBS-T.

RNA extraction and gene expression

Total RNA was extracted from cells using TriReagent (Sigma-Aldrich, Milan, Italy) according to manufacturer's instructions. RNA samples were quantified with a NanoDrop 2000c (ThermoFisher, Life Technologies Italia, Milan, Italy) and run on an agarose gel for quality control.

For real-time quantitative PCR (qPCR), cDNA was obtained from 500 ng of RNA by using the iScript cDNA synthesis kit (Biorad, Milan, Italy). Gene expression analysis was performed in triplicate using a CFX96 thermal cycler (Biorad, Milan, Italy) and the iTAQ Universal Sybr Green Supermix (Biorad, Milan, Italy), using primer pairs specific for *PRODH* (forward primer: 5'-GCAGAGACAAGGAGATGGA-3'; reverse primer: 5'-TGGTATTGCTTGTCCTCCGCTT-3'), *SpB* (forward primer: 5'-GGCCTCACACACAGGATCTC-3'; reverse primer: 5'-CTAGCGCACCTTGGGAAT-3'),

OCIN (forward primer: 5'-ACATTTATGATGAGCAGCCCC-3'; reverse primer: 5'-GTGAAGGCACGTCCTGTGT-3'), *CLDN1* (forward primer: 5'-CCAGTCAATGCCAGGTACGA-3'; reverse primer: 5'-CAAAGTAGGGCACCTCCCAG-3') and *B2M* (forward primer: 5'-AGGCTATCCAGCGTACTCCA-3'; reverse primer: 5'-ATGGATGAAACCCAGACACA-3'). Relative mRNA quantification was obtained by applying the $2^{-\Delta\Delta Cq}$ method, using *B2M* as reference gene, to normalize data (Livak and Schmittgen, 2001).

Melting curve analysis was performed to ensure that single amplicons were obtained for each target.

Plasmid constructs

pRCCMV-TTF1 construct was obtained from Dr. Stefania Guazzi (IIT, Genova) (Zannini et al., 1996); pGL4.26 vector was obtained from the laboratory of Prof. Alberto Inga (University of Trento). pCDNA3.1 vector was already available in the laboratory and was used as a control, because it shares the same characteristics as the pRC-CMV-TTF1 construct.

pGL4.26 was used to clone the sequences of four putative TTF-1 response elements (named RE1, RE2, RE3 and RE4) identified with the rVISTA software in the *PRODH* genomic region encompassing -5000 bp and +1000 bp with respect to the Transcriptional Start Site [numbering is based on alignment of RefSeq NM_016335 on the hg38 genomic assembly in the Blat search engine (<https://genome.ucsc.edu/cgi-bin/hgBlat>)]. The same plasmid was also used to clone the mutagenized sequence of RE1.

Primers were ordered from Metabion International AG (CARLO ERBA Reagents, Milan, Italy). To facilitate cloning, the sequences recognized by specific restriction enzymes and additional nucleotides to obtain a high cutting efficiency were added to the oligonucleotides. Oligonucleotide sequences are shown in Table 1.

Table 1: Characteristics of the synthetic oligonucleotides used for cloning of the single REs in pGL4.26. The sequences of the individual REs are shown in bold and underlined. Restriction sites are indicated in blue (*Xho*I), red (*Bgl*III) and green (*Nde*I).

Name	nt	SEQUENCE (5' → 3')	T _m (°C)
RE1 fw	74	TCCG <u>CTCGAGCATATG</u> GCAGTTTTGTGTCCCTG <u>GGTACTTGA</u> <u>GATT</u> AGGGAGTGGTGATGACT <u>AGATCT</u> TCCA	89
RE1 rv	74	TGGA <u>AGATCT</u> AGTCATCACCCTCCCTA <u>ATCTCAAGTACC</u> CAG GGACACAAA <u>AACTGC</u> <u>CATATGCTCGAG</u> CGGA	89
RE2 fw	80	TCCG <u>CTCGAGCATATG</u> GTCCAGCCTGTAGTCCCAG <u>GCTACTTGG</u> <u>GAG</u> TTGAGGCAGGGGATCACTTGAG <u>AGATCT</u> TCCA	92
RE2 rv	80	TGGA <u>AGATCT</u> CTCAAGTATCCCCTGCCTCAAC <u>CTCCCAAGTA</u> <u>GCT</u> TGGGACTACAGGCTGGAC <u>CATATGCTCGAG</u> CGGA	92
RE3 fw	74	TCCG <u>CTCGAGCATATG</u> TTTCAGGCCAGCCTTGTT <u>CCCACAGGT</u> <u>GCC</u> CTCACAGGTGGGCTCTCC <u>AGATCT</u> TCCA	92
RE3 rv	74	TGGA <u>AGATCT</u> GGAGAGCCCACCTGTGAG <u>GGCACCTGTGGG</u> AA CAAGGCTGGCCTGAAA <u>CATATGCTCGAG</u> CGGA	92
RE4 fw	74	TCCG <u>CTCGAGCATATG</u> TTCATATTTACGATATAT <u>ACCACTTGTG</u> <u>GGA</u> AATACAGAGTTATCACTT <u>AGATCT</u> TCCA	84
RE4 rv	74	TGGA <u>AGATCT</u> AAGTGATAACTCTGTATT <u>CCCACAAGTGGT</u> ATA TATCGTAAATATGAA <u>CATATGCTCGAG</u> CGGA	84
RE1mut fw	74	TCCG <u>CTCGAGCATATG</u> GCAGTTTTGTGTCCCTG <u>GTTAACTCAT</u> <u>ATT</u> AGGGAGTGGTGATGACT <u>AGATCT</u> TCCA	87
RE1mut rv	74	TGGA <u>AGATCT</u> AGTCATCACCCTCCCTA <u>ATATGAGTTAAC</u> CAG GGACACAAA <u>AACTGC</u> <u>CATATGCTCGAG</u> CGGA	87

5 µl of forward and 5 µl of reverse primers (all resuspended at 100 µM final concentration) were mixed with 2X Annealing Buffer (20 mM Tris-HCl, 100 mM NaCl, 2 mM EDTA, pH 8.0) and the reactions were incubated into a T100 Thermal Cycler (Biorad, Milan Italy) at 95 °C for 5 min, followed by a gradual decrease of the temperature of 1 °C/cycle for 1 minute, until 20°C were reached and a final hold at 4 °C.

The double stranded DNAs were then digested with *Xho*I and *Bgl*III and cloned into the pGL4.26 vector. The presence of the insert in the vector was verified through digestion with *Nde*I. The constructs were sequenced to verify the absence of undesired mutations (GATC-Biotech, Germany).

Luciferase assays

For each cell line, 3×10^4 cells were seeded in a 24-well multiwell plate. The following day, transfection was performed with Fugene HD transfection Reagent (Promega, Milan, Italy), according to manufacturer's instructions. Each well was transfected with either 480 ng of the pRcCMV-TTF1 construct or 370 ng of the control pcDNA3.1 empty vector, 400 ng of one of the pGL4.26 constructs containing the single REs or empty vector, 260 ng of the pRL-SV40 plasmid harbouring the luciferase gene from *Renilla reniformis* controlled by a constitutive promoter, for normalisation purposes (Promega, Milan, Italy). 48 hours after transfection, cell cultures were harvested and luciferase activity was measured using the Dual-Luciferase Reporter Assay System (Promega, Milan, Italy) according to manufacturer's protocol. Chemiluminescence was measured with an Infinite F200 microplate reader (Tecan, Cernusco sul Naviglio, Italy), then, for each sample, firefly luciferase activity was normalized with *Renilla* luciferase activity.

Statistical Analysis

Data from gene expression analyses following transfection of the TTF-1 expressing construct or empty vector in the cell lines under study were compared using t-test (GraphPad Prism statistical software program 4.02 version); five independent experiments were done for each cell line. Data from four independent luciferase assay experiments were compared using analysis of variance (ANOVA) with post hoc Dunnett's test (Statistica data analysis and visualization program, version 8.0).

RESULTS

To investigate whether the TTF-1 transcription factor regulates PRODH expression, we performed transient transfection of A549 and NCI-H1299 cells with a TTF-1 expression construct and with empty vector as the control condition. After 48 hours, we observed a strong increase in TTF-1 protein expression, compared to cells transfected with empty vector (Figure 1A), by immunoblotting, that was paralleled by a small but significant ($p=0,0047$) 2,2 fold increase in PRODH transcript A549 cells and a 11,5 fold increase in NCI-H1299 transfected with pRcCMV-TTF-1, compared to control condition (Figure 1B), evaluated by qPCR. The increase in PRODH transcript in the A549 cell line was similar to the fold induction observed for two known TTF-1 target genes, namely occludin (*OCLN*, 1,764 fold, $p = 0.050$) and claudin 1 (*CLDN1*, 2,052 fold, $p = 0.0109$); in the NCI-H1299 we did not observe a significant induction of the two positive control genes (Figure 1B). However, analysis of *SFTPB*, another well known TTF-1 target gene encoding Surfactant protein B (SpB), was induced in both cell lines transfected with the TTF-1 expression construct (1700 fold in A549 cells, $p = 0.0003$; 50 fold in NCI-H1299, $p = 0.0001$) (Figure 1B).

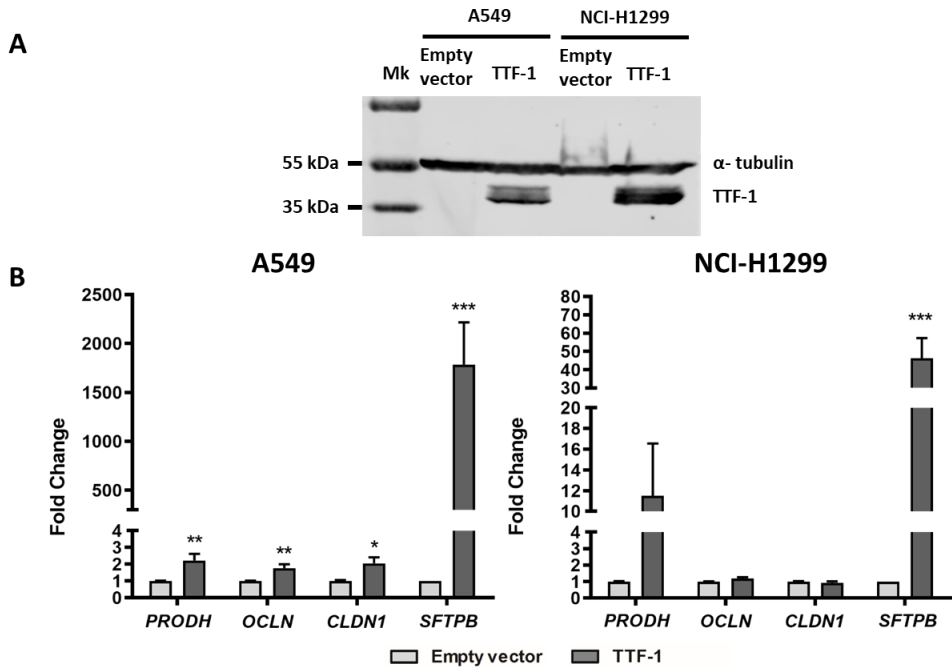


Figure 1. Transient transfection of a TTF-1 expression construct in the A549 and NCI-H1299 cell lines leads to an increase in *PRODHD* expression. **A.** Immunoblotting of TTF-1 and α -Tubulin on cell lysates obtained 48 hours after transfection with pcDNA3.1 and pRcCMV-TTF-1. Mk, Protein Ladder (ThermoFisher Scientific, Milan, Italy). **B.** Graph reporting the mean of qPCR results obtained in 5 experiments for each cell line. The constructs used for transfection are shown along the x axis, while the fold change of *PRODHD*, *OCLN*, *CLDN1* or *SFTPB* expression in cells transfected with the TTF-1 expressing construct compared to empty vector is shown in the y axis. Bars represent the standard error. * $p < 0.05$; ** $p < 0.01$; *** $p < 0.001$ (Student's *t*-test).

We looked for putative TTF-1 binding sites in the *PRODHD* gene. A genomic region encompassing -5000 to +1000 bp (from the transcriptional start site of the *PRODHD* gene) was subjected to bioinformatic analysis with the program "Regulatory Vista" (<http://genome.lbl.gov/vista/rvista/submit.shtml>). Four putative TTF-1 "Response Elements" (RE) were identified in the *PRODHD* gene between 2400 bp upstream and 1000 bp downstream of the transcriptional start site (Figure 2).

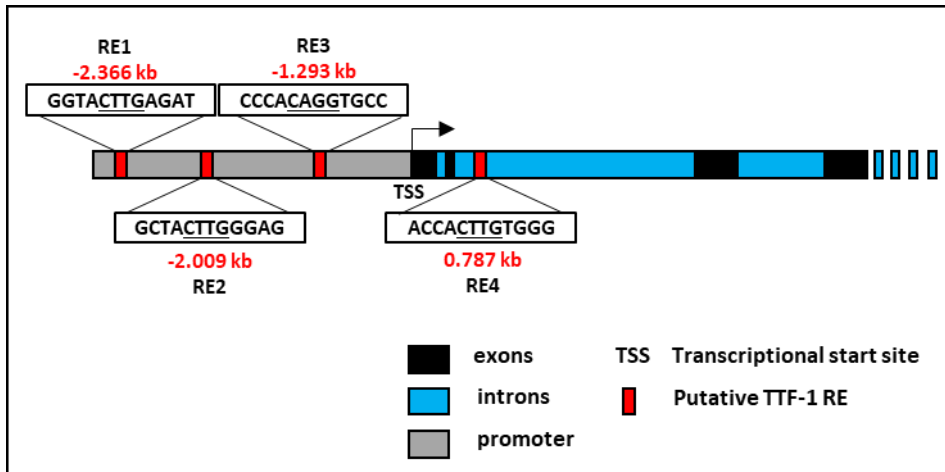


Figure 2. Position and sequence of the four TTF-1 putative “Response Elements”, bioinformatically identified by *rVISTA* in the *PROD H* gene. The numbering refers to their position respect to the transcriptional start site (TSS).

Luciferase assays were used to verify whether these sites are indeed TTF1 responsive sequences. A549 and NCI-H1299 cell lines were transiently co-transfected with pRcCMV-TTF-1 or pcDNA3 as control, pGL4.26 vector or one of the constructs carrying the 4 different Response Elements and finally pRL-SV40, for normalization. Four independent experiments were performed for each cell line. In both cell lines, only the pGL4.26 construct containing the RE1 determined a significant increase in luciferase activity when co-transfected with TTF-1 expressing construct but not with empty vector (A549, $p=0.00002$; NCI-H1299, $p=0.0447$; Anova test) (Figure 3). These results suggest that TTF-1 can bind this sequence and transactivate it.

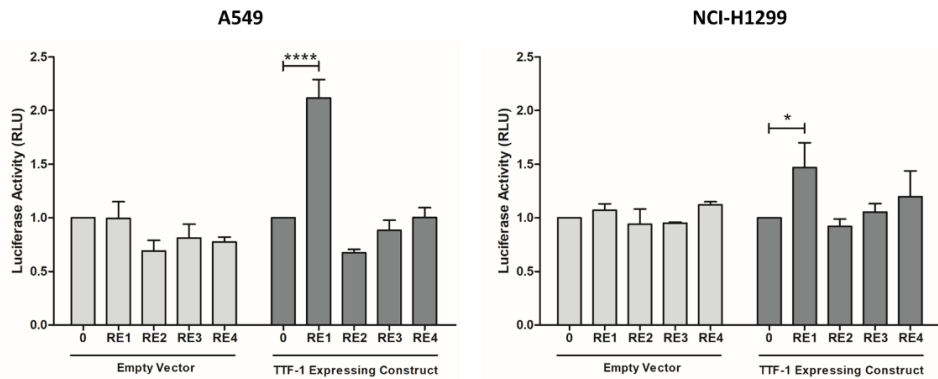


Figure 3: Luciferase assays show transactivation from RE1 in presence of TTF-1. Graphs representing the mean and standard error of the 4 Luciferase assay experiments performed on the A549 and NCI-H1299 cell lines. The analysed REs are indicated along the X axis, while the Y axis shows the luciferase activity in the presence of the various REs (Luciferase Activity, Relative Lights Units). The values obtained in presence of pcDNA3 vector (control) and those in presence of the TTF-1 expression construct (pRcCMV-TTF-1) are shown in light and dark grey, respectively. Asterisks on RE1 with pRcCMV-TTF-1 indicate that the difference in activity is significant compared to controls, * $p < 0.05$; **** $p < 0.0001$ (Anova, Dunnett's test).

To confirm that the increase in *PRODH* expression was due to binding of TTF-1 to RE1 sequence, the sequence of Response Element 1 was modified. The bases to be mutagenized were selected by comparison of RE1 with the consensus sequence published in a work by Guazzi et al., obtained from alignment of 8 sequences from thyroid specific TTF-1 responsive genes (Guazzi et al., 1990). We also compared the sequences of the three response elements identified bioinformatically in the *PRODH* gene but not confirmed in luciferase assays.

The four bases of the CTTG core (positions 5-8) were always present, except the so called RE3. For this reason, 3 of the 4 core bases, as well as 2 further bases which were considered important for binding (position 2, not described in Guazzi et al, that was unique to RE1, and position 10 that is a G in all sequences including the consensus), were mutagenized. The RE1 mutated sequence (RE1mut) is shown in Table 2.

Table 2: Comparison of putative response elements for TTF-1 identified in the *PRODH* gene and the consensus sequence published in the work by Guazzi et al. (Guazzi et al., 1990). The subscript numbers in the Guazzi sequence indicate the frequency at which those specific bases were found in the 8 aligned sequences in their work. The conserved core in the sequence is highlighted in red. The bases that were mutagenized in RE1 are underlined. The final sequence of the mutated RE1 (RE1 mut) is represented in blue.

RE	Putative Response Elements sequences														
	1	2	3	4	5	6	7	8	9	10	11	12	13	14	15
Guazzi et al					C ₇	T ₆	T ₆	G ₈	A ₇	G ₇	T ₈	G ₆	N	N	C ₆
PRODH-RE1	G	<u>G</u>	T	A	<u>C</u>	<u>I</u>	<u>T</u>	<u>G</u>	A	<u>G</u>	A	T			G
PRODH-RE2	G	C	T	A	C	T	T	G	G	G	A	G			T
PRODH-RE3	C	C	C	A	C	A	G	G	T	G	C	C			C
PRODH-RE4	A	C	C	A	C	T	T	G	T	G	G	G			T
PRODH-RE1mut	G	<u>I</u>	T	A	<u>A</u>	<u>C</u>	T	<u>C</u>	A	<u>I</u>	A	T			G

The RE1mut sequence was cloned into pGL4.26 and used for luciferase assays, comparing the luciferase activity from this construct and from empty pLG4.26 to that of wild-type RE1.

Luciferase activity in presence of the RE1mut construct was reduced respect to the wild-type RE1 sequence in both cell lines, with values comparable to those obtained with the empty vector (Figure 4). The data suggest that RE1 is effectively bound by TTF-1 and is responsible for the induction observed when the transcription factor is ectopically expressed in adenocarcinoma cell lines.

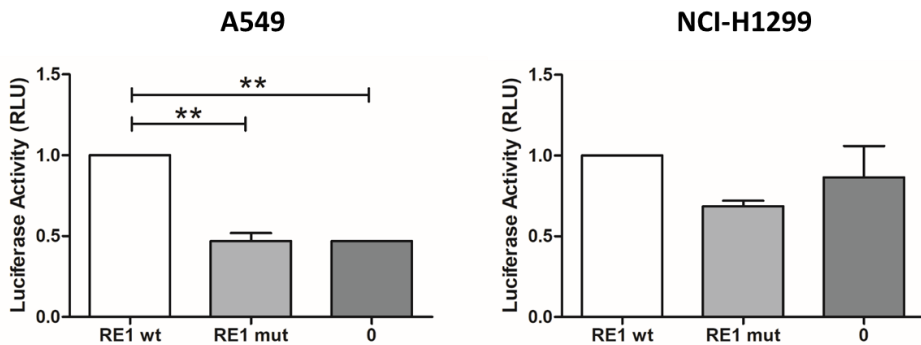


Figure 4: Graph representing the results of luciferase assays performed in A549 and NCI-H1299 cell lines using RE1 wt or RE1 mut sequences in pGL4.26 constructs or empty vector (0), co-transfected with the TTF-1 expression construct and pRL-SV40 for normalisation. The mean and standard error of two experiments are shown. The different constructs expressing Firefly luciferase are shown along the x axis, while in the Y axis the activity of the various constructs related to the activity obtained by the wild-type RE1 construct, after normalization with Renilla luciferase, is reported. ** indicate significant difference, with $p < 0.01$ (Anova, Dunnett's test).

DISCUSSION

Lung cancer is one of the most common types of cancer and the leading cause of cancer-related mortality worldwide. Therefore, to improve diagnosis, prognosis and therapy it is key to understand its biology and to identify novel players in lung tumorigenesis.

In a recent work, we showed that proline dehydrogenase (PRODH) is expressed in the adenocarcinoma subtype of lung cancer, where it appears to be a favourable prognostic factor. In lung adenocarcinoma cell lines its expression influences survival, invasion and the ability to grow in soft agar (Grossi et al., manuscript in preparation). Although we show that PRODH is expressed in lung adenocarcinomas, especially at an early stage and at low grade, neither the factors that control its expression, nor its physiological significance in normal lung cells -type II

pneumocytes and Clara cells – and in the deriving tumours is known (Grossi et al., manuscript in preparation; Angulo et al., 2008).

We were intrigued by the fact that the expression pattern and the effects of *PRODH* in adenocarcinoma cells recapitulate the behaviour of the TTF-1 homeodomain containing and lineage-specific transcription factor, which is a well known marker of lung ADC (Boggaram. 2009; Mu, 2013; Yamaguchi et al., 2013). Its dual role as tumour suppressor or oncogene can be modulated by different factors, including p53 status (Chen et al., 2015) and interaction with other transcription factors (Isogaya et al., 2014).

TTF-1 has clinical application as a marker for the diagnosis of adenocarcinomas, where its expression is detected in 85-90% of cases. This specificity is very important because it allows to identify the origin of metastases when the primary tumour has not been identified (Ordóñez, 2000; Zamecnik and Kodet 2002; Moldvay et al., 2004). Although TTF-1 is an excellent marker for differential diagnosis, it cannot be used as a molecular target for the treatment of this pathology as it performs fundamental functions for the normal physiology of the lung and thyroid.

Several TTF-1 targets have been identified, suggesting its involvement in different biological processes, including cell-cell communication and adhesion, cell survival and invasion, among others (Hosono et al., 2012; Runkle et al., 2012; Yamaguchi et al., 2012). In this work we explored the possible transcriptional regulation of the *PRODH* gene expression by TTF-1. We show that ectopic expression of TTF-1 led to an increase in *PRODH* transcript. RE1, one of the putative response elements identified in *PRODH* regulatory regions by the rVista prediction program, induced an increase of luciferase activity when co-transfected with the TTF-1 expressing construct in the A549 and the NCI-H1299 lung adenocarcinoma cell lines. The presence of RE1 and TTF-1 together significantly increased luciferase activity by a factor of 2.5 in A549 cells ($p = 0.0047$, Anova test) while in the NCI-H1299, a small increase (1.5 fold) was observed compared to cells transfected with empty vector. The other Response Elements determined luciferase activity comparable to the

empty vector, demonstrating that they are not functional. Of note, RE1, located 2366 bp upstream of the Transcriptional Start Site in the human gene, is the only one preserved between man and mouse both in sequence and position.

Although the induction factor is not high, it is similar to that of other TTF-1 targets, such as Claudin-1 (Runkle et al., 2012 and our results). It must be underlined that there is no complete agreement on the actual consensus sequence recognised by TTF-1, compared with other transcriptional factors, such as p53. The two wild-type REs described in the work by Runkle et al for occludin and claudin-1 genes (Runkle et al., 2012) show almost no sequence conservation compared to the REs reported for eight genes in the work by Guazzi et al., 1990. The consensus sequence reported by Guazzi et al. is the one used by the rVISTA program.

In support of a direct binding of *PRODH* RE1 by TTF-1, RE1 mutagenesis led to a reduction in luciferase activity to the levels found when the empty pGL4.26 vector was used. The RE1 sequence was mutagenized in four different positions to differentiate it from the wild-type sequence; in particular, three bases were changed in the core and another base at position 10 (Table 2 in the Results), all considered important for binding to the TTF-1 transcription factor.

TTF-1 can play a double-edged role in cancer (Yamaguchi et al., 2013): on one hand it can play a suppressive role by reducing invasion and metastasis, on the other hand, it can play an oncogenic role, for example by enhancing *EGFR*-driven lung tumorigenesis (Maeda et al., 2012; Yamaguchi et al., 2013).

Evidence suggests that the double role of TTF-1 in lung tumorigenesis may be influenced by interaction with other genetic factors. In particular, p53 status influences TTF-1 induced outcome during lung tumorigenesis (Chen et al., 2015). This is of particular importance considering that *PRODH* is also a target of the p53 family (Raimondi et al., 2013; Monti et al., 2014). Other factors influencing TTF-1 function include the transcription factor Foxp2, which interacts with TTF-1 and provokes its dissociation from DNA and down-regulation of Surfactant Protein C (SP-C) (Zhou et al., 2008), Forkhead Box A2 (FOXA2; Minoo et al., 2007), retinoic acid

receptors (RAR; Yan et al., 2001), GATA6, a member of the GATA family of zinc finger domain containing transcription factors (Liu et al., 2002) and Signal transducer and activator of transcription 3 (STAT3; Yan et al., 2002). The latter is also involved in EGFR signal transduction pathway, thus representing another possible modifier of PRODH expression and function in lung adenocarcinomas. Moreover, the receptor-regulated Smad proteins (Smad2 and Smad3) negatively modulate the transcriptional activity of TTF-1 (Li et al., 2002; Isogaya et al., 2014), whereas the transcriptional co-activator with PDZ-binding motif (TAZ) modulates TTF-1 in positive manner (Park et al., 2004).

This would explain why PRODH, as well as other TTF-1 targets, are expressed at different levels in different cell lines. For these reasons, further experiments are needed in order to define the cofactor(s) that cooperate with TTF-1 to regulate the expression of PRODH in lung adenocarcinoma cell lines.

A limitation of this study is that we investigated the transcriptional control exerted on PRODH expression only following transfection of a TTF-1 encoding construct. TTF-1 activity is induced by glucocorticoids -such as dexamethasone- and cAMP treatment (Li et al., 1998; Gonzales et al., 2002; Kolla et al., 2007). Interestingly, glucocorticoid response elements are also present in the *PRODH* gene, suggesting that PRODH upregulation by glucocorticoids may occur both directly and indirectly, through TTF-1 (Sasse et al., 2015).

In conclusion, our data suggest that PRODH is a favourable prognostic factor in lung adenocarcinoma and its expression is at least partially controlled by TTF-1, one of the most important transcription factor and markers of adenocarcinoma. It will be important to collect as much information as possible about PRODH regulation and biological functions to be able to understand how it could be exploited as a marker and if in some instances it could also be used for targeted therapy.

REFERENCES

- Angulo B, Suarez-Gauthier A, Lopez-Rios F, Medina PP, Conde E, Tang M, Soler G, Lopez-Encuentra A, Cigudosa JC, Sanchez-Cespedes M. Expression signatures in lung cancer reveal a profile for EGFR-mutant tumours and identify selective PIK3CA overexpression by gene amplification. *J Pathol.* 2008 Feb;214(3):347-56.
- Bender HU, Almashanu S, Steel G, Hu CA, Lin WW, Willis A, Pulver A, Valle D. Functional consequences of PRODH missense mutations. *Am J Hum Genet.* 2005 Mar;76(3):409-20.
- Bingle CD. Thyroid transcription factor-1. *Int J Biochem Cell Biol.* 1997 Dec;29(12):1471-3. doi: 10.1016/s1357-2725(97)00007-1. PMID: 9570141.
- Boggaram V. Thyroid transcription factor-1 (TTF-1/Nkx2.1/TITF1) gene regulation in the lung. *Clin Sci (Lond).* 2009 Jan;116(1):27-35.
- Chen Z, Fillmore CM, Hammerman PS, Kim CF, Wong KK. Non-small-cell lung cancers: a heterogeneous set of diseases. *Nat Rev Cancer.* 2014 Aug;14(8):535-46.
- Chen PM, Wu TC, Cheng YW, Chen CY, Lee H. NKX2-1-mediated p53 expression modulates lung adenocarcinoma progression via modulating IKK β /NF- κ B activation. *Oncotarget.* 2015 Jun 10;6(16):14274-89.
- Clelland CL, Read LL, Baraldi AN, Bart CP, Pappas CA, Panek LJ, Nadrich RH, Clelland JD. Evidence for association of hyperprolinemia with schizophrenia and a measure of clinical outcome. *Schizophr Res.* 2011 Sep;131(1-3):139-45.
- Di Rosa G, Pustorino G, Spano M, Campion D, Calabrò M, Aguenouz M, Caccamo D, Legallic S, Sgro DL, Bonsignore M, Tortorella G. Type I hyperprolinemia and proline dehydrogenase (PRODH) mutations in four Italian children with epilepsy and mental retardation. *Psychiatr Genet.* 2008 Feb;18(1):40-2.
- Elia I, Broekaert D, Christen S, Boon R, Radaelli E, Orth MF, Verfaillie C, Grünewald TGP, Fendt SM. Proline metabolism supports metastasis formation

and could be inhibited to selectively target metastasizing cancer cells. *Nat Commun.* 2017 May 11;8:15267.

- Gonzales LW, Guttentag SH, Wade KC, Postle AD, Ballard PL. Differentiation of human pulmonary type II cells in vitro by glucocorticoid plus cAMP. *Am J Physiol Lung Cell Mol Physiol.* 2002 Nov;283(5):L940-51.
- Guazzi S, Price M, De Felice M, Damante G, Mattei MG, Di Lauro R. Thyroid nuclear factor 1 (TTF-1) contains a homeodomain and displays a novel DNA binding specificity. *EMBO J.* 1990 Nov;9(11):3631-9.
- Guilmatre A, Legallic S, Steel G, Willis A, Di Rosa G, Goldenberg A, Drouin-Garraud V, Guet A, Mignot C, Des Portes V, Valayannopoulos V, Van Maldergem L, Hoffman JD, Izzi C, Espil-Taris C, Orcesi S, Bonafé L, Le Galloudec E, Maurey H, Ioos C, Afenjar A, Blanchet P, Echenne B, Roubertie A, Frebourg T, Valle D, Champion D. Type I hyperprolinemia: genotype/phenotype correlations. *Hum Mutat.* 2010 Aug;31(8):961-5.
- Hosono Y, Yamaguchi T, Mizutani E, Yanagisawa K, Arima C, Tomida S, Shimada Y, Hiraoka M, Kato S, Yokoi K, Suzuki M, Takahashi T. MYBPH, a transcriptional target of TTF-1, inhibits ROCK1, and reduces cell motility and metastasis. *EMBO J.* 2012 Jan 18;31(2):481-93.
- Isogaya K, Koinuma D, Tsutsumi S, Saito RA, Miyazawa K, Aburatani H, Miyazono K. A Smad3 and TTF-1/NKX2-1 complex regulates Smad4-independent gene expression. *Cell Res.* 2014 Aug;24(8):994-1008.
- Jacquet H, Raux G, Thibaut F, Hecketsweiler B, Houy E, Demilly C, Haouzir S, Allio G, Fouldrin G, Drouin V, Bou J, Petit M, Champion D, Frébourg T. PRODH mutations and hyperprolinemia in a subset of schizophrenic patients. *Hum Mol Genet.* 2002 Sep 15;11(19):2243-9.
- Jacquet H, Demily C, Houy E, Hecketsweiler B, Bou J, Raux G, Lerond J, Allio G, Haouzir S, Tillaux A, Bellegou C, Fouldrin G, Delamillieure P, Ménard JF, Dollfus

- S, D'Amato T, Petit M, Thibaut F, Frébourg T, Campion D. Hyperprolinemia is a risk factor for schizoaffective disorder. *Mol Psychiatry*. 2005 May;10(5):479-85.
- Kolla V, Gonzales LW, Gonzales J, Wang P, Angampalli S, Feinstein SI, Ballard PL. Thyroid transcription factor in differentiating type II cells: regulation, isoforms, and target genes. *Am J Respir Cell Mol Biol*. 2007 Feb;36(2):213-25.
 - Li J, Gao E, Mendelson CR. Cyclic AMP-responsive expression of the surfactant protein-A gene is mediated by increased DNA binding and transcriptional activity of thyroid transcription factor-1. *J Biol Chem*. 1998 Feb 20;273(8):4592-600.
 - Li C, Zhu NL, Tan RC, Ballard PL, Derynck R, Mino P. Transforming growth factor-beta inhibits pulmonary surfactant protein B gene transcription through SMAD3 interactions with NKX2.1 and HNF-3 transcription factors. *J Biol Chem*. 2002 Oct 11;277(41):38399-408.
 - Liang X, Zhang L, Natarajan SK, Becker DF. Proline mechanisms of stress survival. *Antioxid Redox Signal*. 2013 Sep 20;19(9):998-1011.
 - Liu C, Glasser SW, Wan H, Whitsett JA. GATA-6 and thyroid transcription factor-1 directly interact and regulate surfactant protein-C gene expression. *J Biol Chem*. 2002 Feb 8;277(6):4519-25.
 - Liu C, Glasser SW, Wan H, Whitsett JA. GATA-6 and thyroid transcription factor-1 directly interact and regulate surfactant protein-C gene expression. *J Biol Chem*. 2002 Feb 8;277(6):4519-25.
 - Liu Y, Borchert GL, Donald SP, Diwan BA, Anver M, Phang JM. Proline oxidase functions as a mitochondrial tumor suppressor in human cancers. *Cancer Res*. 2009 Aug 15;69(16):6414-22.
 - Liu W, Phang JM. Proline dehydrogenase (oxidase) in cancer. *Biofactors*. 2012 Nov-Dec;38(6):398-406.
 - Liu Y, Mao C, Wang M, Liu N, Ouyang L, Liu S, Tang H, Cao Y, Liu S, Wang X, Xiao D, Chen C, Shi Y, Yan Q, Tao Y. Cancer progression is mediated by proline

catabolism in non-small cell lung cancer. *Oncogene*. 2020 Mar;39(11):2358-2376. Maeda Y, Tsuchiya T, Hao H, Tompkins DH, Xu Y, Mucenski ML, Du L, Keiser AR, Fukazawa T, Naomoto Y, Nagayasu T, Whitsett JA. Kras(G12D) and Nkx2-1 haploinsufficiency induce mucinous adenocarcinoma of the lung. *J Clin Invest*. 2012 Dec;122(12):4388-400.

- Liu Y, Mao C, Wang M, Liu N, Ouyang L, Liu S, Tang H, Cao Y, Liu S, Wang X, Xiao D, Chen C, Shi Y, Yan Q, Tao Y. Cancer progression is mediated by proline catabolism in non-small cell lung cancer. *Oncogene*. 2020 Mar;39(11):2358-2376.
- Livak KJ, Schmittgen TD. Analysis of relative gene expression data using real-time quantitative PCR and the $2^{-\Delta\Delta C(T)}$ Method. *Methods*. 2001 Dec;25(4):402-8. doi: 10.1006/meth.2001.1262. PMID: 11846609.
- Maeda Y, Tsuchiya T, Hao H, Tompkins DH, Xu Y, Mucenski ML, Du L, Keiser AR, Fukazawa T, Naomoto Y, Nagayasu T, Whitsett JA. Kras(G12D) and Nkx2-1 haploinsufficiency induce mucinous adenocarcinoma of the lung. *J Clin Invest*. 2012 Dec;122(12):4388-400.
- Maxwell SA, Rivera A. Proline oxidase induces apoptosis in tumor cells, and its expression is frequently absent or reduced in renal carcinomas. *J Biol Chem*. 2003 Mar 14;278(11):9784-9.
- Maxwell SA, Kochevar GJ. Identification of a p53-response element in the promoter of the proline oxidase gene. *Biochem Biophys Res Commun*. 2008 May 2;369(2):308-13.
- Minoo P, Hu L, Xing Y, Zhu NL, Chen H, Li M, Borok Z, Li C. Physical and functional interactions between homeodomain NKX2.1 and winged helix/forkhead FOXA1 in lung epithelial cells. *Mol Cell Biol*. 2007 Mar;27(6):2155-65.
- Mitsubuchi H, Nakamura K, Matsumoto S, Endo F. Inborn errors of proline metabolism. *J Nutr*. 2008 Oct;138(10):2016S-2020S.

- Moldvay J, Jackel M, Bogos K, Soltész I, Agócs L, Kovács G, Schaff Z. The role of TTF-1 in differentiating primary and metastatic lung adenocarcinomas. *Pathol Oncol Res.* 2004;10(2):85-8.
- Monti P, Ciribilli Y, Bisio A, Foggetti G, Raimondi I, Campomenosi P, Menichini P, Fronza G, Inga A. Δ N-P63 α and TA-P63 α exhibit intrinsic differences in transactivation specificities that depend on distinct features of DNA target sites. *Oncotarget.* 2014 Apr 30;5(8):2116-30.
- Mu D. The complexity of thyroid transcription factor 1 with both pro- and anti-oncogenic activities. *J Biol Chem.* 2013 Aug 30;288(35):24992-5000.
- Olivares O, Mayers JR, Gouirand V, Torrence ME, Gicquel T, Borge L, Lac S, Roques J, Lavaut MN, Berthezène P, Rubis M, Secq V, Garcia S, Moutardier V, Lombardo D, Iovanna JL, Tomasini R, Guillaumond F, Vander Heiden MG, Vasseur S. Collagen-derived proline promotes pancreatic ductal adenocarcinoma cell survival under nutrient limited conditions. *Nat Commun.* 2017 Jul 7;8:16031.
- Ordóñez NG. Thyroid transcription factor-1 is a marker of lung and thyroid carcinomas. *Adv Anat Pathol.* 2000 Mar;7(2):123-7.
- Park KS, Whitsett JA, Di Palma T, Hong JH, Yaffe MB, Zannini M. TAZ interacts with TTF-1 and regulates expression of surfactant protein-C. *J Biol Chem.* 2004 Apr 23;279(17):17384-90.
- Phang JM, Liu W, Hancock CN, Fischer JW. Proline metabolism and cancer: emerging links to glutamine and collagen. *Curr Opin Clin Nutr Metab Care.* 2015 Jan;18(1):71-7.
- Raimondi I, Ciribilli Y, Monti P, Bisio A, Pollegioni L, Fronza G, Inga A, Campomenosi P. P53 family members modulate the expression of PRODH, but not PRODH2, via intronic p53 response elements. *PLoS One.* 2013 Jul 8;8(7):e69152.

- Runkle EA, Rice SJ, Qi J, Masser D, Antonetti DA, Winslow MM, Mu D. Occludin is a direct target of thyroid transcription factor-1 (TTF-1/NKX2-1). *J Biol Chem.* 2012 Aug 17;287(34):28790-801.
- Sasse SK, Zuo Z, Kadiyala V, Zhang L, Pufall MA, Jain MK, Phang TL, Stormo GD, Gerber AN. Response Element Composition Governs Correlations between Binding Site Affinity and Transcription in Glucocorticoid Receptor Feed-forward Loops. *J Biol Chem.* 2015 Aug 7;290(32):19756-69.
- Tang J, Hu M, Lee S, Roblin R. A polymerase chain reaction based method for detecting Mycoplasma/Acholeplasma contaminants in cell culture. *J Microbiol Methods.* 2000 Jan;39(2):121-6.
- Yamaguchi T, Hosono Y, Yanagisawa K, Takahashi T. NKX2-1/TTF-1: an enigmatic oncogene that functions as a double-edged sword for cancer cell survival and progression. *Cancer Cell.* 2013 Jun 10;23(6):718-23.
- Yan C, Naltner A, Conkright J, Ghaffari M. Protein-protein interaction of retinoic acid receptor alpha and thyroid transcription factor-1 in respiratory epithelial cells. *J Biol Chem.* 2001 Jun 15;276(24):21686-91.
- Yan C, Naltner A, Martin M, Naltner M, Fangman JM, Gurel O. Transcriptional stimulation of the surfactant protein B gene by STAT3 in respiratory epithelial cells. *J Biol Chem.* 2002 Mar 29;277(13):10967-72.
- Zannini M, Acebron A, De Felice M, Arnone MI, Martin-Pérez J, Santisteban P, Di Lauro R. Mapping and functional role of phosphorylation sites in the thyroid transcription factor-1 (TTF-1). *J Biol Chem.* 1996 Jan 26;271(4):2249-54.
- Zamecnik J, Kodet R. Value of thyroid transcription factor-1 and surfactant apoprotein A in the differential diagnosis of pulmonary carcinomas: a study of 109 cases. *Virchows Arch.* 2002 Apr;440(4):353-61.
- Zhou B, Zhong Q, Minoo P, Li C, Ann DK, Frenkel B, Morrisey EE, Crandall ED, Borok Z. Foxp2 inhibits Nkx2.1-mediated transcription of SP-C via interactions

with the Nkx2.1 homeodomain. Am J Respir Cell Mol Biol. 2008 Jun;38(6):750-8.

AUTHOR CONTRIBUTION STATEMENTS

S.G. carried out the experiments and wrote the draft of the manuscript.

A.P. and R.C. contributed to cloning of the RE and to cell line maintenance.

P.C. supervised the work and contributed to the final draft.

All authors read and approved the manuscript.

CONCLUSIONS AND FUTURE PERSPECTIVES

The aim of this PhD project was to investigate proline dehydrogenase (PRODH) expression and function in lung cancer and to investigate regulation of its gene by the TTF-1 transcription factor.

PRODH expression, characterized by immunohistochemical analysis in NSCLC and SCLC cases, was shown to be present in the majority of ADCs, rare in SCCs and absent in SCLC. Moreover, PRODH expression was higher in tumours at an early stage, characterized by small size and absence of metastases, and low grade. PRODH expression appeared to improve cancer-specific survival and overall survival by Kaplan-Meier curves.

Investigation of the effects of PRODH expression in adenocarcinoma cell lines did not lead to univocal results, although the majority of the cell lines had the same behaviour, in particular in terms of cell survival. We hypothesized that the different genetic background of the cell lines under analysis could play a role.

Among the possible modifiers to be investigated in order to analyse in more detail the effects that an overexpression of PRODH has on cell growth, it is worth mentioning p53, because *PRODH* gene is a target of the p53 family (Raimondi et al., 2013), and PRODH was shown to contribute to p53-induced apoptosis (Liu and Phang, 2012).

Another factor that could act as modifier of PRODH effects is EGFR. Indeed, a study by Angulo et al. showed that PRODH is expressed in a subset of lung adenocarcinomas as part of a 13 genes signature induced by EGFR mutations (Angulo et al., 2008). These results are in agreement with our findings in ADC samples, obtained by immunohistochemical analysis, in which PRODH expression correlated with the presence of EGFR activating mutations. However, EGFR status alone does not completely explain our findings regarding survival in the cell lines under study.

In considering the role that a different genetic background plays in tumorigenesis, the importance of chromatin-modifying enzymes must also be highlighted (Jones et al., 2016). Indeed, it was demonstrated that the chromatin remodelling factor lymphoid-specific helicase (LSH) regulated *PRODH* expression through the recruitment of p53 to *PRODH* promoter (Liu et al., 2020).

The same authors found a correlation between *PRODH* and inflammation. In particular, they showed that, by the induction of ROS, *PRODH* could induce three inflammatory genes (*CXCL1*, *LCN2* and *IL17C*) in a manner dependent on IKK α and I κ B phosphorylation (Liu et al., 2020).

In this PhD project I also suggest that the Thyroid Transcription Factor-1 (TTF-1) activates *PRODH* gene expression. However, I used ectopic expression of TTF-1 for these experiments. Studies on *PRODH* regulation following induction of TTF-1 transactivating activity with glucocorticoids / cAMP will confirm my preliminary findings. It must be considered that the picture about *PRODH* regulation that I am presenting is likely to be more complex. TTF-1, p53 and Nf κ B were shown to be interconnected and the effects of TTF-1 on cellular phenotypes (seen by invasion, soft agar growth, xenograft models) was shown to be different depending on p53 status (Chen et al., 2015). Additionally, the EGFR pathway is connected to TTF-1 by the orphan tyrosine kinase-like receptor ROR1, that is a transcriptional target of TTF-1 and sustains cell survival mediated by EGFR (Yamaguchi et al., 2012).

Further studies are therefore needed to investigate how the crosstalk among these different pathways could influence *PRODH* induced cellular outcomes.

In this study, *PRODH* overexpression increased cell motility of tested lung ADC cell lines, but decreased anchorage independence during soft agar growth. In a recent work, Liu et al. described that *PRODH* increases invasion, epithelial to mesenchymal transition and production of inflammatory cytokines via ROS production in lung ADC cell lines; moreover, *in vivo*, *PRODH* expressing tumours were bigger than control tumours in nude mice (Liu et al., 2020), confirming its function as an oncogene, that had already been proposed for *PRODH* in breast cancer cells (Elia et al., 2017). The

authors used the A549 cell model, that also in our clonogenic assay behaved differently from other cell lines. The other two cell lines used by Liu et al., PC9 and 95D, are not among the cell lines we analysed in our study (Liu et al., 2020).

Therefore, further experiments need to be performed, focusing on 3D cells growth, invasion and the characterisation of epithelial to mesenchymal transition also in our models, to draw a clear picture of PRODH effects in these cell lines.

Another aspect to take into consideration is the type of construct used to drive PRODH expression. I used a pcDNA3.1 vector, in which transgene expression is controlled by the strong CMV viral promoter. Transgene expression could be too high (resulting in toxicity of specific proteins) or unstable with this promoter, due to silencing, as it has been shown for ectopic expression of transgenes under control of the CMV promoter in CHO cells (Yang et al., 2010; Wang et al., 2017).

Indeed, new cellular models in which PRODH expression is modulated by an inducible promoter are desirable to apply these models also for *in vivo* tumorigenesis experiments in nude mice.

It is well known that metabolic reprogramming is an important hallmark of cancer (Hanahan and Weinberg, 2011). For this reason, the search for metabolic pathways that are altered in various types of tumours, and therefore the development of new metabolic inhibitors as novel cancer therapy has developed in recent years. Modulation of PRODH activity seems very promising, as evidence for an altered proline metabolism during tumorigenesis accumulates (Frank et al., 2010; Sasada et al., 2013; Elia et al., 2017; Panosyan et al., 2017; Olivares et al., 2017; Zareba et al., 2017; Tanner et al., 2018; Fang et al., 2019; Huynh et al., 2020).

Among the most promising chemical compounds, L-tetrahydro-2-furoic acid (L-THFA) was demonstrated to inhibit PRODH activity in HEK 293 and MCF7 cell lines (Krishnan et al., 2008; Elia et al., 2017). Moreover, treatment with this compound did not show adverse effects on normal cells in *in vitro* and *in vivo* experiments (Elia et al., 2017). Other compounds with anticancer activity are contained in propolis (chrysin, caffeic acid, p-coumaric acid, and ferulic acid) and were shown to

contribute to the induction of PRODH dependent apoptosis in the Cal-27 tongue squamous cell line (Celinska-Janowicz et al., 2018).

N-propargylglycine (N-PPPG) is another promising compound, capable of inhibiting PRODH specifically and irreversibly, and apparently well tolerated in mice at effective doses (Scott et al., 2019).

It is important to underline that the switching mechanism of PRODH-dependent apoptosis/survival in lung cancer was unknown so far. The data reported in this PhD thesis suggest that the differential expression and/or mutations of PRODH and its regulation by TTF-1 and possibly EGFR may play a role in this type of tumour.

In conclusion, PRODH is demonstrating to be a challenging protein, whose effects can be different in different cell types and tissues, likely depending also on the genetic background. Further and more in-depth studies need to be performed in order to better characterize the role this protein plays in lung tumourigenesis, and to identify possible genetic modifiers of PRODH function.

REFERENCES

- Adams E. Metabolism of proline and of hydroxyproline. *Int Rev Connect Tissue Res.* 1970;5:1-91.
- Adams E, Frank L. Metabolism of proline and the hydroxyprolines. *Annu Rev Biochem.* 1980;49:1005-61.
- Amos CI, Xu W, Spitz MR. Is there a genetic basis for lung cancer susceptibility? *Recent Results Cancer Res.* 1999;151:3-12.
- Anagnostou VK, Syrigos KN, Bepler G, Homer RJ, Rimm DL. Thyroid transcription factor 1 is an independent prognostic factor for patients with stage I lung adenocarcinoma. *J Clin Oncol.* 2009 Jan 10;27(2):271-8.
- Angulo B, Suarez-Gauthier A, Lopez-Rios F, Medina PP, Conde E, Tang M, Soler G, Lopez-Encuentra A, Cigudosa JC, Sanchez-Cespedes M. Expression signatures in lung cancer reveal a profile for EGFR-mutant tumours and identify selective PIK3CA overexpression by gene amplification. *J Pathol.* 2008 Feb;214(3):347-56.
- Baron M. Genetics of schizophrenia and the new millennium: progress and pitfalls. *Am J Hum Genet.* 2001 Feb;68(2):299-312.
- Bender HU, Almashanu S, Steel G, Hu CA, Lin WW, Willis A, Pulver A, Valle D. Functional consequences of PRODH missense mutations. *Am J Hum Genet.* 2005 Mar;76(3):409-20.
- Bingle CD. Thyroid transcription factor-1. *Int J Biochem Cell Biol.* 1997 Dec;29(12):1471-3.
- Boggaram V. Thyroid transcription factor-1 (TTF-1/Nkx2.1/TITF1) gene regulation in the lung. *Clin Sci (Lond).* 2009 Jan;116(1):27-35.
- Bohinski RJ, Di Lauro R, Whitsett JA. The lung-specific surfactant protein B gene promoter is a target for thyroid transcription factor 1 and hepatocyte nuclear factor 3, indicating common factors for organ-specific gene expression along the foregut axis. *Mol Cell Biol.* 1994 Sep;14(9):5671-81.

- Bray F, Ferlay J, Soerjomataram I, Siegel RL, Torre LA, Jemal A. Global cancer statistics 2018: GLOBOCAN estimates of incidence and mortality worldwide for 36 cancers in 185 countries. *CA Cancer J Clin*. 2018 Nov;68(6):394-424.
- Cairns RA, Harris I, McCracken S, Mak TW. Cancer cell metabolism. *Cold Spring Harb Symp Quant Biol*. 2011;76:299-311.
- Celińska-Janowicz K, Zaręba I, Lazarek U, Teul J, Tomczyk M, Pałka J, Milyk W. Constituents of Propolis: Chrysin, Caffeic Acid, p-Coumaric Acid, and Ferulic Acid Induce PRODH/POX-Dependent Apoptosis in Human Tongue Squamous Cell Carcinoma Cell (CAL-27). *Front Pharmacol*. 2018 Apr 6;9:336.
- Chen Z, Fillmore CM, Hammerman PS, Kim CF, Wong KK. Non-small-cell lung cancers: a heterogeneous set of diseases. *Nat Rev Cancer*. 2014 Aug;14(8):535-46.
- Chen PM, Wu TC, Cheng YW, Chen CY, Lee H. NKX2-1-mediated p53 expression modulates lung adenocarcinoma progression via modulating IKK β /NF- κ B activation. *Oncotarget*. 2015 Jun 10;6(16):14274-89.
- Davidson MR, Gazdar AF, Clarke BE. The pivotal role of pathology in the management of lung cancer. *J Thorac Dis*. 2013 Oct;5 Suppl 5(Suppl 5):S463-78.
- DeBerardinis RJ, Chandel NS. We need to talk about the Warburg effect. *Nat Metab*. 2020 Feb;2(2):127-129.
- De Felice M, Damante G, Zannini M, Francis-Lang H, Di Lauro R. Redundant domains contribute to the transcriptional activity of the thyroid transcription factor 1. *J Biol Chem*. 1995 Nov 3;270(44):26649-56.
- Devriendt K, Vanhole C, Matthijs G, de Zegher F. Deletion of thyroid transcription factor-1 gene in an infant with neonatal thyroid dysfunction and respiratory failure. *N Engl J Med*. 1998 Apr 30;338(18):1317-8.
- Di Palma T, Nitsch R, Mascia A, Nitsch L, Di Lauro R, Zannini M. The paired domain-containing factor Pax8 and the homeodomain-containing factor TTF-1

directly interact and synergistically activate transcription. *J Biol Chem*. 2003 Jan 31;278(5):3395-402.

- Elia I, Broekaert D, Christen S, Boon R, Radaelli E, Orth MF, Verfaillie C, Grünewald TGP, Fendt SM. Proline metabolism supports metastasis formation and could be inhibited to selectively target metastasizing cancer cells. *Nat Commun*. 2017 May 11;8:15267.
- Fang H, Du G, Wu Q, Liu R, Chen C, Feng J. HDAC inhibitors induce proline dehydrogenase (POX) transcription and anti-apoptotic autophagy in triple negative breast cancer. *Acta Biochim Biophys Sin (Shanghai)*. 2019 Sep 6;51(10):1064-1070.
- Frank B, Hoffmeister M, Klopp N, Illig T, Chang-Claude J, Brenner H. Polymorphisms in inflammatory pathway genes and their association with colorectal cancer risk. *Int J Cancer*. 2010 Dec 15;127(12):2822-30.
- Galluzzi L, Kepp O, Vander Heiden MG, Kroemer G. Metabolic targets for cancer therapy. *Nat Rev Drug Discov*. 2013 Nov;12(11):829-46.
- Gehring WJ. Homeo boxes in the study of development. *Science*. 1987 Jun 5;236(4806):1245-52.
- Goldstraw P, Crowley J, Chansky K, Giroux DJ, Groome PA, Rami-Porta R, Postmus PE, Rusch V, Sobin L; International Association for the Study of Lung Cancer International Staging Committee; Participating Institutions. The IASLC Lung Cancer Staging Project: proposals for the revision of the TNM stage groupings in the forthcoming (seventh) edition of the TNM Classification of malignant tumours. *J Thorac Oncol*. 2007 Aug;2(8):706-14.
- Gottlieb E, Tomlinson IP. Mitochondrial tumour suppressors: a genetic and biochemical update. *Nat Rev Cancer*. 2005 Nov;5(11):857-66.
- Guazzi S, Price M, De Felice M, Damante G, Mattei MG, Di Lauro R. Thyroid nuclear factor 1 (TTF-1) contains a homeodomain and displays a novel DNA binding specificity. *EMBO J*. 1990 Nov;9(11):3631-9.

- Hagland H, Nikolaisen J, Hodneland LI, Gjertsen BT, Bruserud Ø, Tronstad KJ. Targeting mitochondria in the treatment of human cancer: a coordinated attack against cancer cell energy metabolism and signalling. *Expert Opin Ther Targets*. 2007 Aug;11(8):1055-69.
- Hamdan H, Liu H, Li C, Jones C, Lee M, deLemos R, Minoo P. Structure of the human Nkx2.1 gene. *Biochim Biophys Acta*. 1998 Mar 13;1396(3):336-48.
- Hanahan D, Weinberg RA. Hallmarks of cancer: the next generation. *Cell*. 2011 Mar 4;144(5):646-74.
- Haque AK, Syed S, Lele SM, Freeman DH, Adegboyega PA. Immunohistochemical study of thyroid transcription factor-1 and HER2/neu in non-small cell lung cancer: strong thyroid transcription factor-1 expression predicts better survival. *Appl Immunohistochem Mol Morphol*. 2002 Jun;10(2):103-9.
- Hecht SS. Lung carcinogenesis by tobacco smoke. *Int J Cancer*. 2012 Dec 15;131(12):2724-32.
- Herbst RS, Heymach JV, Lippman SM. Lung cancer. *N Engl J Med*. 2008 Sep 25;359(13):1367-80.
- Huynh TYL, Zareba I, Baszanowska W, Lewoniewska S, Palka J. Understanding the role of key amino acids in regulation of proline dehydrogenase/proline oxidase (prodh/pox)-dependent apoptosis/autophagy as an approach to targeted cancer therapy. *Mol Cell Biochem*. 2020 Mar;466(1-2):35-44
- Ikeda K, Clark JC, Shaw-White JR, Stahlman MT, Boutell CJ, Whitsett JA. Gene structure and expression of human thyroid transcription factor-1 in respiratory epithelial cells. *J Biol Chem*. 1995 Apr 7;270(14):8108-14.
- Islami F, Torre LA, Jemal A. Global trends of lung cancer mortality and smoking prevalence. *Transl Lung Cancer Res*. 2015 Aug;4(4):327-38.
- Jacquet H, Raux G, Thibaut F, Hecketsweiler B, Houy E, Demilly C, Haouzir S, Allio G, Fouldrin G, Drouin V, Bou J, Petit M, Campion D, Frébourg T. PRODH

mutations and hyperprolinemia in a subset of schizophrenic patients. *Hum Mol Genet.* 2002 Sep 15;11(19):2243-9.

- Jones PA, Issa JP, Baylin S. Targeting the cancer epigenome for therapy. *Nat Rev Genet.* 2016 Sep 15;17(10):630-41.
- Kandoth C, McLellan MD, Vandin F, Ye K, Niu B, Lu C, Xie M, Zhang Q, McMichael JF, Wyczalkowski MA, Leiserson MDM, Miller CA, Welch JS, Walter MJ, Wendl MC, Ley TJ, Wilson RK, Raphael BJ, Ding L. Mutational landscape and significance across 12 major cancer types. *Nature.* 2013 Oct 17;502(7471):333-339.
- Karayiorgou M, Gogos JA. The molecular genetics of the 22q11-associated schizophrenia. *Brain Res Mol Brain Res.* 2004 Dec 20;132(2):95-104.
- Karna E, Szoka L, Huynh TYL, Palka JA. Proline-dependent regulation of collagen metabolism. *Cell Mol Life Sci.* 2020 May;77(10):1911-1918.
- Kazberuk A, Zareba I, Palka J, Surazynski A. A novel plausible mechanism of NSAIDs-induced apoptosis in cancer cells: the implication of proline oxidase and peroxisome proliferator-activated receptor. *Pharmacol Rep.* 2020 Oct;72(5):1152-1160.
- Kimura S, Hara Y, Pineau T, Fernandez-Salguero P, Fox CH, Ward JM, Gonzalez FJ. The T/ebp null mouse: thyroid-specific enhancer-binding protein is essential for the organogenesis of the thyroid, lung, ventral forebrain, and pituitary. *Genes Dev.* 1996 Jan 1;10(1):60-9.
- Krishnan N, Dickman MB, Becker DF. Proline modulates the intracellular redox environment and protects mammalian cells against oxidative stress. *Free Radic Biol Med.* 2008 Feb 15;44(4):671-81.
- Kruse JP, Gu W. Modes of p53 regulation. *Cell.* 2009 May 15;137(4):609-22.
- Kwei KA, Kim YH, Girard L, Kao J, Pacyna-Gengelbach M, Salari K, Lee J, Choi YL, Sato M, Wang P, Hernandez-Boussard T, Gazdar AF, Petersen I, Minna JD, Pollack JR. Genomic profiling identifies TTF1 as a lineage-specific oncogene amplified in lung cancer. *Oncogene.* 2008 Jun 5;27(25):3635-40.

- Lane DP. Cancer. p53, guardian of the genome. *Nature*. 1992 Jul 2;358(6381):15-6.
- Lazzaro D, Price M, de Felice M, Di Lauro R. The transcription factor TTF-1 is expressed at the onset of thyroid and lung morphogenesis and in restricted regions of the foetal brain. *Development*. 1991 Dec;113(4):1093-104.
- Levine AJ, Hu W, Feng Z. The P53 pathway: what questions remain to be explored? *Cell Death Differ*. 2006 Jun;13(6):1027-36.
- Liang X, Zhang L, Natarajan SK, Becker DF. Proline mechanisms of stress survival. *Antioxid Redox Signal*. 2013 Sep 20;19(9):998-1011.
- Liu H, Heath SC, Sobin C, Roos JL, Galke BL, Blundell ML, Lenane M, Robertson B, Wijsman EM, Rapoport JL, Gogos JA, Karayiorgou M. Genetic variation at the 22q11 PRODH2/DGCR6 locus presents an unusual pattern and increases susceptibility to schizophrenia. *Proc Natl Acad Sci U S A*. 2002 Mar 19;99(6):3717-22.
- Liu Y, Borchert GL, Surazynski A, Hu CA, Phang JM. Proline oxidase activates both intrinsic and extrinsic pathways for apoptosis: the role of ROS/superoxides, NFAT and MEK/ERK signaling. *Oncogene*. 2006 Sep 14;25(41):5640-7.
- Liu Y, Borchert GL, Surazynski A, Phang JM. Proline oxidase, a p53-induced gene, targets COX-2/PGE2 signaling to induce apoptosis and inhibit tumor growth in colorectal cancers. *Oncogene*. 2008 Dec 4;27(53):6729-37.
- Liu Y, Borchert GL, Donald SP, Diwan BA, Anver M, Phang JM. Proline oxidase functions as a mitochondrial tumor suppressor in human cancers. *Cancer Res*. 2009 Aug 15;69(16):6414-22.
- Liu W, Zahirnyk O, Wang H, Shiao YH, Nickerson ML, Khalil S, Anderson LM, Perantoni AO, Phang JM. miR-23b targets proline oxidase, a novel tumor suppressor protein in renal cancer. *Oncogene*. 2010 Sep 2;29(35):4914-24.
- Liu W, Le A, Hancock C, Lane AN, Dang CV, Fan TW, Phang JM. Reprogramming of proline and glutamine metabolism contributes to the proliferative and

metabolic responses regulated by oncogenic transcription factor c-MYC. *Proc Natl Acad Sci U S A*. 2012 Jun 5;109(23):8983-8.

- Liu W, Phang JM. Proline dehydrogenase (oxidase) in cancer. *Biofactors*. 2012 Nov-Dec;38(6):398-406.
- Liu W, Phang JM. Proline dehydrogenase (oxidase), a mitochondrial tumor suppressor, and autophagy under the hypoxia microenvironment. *Autophagy*. 2012 Sep;8(9):1407-9.
- Liu W, Hancock CN, Fischer JW, Harman M, Phang JM. Proline biosynthesis augments tumor cell growth and aerobic glycolysis: involvement of pyridine nucleotides. *Sci Rep*. 2015 Nov 24;5:17206.
- Liu Y, Mao C, Wang M, Liu N, Ouyang L, Liu S, Tang H, Cao Y, Liu S, Wang X, Xiao D, Chen C, Shi Y, Yan Q, Tao Y. Cancer progression is mediated by proline catabolism in non-small cell lung cancer. *Oncogene*. 2020 Mar;39(11):2358-2376.
- Maeda Y, Tsuchiya T, Hao H, Tompkins DH, Xu Y, Mucenski ML, Du L, Keiser AR, Fukazawa T, Naomoto Y, Nagayasu T, Whitsett JA. *Kras*(G12D) and *Nkx2-1* haploinsufficiency induce mucinous adenocarcinoma of the lung. *J Clin Invest*. 2012 Dec;122(12):4388-400.
- Maxwell SA, Rivera A. Proline oxidase induces apoptosis in tumor cells, and its expression is frequently absent or reduced in renal carcinomas. *J Biol Chem*. 2003 Mar 14;278(11):9784-9.
- McDermid HE, Morrow BE. Genomic disorders on 22q11. *Am J Hum Genet*. 2002 May;70(5):1077-88.
- McDonald-McGinn DM, Reilly A, Wallgren-Pettersson C, Hoyme HE, Yang SP, Adam MP, Zackai EH, Sullivan KE. Malignancy in chromosome 22q11.2 deletion syndrome (DiGeorge syndrome/velocardiofacial syndrome). *Am J Med Genet A*. 2006 Apr 15;140(8):906-9.

- Mitsubuchi H, Nakamura K, Matsumoto S, Endo F. Inborn errors of proline metabolism. *J Nutr.* 2008 Oct;138(10):2016S-2020S.
- Mizuno K, Gonzalez FJ, Kimura S. Thyroid-specific enhancer-binding protein (T/EBP): cDNA cloning, functional characterization, and structural identity with thyroid transcription factor TTF-1. *Mol Cell Biol.* 1991 Oct;11(10):4927-33.
- Mizushima N, Komatsu M. Autophagy: renovation of cells and tissues. *Cell.* 2011 Nov 11;147(4):728-41.
- Moldvay J, Jackel M, Bogos K, Soltész I, Agócs L, Kovács G, Schaff Z. The role of TTF-1 in differentiating primary and metastatic lung adenocarcinomas. *Pathol Oncol Res.* 2004;10(2):85-8.
- Moxley AH, Reisman D. Context is key: Understanding the regulation, functional control, and activities of the p53 tumour suppressor. *Cell Biochem Funct.* 2020 Sep 30.
- Mu D. The complexity of thyroid transcription factor 1 with both pro- and anti-oncogenic activities. *J Biol Chem.* 2013 Aug 30;288(35):24992-5000.
- Myong NH. Thyroid transcription factor-1 (TTF-1) expression in human lung carcinomas: its prognostic implication and relationship with wxpressions of p53 and Ki-67 proteins. *J Korean Med Sci.* 2003 Aug;18(4):494-500.
- National Lung Screening Trial Research Team, Aberle DR, Adams AM, Berg CD, Black WC, Clapp JD, Fagerstrom RM, Gareen IF, Gatsonis C, Marcus PM, Sicks JD. Reduced lung-cancer mortality with low-dose computed tomographic screening. *N Engl J Med.* 2011 Aug 4;365(5):395-409.
- Niimi T, Nagashima K, Ward JM, Minoo P, Zimonjic DB, Popescu NC, Kimura S. claudin-18, a novel downstream target gene for the T/EBP/NKX2.1 homeodomain transcription factor, encodes lung- and stomach-specific isoforms through alternative splicing. *Mol Cell Biol.* 2001 Nov;21(21):7380-90.
- Oguchi H, Pan YT, Kimura S. The complete nucleotide sequence of the mouse thyroid-specific enhancer-binding protein (T/EBP) gene: extensive identity of

the deduced amino acid sequence with the human protein. *Biochim Biophys Acta*. 1995 Apr 4;1261(2):304-6.

- Olivares O, Mayers JR, Gouirand V, Torrence ME, Gicquel T, Borge L, Lac S, Roques J, Lavaut MN, Berthezène P, Rubis M, Secq V, Garcia S, Moutardier V, Lombardo D, Iovanna JL, Tomasini R, Guillaumond F, Vander Heiden MG, Vasseur S. Collagen-derived proline promotes pancreatic ductal adenocarcinoma cell survival under nutrient limited conditions. *Nat Commun*. 2017 Jul 7;8:16031.
- Ordóñez NG. Thyroid transcription factor-1 is a marker of lung and thyroid carcinomas. *Adv Anat Pathol*. 2000 Mar;7(2):123-7.
- Ordóñez NG. Value of thyroid transcription factor-1 immunostaining in distinguishing small cell lung carcinomas from other small cell carcinomas. *Am J Surg Pathol*. 2000 Sep;24(9):1217-23.
- Pandhare J, Cooper SK, Phang JM. Proline oxidase, a proapoptotic gene, is induced by troglitazone: evidence for both peroxisome proliferator-activated receptor gamma-dependent and -independent mechanisms. *J Biol Chem*. 2006 Jan 27;281(4):2044-52.
- Pandhare J, Donald SP, Cooper SK, Phang JM. Regulation and function of proline oxidase under nutrient stress. *J Cell Biochem*. 2009 Jul 1;107(4):759-68.
- Panosyan EH, Lin HJ, Koster J, Lasky JL 3rd. In search of druggable targets for GBM amino acid metabolism. *BMC Cancer*. 2017 Feb 28;17(1):162.
- Peng Z, Lu Q, Verma DP. Reciprocal regulation of delta 1-pyrroline-5-carboxylate synthetase and proline dehydrogenase genes controls proline levels during and after osmotic stress in plants. *Mol Gen Genet*. 1996 Dec 13;253(3):334-41.
- Phang JM, Downing SJ, Yeh GC, Smith RJ, Williams JA, Hagedorn CH. Stimulation of the hexosemonophosphate-pentose pathway by pyrroline-5-carboxylate in cultured cells. *J Cell Physiol*. 1982 Mar;110(3):255-61.

- Phang JM. The regulatory functions of proline and pyrroline-5-carboxylic acid. *Curr Top Cell Regul.* 1985;25:91-132.
- Phang JM, Donald SP, Pandhare J, Liu Y. The metabolism of proline, a stress substrate, modulates carcinogenic pathways. *Amino Acids.* 2008 Nov;35(4):681-90.
- Phang JM, Liu W, Zahirnyk O. Proline metabolism and microenvironmental stress. *Annu Rev Nutr.* 2010 Aug 21;30:441-63.
- Phang JM, Liu W, Hancock C, Christian KJ. The proline regulatory axis and cancer. *Front Oncol.* 2012 Jun 21;2:60.
- Phang JM, Liu W, Hancock CN, Fischer JW. Proline metabolism and cancer: emerging links to glutamine and collagen. *Curr Opin Clin Nutr Metab Care.* 2015 Jan;18(1):71-7.
- Phang JM. Proline Metabolism in Cell Regulation and Cancer Biology: Recent Advances and Hypotheses. *Antioxid Redox Signal.* 2019 Feb 1;30(4):635-649.
- Polyak K, Xia Y, Zweier JL, Kinzler KW, Vogelstein B. A model for p53-induced apoptosis. *Nature.* 1997 Sep 18;389(6648):300-5.
- Puglisi F, Barbone F, Damante G, Bruckbauer M, Di Lauro V, Beltrami CA, Di Loreto C. Prognostic value of thyroid transcription factor-1 in primary, resected, non-small cell lung carcinoma. *Mod Pathol.* 1999 Mar;12(3):318-24.
- Raimondi I, Ciribilli Y, Monti P, Bisio A, Pollegioni L, Fronza G, Inga A, Campomenosi P. P53 family members modulate the expression of PRODH, but not PRODH2, via intronic p53 response elements. *PLoS One.* 2013 Jul 8;8(7):e69152.
- Ristow M. Oxidative metabolism in cancer growth. *Curr Opin Clin Nutr Metab Care.* 2006 Jul;9(4):339-45.
- Rivera A, Maxwell SA. The p53-induced gene-6 (proline oxidase) mediates apoptosis through a calcineurin-dependent pathway. *J Biol Chem.* 2005 Aug 12;280(32):29346-54.

- Rivlin N, Brosh R, Oren M, Rotter V. Mutations in the p53 Tumor Suppressor Gene: Important Milestones at the Various Steps of Tumorigenesis. *Genes Cancer*. 2011 Apr;2(4):466-74.
- Runkle EA, Rice SJ, Qi J, Masser D, Antonetti DA, Winslow MM, Mu D. Occludin is a direct target of thyroid transcription factor-1 (TTF-1/NKX2-1). *J Biol Chem*. 2012 Aug 17;287(34):28790-801.
- Saad RS, Liu YL, Han H, Landreneau RJ, Silverman JF. Prognostic significance of thyroid transcription factor-1 expression in both early-stage conventional adenocarcinoma and bronchioloalveolar carcinoma of the lung. *Hum Pathol*. 2004 Jan;35(1):3-7.
- Sacktor B. Biochemical adaptations for flight in the insect. *Biochem Soc Symp*. 1976;(41):111-31.
- Sasada S, Miyata Y, Tsutani Y, Tsuyama N, Masujima T, Hihara J, Okada M. Metabolomic analysis of dynamic response and drug resistance of gastric cancer cells to 5-fluorouracil. *Oncol Rep*. 2013 Mar;29(3):925-31.
- Sato M, Shames DS, Gazdar AF, Minna JD. A translational view of the molecular pathogenesis of lung cancer. *J Thorac Oncol*. 2007 Apr;2(4):327-43.
- Scaraffia PY, Wells MA. Proline can be utilized as an energy substrate during flight of *Aedes aegypti* females. *J Insect Physiol*. 2003 Jun;49(6):591-601.
- Scott MP, Tamkun JW, Hartzell GW 3rd. The structure and function of the homeodomain. *Biochim Biophys Acta*. 1989 Jul 28;989(1):25-48.
- Scott GK, Yau C, Becker BC, Khateeb S, Mahoney S, Jensen MB, Hann B, Cowen BJ, Pegan SD, Benz CC. Targeting Mitochondrial Proline Dehydrogenase with a Suicide Inhibitor to Exploit Synthetic Lethal Interactions with p53 Upregulation and Glutaminase Inhibition. *Mol Cancer Ther*. 2019 Aug;18(8):1374-1385.
- Snyder EL, Watanabe H, Magendantz M, Hoersch S, Chen TA, Wang DG, Crowley D, Whittaker CA, Meyerson M, Kimura S, Jacks T. Nkx2-1 represses a latent

gastric differentiation program in lung adenocarcinoma. *Mol Cell*. 2013 Apr 25;50(2):185-99.

- Stahlman MT, Gray ME, Whitsett JA. Expression of thyroid transcription factor-1(TTF-1) in fetal and neonatal human lung. *J Histochem Cytochem*. 1996 Jul;44(7):673-8.
- Sun S, Schiller JH, Gazdar AF. Lung cancer in never smokers--a different disease. *Nat Rev Cancer*. 2007 Oct;7(10):778-90.
- Takeuchi T, Tomida S, Yatabe Y, Kosaka T, Osada H, Yanagisawa K, Mitsudomi T, Takahashi T. Expression profile-defined classification of lung adenocarcinoma shows close relationship with underlying major genetic changes and clinicopathologic behaviors. *J Clin Oncol*. 2006 Apr 10;24(11):1679-88.
- Tallarita E, Pollegioni L, Servi S, Molla G. Expression in *Escherichia coli* of the catalytic domain of human proline oxidase. *Protein Expr Purif*. 2012 Apr;82(2):345-51.
- Tan D, Li Q, Deeb G, Ramnath N, Slocum HK, Brooks J, Cheney R, Wiseman S, Anderson T, Loewen G. Thyroid transcription factor-1 expression prevalence and its clinical implications in non-small cell lung cancer: a high-throughput tissue microarray and immunohistochemistry study. *Hum Pathol*. 2003 Jun;34(6):597-604.
- Tanaka H, Yanagisawa K, Shinjo K, Taguchi A, Maeno K, Tomida S, Shimada Y, Osada H, Kosaka T, Matsubara H, Mitsudomi T, Sekido Y, Tanimoto M, Yatabe Y, Takahashi T. Lineage-specific dependency of lung adenocarcinomas on the lung development regulator TTF-1. *Cancer Res*. 2007 Jul 1;67(13):6007-11.
- Tanner JJ, Fendt SM, Becker DF. The Proline Cycle As a Potential Cancer Therapy Target. *Biochemistry*. 2018 Jun 26;57(25):3433-3444.
- Tell G, Pines A, Paron I, D'Elia A, Bisca A, Kelley MR, Manzini G, Damante G. Redox effector factor-1 regulates the activity of thyroid transcription factor 1 by

controlling the redox state of the N transcriptional activation domain. *J Biol Chem*. 2002 Apr 26;277(17):14564-74.

- Tołoczko-Iwaniuk N, Dziemiańczyk-Pakieła D, Celińska-Janowicz K, Zaręba I, Klupczyńska A, Kokot ZJ, Nowaszewska BK, Reszeć J, Borys J, Milyk W. Proline-Dependent Induction of Apoptosis in Oral Squamous Cell Carcinoma (OSCC)-The Effect of Celecoxib. *Cancers (Basel)*. 2020 Jan 6;12(1):136.
- Torre LA, Siegel RL, Jemal A. Lung Cancer Statistics. *Adv Exp Med Biol*. 2016;893:1-19.
- Travis WD, Brambilla E, Nicholson AG, Yatabe Y, Austin JHM, Beasley MB, Chirieac LR, Dacic S, Duhig E, Flieder DB, Geisinger K, Hirsch FR, Ishikawa Y, Kerr KM, Noguchi M, Pelosi G, Powell CA, Tsao MS, Wistuba I; WHO Panel. The 2015 World Health Organization Classification of Lung Tumors: Impact of Genetic, Clinical and Radiologic Advances Since the 2004 Classification. *J Thorac Oncol*. 2015 Sep;10(9):1243-1260.
- Vousden KH, Lu X. Live or let die: the cell's response to p53. *Nat Rev Cancer*. 2002 Aug;2(8):594-604.
- Vousden KH, Prives C. Blinded by the Light: The Growing Complexity of p53. *Cell*. 2009 May 1;137(3):413-31.
- Wang X, Xu Z, Tian Z, Zhang X, Xu D, Li Q, Zhang J, Wang T. The EF-1 α promoter maintains high-level transgene expression from episomal vectors in transfected CHO-K1 cells. *J Cell Mol Med*. 2017 Nov;21(11):3044-3054.
- Warburg O. On the origin of cancer cells. *Science*. 1956 Feb 24;123(3191):309-14.
- Willis A, Bender HU, Steel G, Valle D. PRODH variants and risk for schizophrenia. *Amino Acids*. 2008 Nov;35(4):673-9.
- Wistuba II, Gazdar AF. Lung cancer preneoplasia. *Annu Rev Pathol*. 2006;1:331-48.

- Yamaguchi T, Yanagisawa K, Sugiyama R, Hosono Y, Shimada Y, Arima C, Kato S, Tomida S, Suzuki M, Osada H, Takahashi T. NKX2-1/TITF1/TTF-1-Induced ROR1 is required to sustain EGFR survival signaling in lung adenocarcinoma. *Cancer Cell*. 2012 Mar 20;21(3):348-61.
- Yamaguchi T, Hosono Y, Yanagisawa K, Takahashi T. NKX2-1/TTF-1: an enigmatic oncogene that functions as a double-edged sword for cancer cell survival and progression. *Cancer Cell*. 2013 Jun 10;23(6):718-23.
- Yang Y, Mariati, Chusainow J, Yap MG. DNA methylation contributes to loss in productivity of monoclonal antibody-producing CHO cell lines. *J Biotechnol*. 2010 Jun;147(3-4):180-5.
- Yatabe Y, Kosaka T, Takahashi T, Mitsudomi T. EGFR mutation is specific for terminal respiratory unit type adenocarcinoma. *Am J Surg Pathol*. 2005 May;29(5):633-9.
- Yokota J, Shiraishi K, Kohno T. Genetic basis for susceptibility to lung cancer: Recent progress and future directions. *Adv Cancer Res*. 2010;109:51-72.
- Zamecnik J, Kodet R. Value of thyroid transcription factor-1 and surfactant apoprotein A in the differential diagnosis of pulmonary carcinomas: a study of 109 cases. *Virchows Arch*. 2002 Apr;440(4):353-61.
- Zareba I, Palka J. Prolidase-proline dehydrogenase/proline oxidase-collagen biosynthesis axis as a potential interface of apoptosis/autophagy. *Biofactors*. 2016 Jul 8;42(4):341-8.
- Zareba I, Surazynski A, Chrusciel M, Milyk W, Doroszko M, Rahman N, Palka J. Functional Consequences of Intracellular Proline Levels Manipulation Affecting PRODH/POX-Dependent Pro-Apoptotic Pathways in a Novel in Vitro Cell Culture Model. *Cell Physiol Biochem*. 2017;43(2):670-684.
- Zareba I, Celinska-Janowicz K, Surazynski A, Milyk W, Palka J. Proline oxidase silencing induces proline-dependent pro-survival pathways in MCF-7 cells. *Oncotarget*. 2018 Feb 9;9(17):13748-13757.

- Zhang L, Becker DF. Connecting proline metabolism and signaling pathways in plant senescence. *Front Plant Sci.* 2015 Jul 22;6:552.
- Zhou L, Lim L, Costa RH, Whitsett JA. Thyroid transcription factor-1, hepatocyte nuclear factor-3beta, surfactant protein B, C, and Clara cell secretory protein in developing mouse lung. *J Histochem Cytochem.* 1996 Oct;44(10):1183-93.
- AJCC Cancer Staging Manual, Seventh Edition 2010 American Joint Committee on Cancer.
- Humphrey EW, et al. The American Cancer Society Textbook of Clinical Oncology, 1995; 220-35.

Human Primary Dermal Fibroblasts Interacting with 3-Dimensional Matrices for Surgical Application Show Specific Growth and Gene Expression Programs





International Journal of
Molecular Sciences



Article

Human Primary Dermal Fibroblasts Interacting with 3-Dimensional Matrices for Surgical Application Show Specific Growth and Gene Expression Programs

Sarah Grossi ¹, Annalisa Grimaldi ¹ , Tenzio Congiu ², Arianna Parnigoni ¹, Giampiero Campanelli ^{3,4} and Paola Campomenosi ^{1,*} 

¹ Department of Biotechnology and Life Sciences, University of Insubria, DBSV, Via J.H. Dunant 3, 21100 Varese, Italy; s.grossi1@uninsubria.it (S.G.); annalisa.grimaldi@uninsubria.it (A.G.); a.parnigoni@uninsubria.it (A.P.)

² Department of Surgical Sciences, University of Cagliari, 09100 Cagliari, Italy; tenzio.congiu@unica.it
³ Milano Hernia Center, Department of Surgical Science, Istituto Clinico Sant'Ambrogio, Via Luigi Giuseppe Faravelli 16, 20149 Milan, Italy; giampiero.campanelli@uninsubria.it

⁴ Department of Medicine and Surgery, University of Insubria, DMC, Via Guicciardini 9, 21100 Varese, Italy

* Correspondence: paola.campomenosi@uninsubria.it; Tel.: +39-0332-421322

Abstract: Several types of 3-dimensional (3D) biological matrices are employed for clinical and surgical applications, but few indications are available to guide surgeons in the choice among these materials. Here we compare the in vitro growth of human primary fibroblasts on different biological matrices commonly used for clinical and surgical applications and the activation of specific molecular pathways over 30 days of growth. Morphological analyses by Scanning Electron Microscopy and proliferation curves showed that fibroblasts have different ability to attach and proliferate on the different biological matrices. They activated similar gene expression programs, reducing the expression of collagen genes and myofibroblast differentiation markers compared to fibroblasts grown in 2D. However, differences among 3D matrices were observed in the expression of specific metalloproteinases and interleukin-6. Indeed, cell proliferation and expression of matrix degrading enzymes occur in the initial steps of interaction between fibroblast and the investigated meshes, whereas collagen and interleukin-6 expression appear to start later. The data reported here highlight features of fibroblasts grown on different 3D biological matrices and warrant further studies to understand how these findings may be used to help the clinicians choose the correct material for specific applications.

Keywords: 3D-biomaterials; human primary fibroblasts; gene expression; cell growth; surgery



Citation: Grossi, S.; Grimaldi, A.; Congiu, T.; Parnigoni, A.; Campanelli, G.; Campomenosi, P. Human Primary Dermal Fibroblasts Interacting with 3-Dimensional Matrices for Surgical Application Show Specific Growth and Gene Expression Programs. *Int. J. Mol. Sci.* **2021**, *22*, 526. <https://doi.org/10.3390/ijms220526>

Received: 6 November 2020

Accepted: 5 January 2021

Published: 7 January 2021

Publisher's Note: MDPI stays neutral with regard to jurisdictional claims in published maps and institutional affiliations.



Copyright: © 2021 by the authors. Licensee MDPI, Basel, Switzerland. This article is an open access article distributed under the terms and conditions of the Creative Commons Attribution (CC BY) license (<https://creativecommons.org/licenses/by/4.0/>).

1. Introduction

Prosthetic abdominal wall surgical repair is a common procedure for the treatment of several types of hernias or lesions of the muscular inner body walls. About one million prostheses for abdominal wall repair per year are used worldwide, and, since the first description of the use of a synthetic mesh for this surgery, plenty of new materials have been introduced as repairing options, leading to a considerable reduction in recurrence rates [1]. Moreover, prosthetic materials are increasingly used for other applications, such as mammary plastic surgery [2].

These materials can be synthetic or of biological derivation. Synthetic meshes are generally made of polypropylene, polyethylene-terephthalate, polytetrafluoroethylene, polyester, or polyvinylidene-fluoride, and their features depend on the material weight and size of pores [3,4]. They confer strength and stability to the abdominal wall. However, synthetic meshes can give rise to fibrotic responses and adherence. Moreover, their use in surgery at risk for infection (classified by the Centers for Disease Control and Prevention as “clean-contaminated”) is debated [5]. Biological 3D matrices are derived from the extracellular matrix (ECM) of a variety of tissues and species. They undergo sterilization, albeit

different procedures can be used to this aim, and can be further processed by crosslinking. All these processes can lead to alterations of the matrix and, therefore, once implanted in the patient, affect the pathways inducing foreign body response (FBR) [6]. Other characteristics considered specifically in the instance of biological meshes include resistance to microbial infection, the ability to provide a barrier to visceral adhesion formation, and the capacity to respond in a fashion similar to native tissue [7,8].

A proper body-mesh response is fundamental for successful abdominal wall repair, but the mechanisms underlying the interactions between the 3D matrices and patient cells and tissues are still not clear and need to be further investigated [3,9,10]. A hypothesis is that operational outcome during the use of biological prostheses depends on the growth of patient cells. The balance between ECM synthesis and degradation may ultimately contribute to the success of hernia repair.

However, the number of studies dealing with the biology of these materials and their interaction with host tissues is not as wide as one could expect. Moreover, scarce information is available on the application of one or the other biological matrices in relation to specific clinical indications [11,12].

To identify possible differences among specific 3D matrices commonly used in abdominal wall repair that may guide the choice of the best one suited for specific applications, thus improving clinical outcomes, in this study, we investigated fibroblast-matrix interactions by morphological analysis and by monitoring cell proliferation. We also aimed to identify the molecular pathways activated by fibroblasts during the first phases of their interaction with the different types of 3D biological matrices. In particular, we investigated the expression of genes involved in the degradation or biosynthesis of collagen, as well as some cytokines and markers of differentiation into myofibroblasts. Human primary fibroblasts have been used for this study because of their central role in foreign body reaction and wound healing process [3,10].

2. Results

2.1. Growth of Fibroblasts on the Different 3D Matrices

2.1.1. Morphological Examination by SEM

The morphology of fibroblasts grown on different types of 3D matrices was analyzed by scanning electron microscopy (SEM) 10, 20, and 30 days after their seeding. Three independent experiments were carried out, and exemplificative pictures are shown in Figure 1.

The surface of the Strattice biomaterial appeared non-homogeneous: irregular areas alternated with smoother ones, suggesting a multidirectional organization of collagen fibers in the scaffold (Figure 1a'). Ten days after seeding, few cells were visible on the Strattice mesh surface, and they were not uniformly distributed (Figure 1b'). The number of cells progressively increased at 20 and 30 days; however, a non-homogeneous distribution was also observed at these time points (Figure 1c,d). Cells appeared to be healthy and seemed to firmly adhere to the matrix, as shown in Figure 1b'-d'.

The surface of the Permacol scaffold appeared similar to Strattice, alternating rough and smooth areas (Figure 1e'). The number of cells at 10 days was higher on Permacol than on Strattice and progressively increased at 20 and 30 days. However, a non-homogeneous distribution was also observed, with groups of healthy cells scattered on the scaffold surface (Figure 1f-h, f'-h').

The surface of the Biodesign scaffold appeared smoother than Strattice and Permacol (Figure 1i'). This matrix presented the greatest number of cells among all matrices at all analyzed times. After 10 days from seeding, cells covered the surface of the biomaterial homogeneously (Figure 1j). At 20 days, cells appeared in close contact with each other, forming a monolayer (Figure 1k). However, they did not seem to firmly adhere to the scaffold, since at 30 days, the monolayer seemed to bend out and to detach from the matrix (Figure 1l). Details at higher magnification are provided in Figure 1j'-l'.

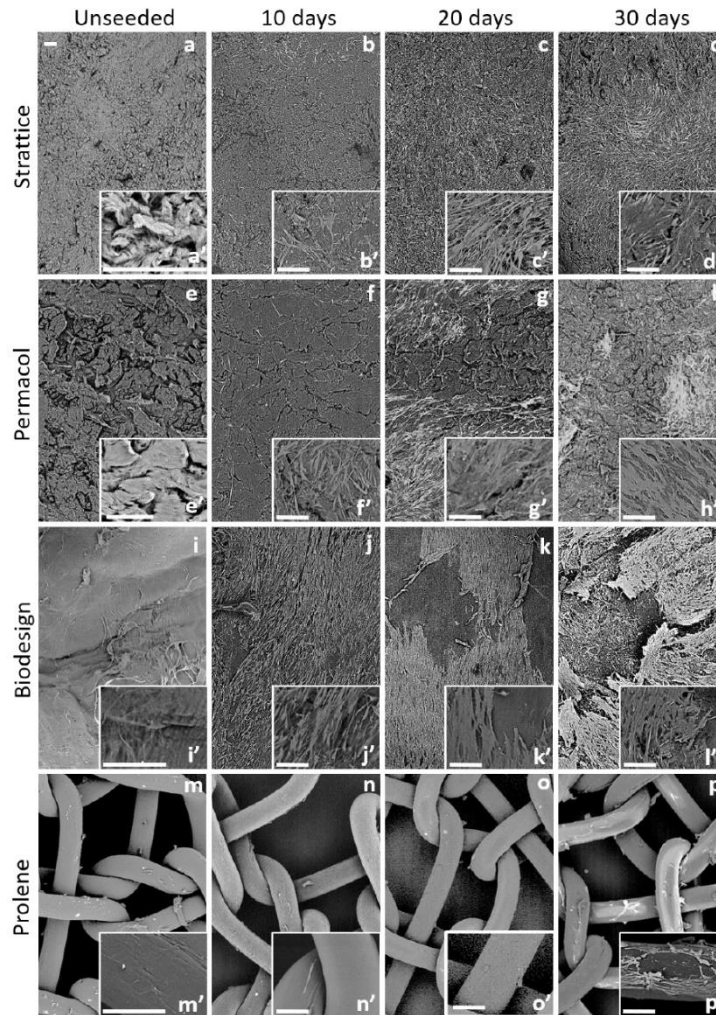


Figure 1. Scanning Electron Microscopy (SEM) images of human dermal fibroblasts cultured on tested matrices for 10, 20, or 30 days and corresponding unseeded controls, as indicated above the panels. Inserts represent images at higher magnification. Strattice (a–d,a'–d'), Permacol (e–h,e'–h'), Biodesign (i–l,i'–l'), Prolene (m–p,m'–p'). Bars indicate 100 μ m.

Finally, we observed very few cells adhering to the Prolene small pore synthetic matrix at all times. Cells did not seem to easily attach and grow on this material. At 30 days, only a few cells were present on the scaffold (Figure 1n–p,n'–p').

High magnification images are also shown in Supplementary Figure S1.

2.1.2. Cell Growth Curves

The growth of cells on the different 3D matrices was monitored at the three chosen time points by two different methods, as detailed in Materials and Methods. Data presented are the averages of three independent experiments taking into account the values obtained by the two methods used for cell counting for each matrix at each time point (Figure 2).

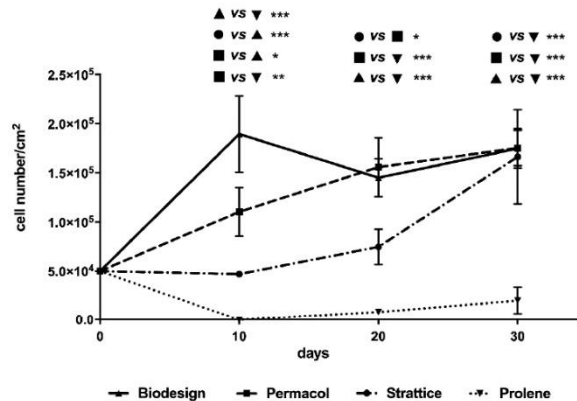


Figure 2. Growth of human dermal fibroblasts on tested matrices at 10, 20, and 30 days. Biodesign: line with upwards pointing triangles; Permacol: dashed line with squares; Strattice: dash-dot line with circles; Prolene: dotted line with downwards pointing triangles. Average number of cells (\pm SE) obtained at each time point with two methods (Cell Titer Glo Promega kit and manual count after detachment with an enzymatic cocktail) in three independent experiments were analyzed with analysis of variance (ANOVA) using a *post-hoc* Bonferroni test. Asterisks indicate significant differences (* $p < 0.05$; ** $p < 0.01$; *** $p < 0.001$).

At 10 days from seeding, the Biodesign mesh showed the highest number of cells among all tested scaffolds. At 20 days, a slight, temporary decrease in cell number compared to 10 days was observed on this matrix, whereas at 30 days, the number of cells was similar to that observed at 10 days (line with upwards pointing triangles). On Permacol scaffolds, cells increased in numbers from seeding to 30 days (dashed line with squares). On Strattice, the number of cells at 10 days was the same seeded at the beginning of the experiment; then it increased until it reached the number present on the other biological matrices at 30 days (dash-dot line with circles).

Indeed, whereas at 10 days, the number of cells was higher on Biodesign, followed by Permacol and Strattice, at 30 days, the number of cells grown on biological scaffolds was comparable. Very few cells were recovered in the Prolene samples, in keeping with morphological observation of a lower number of cells attaching to this synthetic mesh. However, the cell number showed a modest increase over time (dotted line with downwards pointing triangles).

2.2. Gene and Protein Expression

Although in our study we included for comparison a synthetic mesh together with biological matrices, gene and protein expression analyses from fibroblasts grown on Prolene were impaired by the small number of cells recovered from this type of mesh.

For all 3D matrices, no difference was observed in the results obtained with fibroblasts from the two donors; therefore, the results were pooled together.

2.2.1. Expression of Collagen Genes

Fibroblasts grown on the different types of mesh may activate either new matrix deposition or degradation of the scaffold as a first transcriptional program. Therefore, we examined collagen I and collagen III production, the types of collagen produced by primary dermal fibroblasts used in this study. At 10 days, fibroblasts showed a significant decrease in all collagen transcripts when grown on all meshes compared to those grown on plastics ($p < 0.005$, ANOVA using a *post-hoc* Duncan's test) (Figure 3, left panel). At 30 days, collagen transcript levels in cells grown on meshes were still reduced compared to control cells, although the difference was less pronounced (Figure 3, right panel).

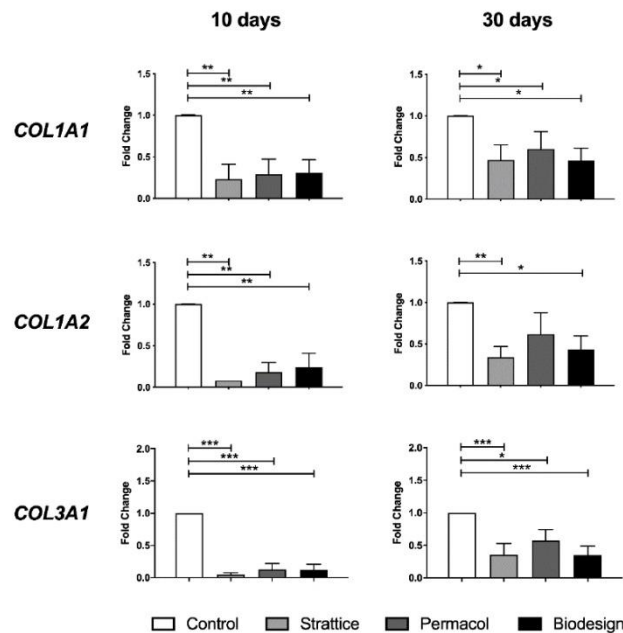


Figure 3. Changes in the levels of collagen transcripts following fibroblast growth on the different types of matrices for 10 or 30 days compared to the control condition—expression from fibroblasts grown on plastics (control), Strattice, Permacol, and Biodesign. Values are the means of four independent experiments \pm standard error (SE). The results were analyzed with ANOVA. Asterisks indicate significant differences (* $p < 0.05$; ** $p < 0.01$; *** $p < 0.001$).

No significant difference between the examined biological matrices was observed. Our data suggest that new collagen deposition seems unlikely during the analyzed timeframe.

2.2.2. Expression and Activity of Extracellular Matrix Degrading Enzymes

Then we investigated if, in the same timeframe, specific matrix metalloproteinase levels were modified.

We observed an increase in MMP-1 transcripts in fibroblasts grown on all 3D biological matrices compared to cells grown in 2D on plastics (Figure 4A). Due to the high variability in the biological replicates, after 10 days, the increase was not significant (Figure 4A); at 30 days, fibroblasts cultured on Strattice showed a significant increase in MMP-1, compared not only with control cells but also to cells grown on the other two biological matrices (Figure 4A, right panel). Moreover, at 30 days, MMP-1 expression by fibroblasts grown on Permacol and Biodesign scaffolds was also increased compared to that of control cells (Figure 4A). Measurement of MMP-1 protein in cell supernatants by enzyme-linked immunosorbent assay (ELISA) confirmed the results of MMP-1 transcript levels (Figure 4A). Fibroblasts grown on Strattice had the highest levels of this protease at both time points, whereas cells grown on Biodesign had the lowest increase among those grown on the three 3D matrices, but still higher than control cells (Figure 4A). We did not observe significant changes in MMP-13 transcripts (Figure 4A).

To investigate if, in the presence of 3D biological matrices, the proportion of active collagenases was also increased, we performed collagen zymography. Supernatants from fibroblasts grown in 2D on plastics expressed only pro-MMP1, whereas those from fibroblasts grown on biological matrices showed an equal proportion of pro- and active MMP-1, or even a preponderance of active form in the case of cells grown on Strattice at 30 days (Figure 4B). No evidence of MMP-13 activity was observed in these zymograms (Figure 4B). It must be said that the Cq values in qPCR were above 30 for this metalloproteinase even when induced, suggesting that levels of expression remained low (Supplementary Table S1). Our results suggest that MMP-13 expression and activity were negligible in the conditions tested.

MMP-2 transcript levels showed small but significant changes not only between controls and fibroblasts grown on biological meshes but also among the different matrices. Transcript levels were modestly but consistently increased in the Strattice samples compared to control at 30 days, and the increase was confirmed by quantification of protein levels (Figure 4C). On the contrary, cells grown on Biodesign showed a 50% decrease in the transcript when compared to control at both times. Interestingly, while no increase in MMP-2 protein was observed at 10 days compared to control cells, an eight-fold increase was measured in supernatants from cells cultured on the Biodesign sample for 30 days (Figure 4C). However, the difference described in MMP-2 protein levels was statistically significant only for Strattice. MMP-2 expression in cells grown on Permacol was more variable in time, and transcript and protein levels did not correlate (Figure 4C).

MMP-9 transcript levels were increased in cells grown on all biological matrices compared to control conditions, albeit not significantly, due to high variability among experiments. For cells grown on Strattice for 10 days, the number of cells did not allow to extract sufficient amounts of RNA to analyze all genes of interest (Figure 4C).

We then performed gelatin zymography to assay for the presence of pro- and active forms of MMP-2 and MMP-9 gelatinases. Supernatants from fibroblasts grown on plastics showed only pro-MMP-2, whereas fibroblasts grown on biological matrices showed either a shift towards the active form or an increase in the total activity of MMP-2, variably distributed between the two forms (Figure 4D). MMP-9 activity was not detected in our gels. Indeed, as for MMP-13, also for MMP-9, the levels of transcript were low, even after induction: the Cq from fibroblasts grown on plastics was above 35 and was no more than 30 when cells grown on biological matrices were analyzed (Supplementary Table S1). In conclusion, fibroblasts grown on biological matrices showed an increase in the expression

and activity of only specific metalloproteinases (MMP-1 and MMP-2) during the first weeks of growth. For both enzymes, the expression was Strattice > Permacol > Biodesign.

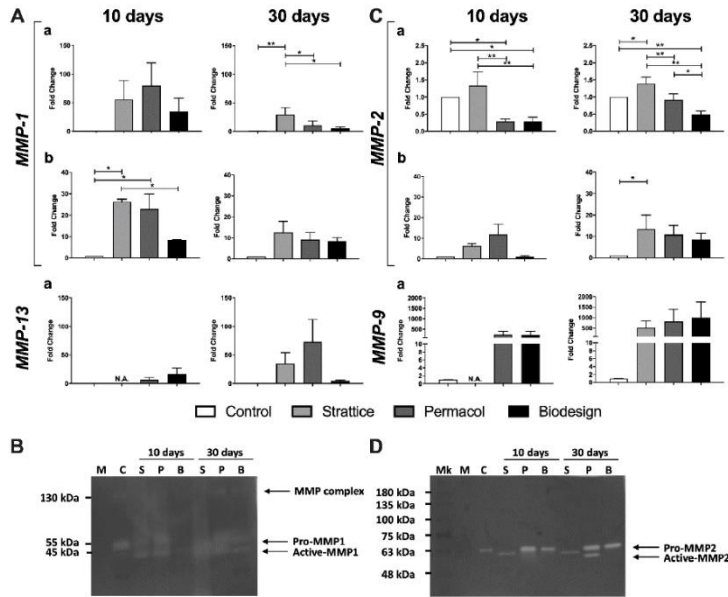


Figure 4. Changes in the levels of metalloproteinases transcripts, proteins, and in their activity following growth on the different types of matrices for 10 or 30 days, compared to control condition. (A) Expression of MMP-1 and MMP-13 collagenases from fibroblasts grown on plastics (control), Strattice, Permacol, Biodesign at transcript (a) and protein (b) levels. (B) Representative image of collagen zymography using supernatants from fibroblasts grown on plastics (C), Strattice (S), Permacol (P), and Biodesign (B) for 10 and 30 days. Complete medium (M) was used as a negative control. (C) Expression of MMP-2 and MMP-9 gelatinases from fibroblasts grown on plastics (control), Strattice, Permacol, Biodesign at transcript (a) and protein (b) levels. (D) Representative image of gelatin zymography using supernatants from fibroblasts grown on plastics (C), Strattice (S), Permacol (P), and Biodesign (B) for 10 and 30 days. Complete medium (M) was used as a negative control. Values in (A,C) are means of four independent experiments \pm SE. The results were analyzed with ANOVA. Asterisks indicate significant differences (* $p < 0.05$; ** $p < 0.01$). N.A. indicates that the sample was not analyzed since the amount of RNA extracted from the sample was not sufficient to analyze all genes of interest.

2.2.3. Expression of Metalloproteinase Inhibitors

Next, we investigated whether TIMP-1, MMP-1 specific inhibitor, was expressed by fibroblasts grown on meshes. Although a slight increase in TIMP-1 was observed at 30 days after cell seeding in all biological matrices compared to control cells, the difference was not significant (Figure 5). TIMP-2, analyzed as a control, did not show any change in the conditions tested (Figure 5).

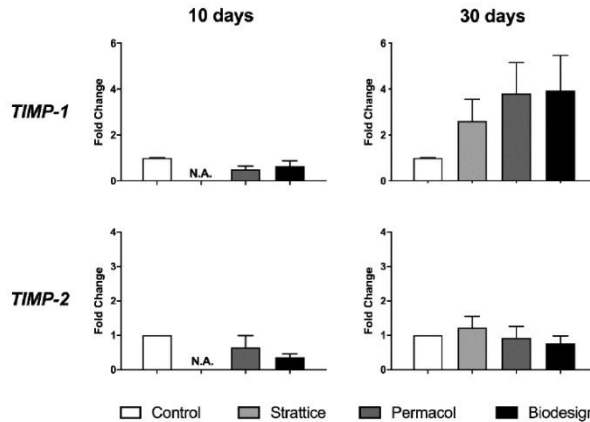


Figure 5. Changes in the transcript levels of metalloproteinase inhibitors following growth on the different types of matrices for 10 or 30 days compared to the control condition—expression from fibroblasts grown on plastics (control), Strattice, Permacol, and Biodesign. Values are the means of four independent experiments \pm SE. The results were analyzed with ANOVA. N.A. indicates that the sample was not analyzed since the amount of RNA extracted from the sample was not sufficient to analyze all genes of interest.

2.2.4. Expression of Cytokines and Alpha-Smooth Muscle Actin (α -SMA)

Finally, we investigated if specific cytokines, namely Interleukin-6 (IL-6) and Connective Tissue Growth Factor (CTGF), were differentially expressed by fibroblasts grown on the different types of matrices. IL-6 transcript levels were increased, in particular in fibroblasts grown on the Biodesign samples at both 10 and 30 days. At 30 days, the difference was significant not only compared to control conditions but also compared to cells grown on the other types of matrices (Figure 6). Levels of interleukin-6 protein were not affected at 10 days by any of the matrices; however, an increase was observed at 30 days in supernatants from cells grown on all biological meshes compared to control (Figure 6, right panel).

CTGF is considered a marker of myofibroblast differentiation together with alpha-smooth muscle actin (α -SMA), the product of the *ACTA2* gene. Expression of both genes was examined to investigate the possible differentiation of fibroblasts, cultured on the different scaffolds, into myofibroblasts, responsible for the induction of the fibrotic reaction. A highly significant and consistent reduction in CTGF transcript was observed in fibroblasts grown on all types of biological matrices compared to cells grown on plastics for the whole duration of the experiment (Figure 6).

Also, *ACTA2* transcript levels were reduced in fibroblasts grown on biological matrices compared to cells grown on plastics, in particular after 30 days of growth (Figure 6).

Cumulatively, these results suggest that fibroblasts do not undergo differentiation into myofibroblasts when grown on 3D biological matrices in the studied timeframe.

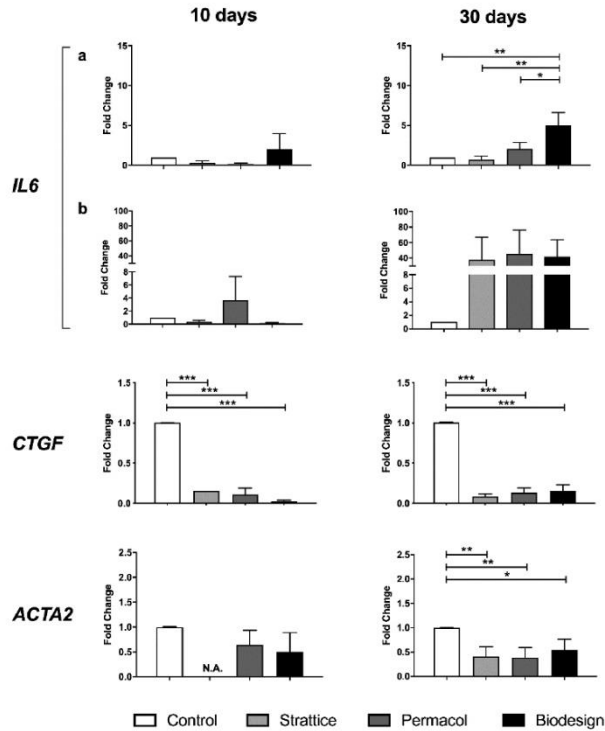


Figure 6. Changes in the levels of IL-6, CTGF, and α -smooth muscle actin following growth on the different types of matrices for 10 or 30 days, compared to the control condition. Expression from fibroblasts grown on plastics (control), Strattice, Permacol, Biodesign at transcript (a) and protein (b) levels. Values are the means of four independent experiments \pm SE. The results were analyzed with ANOVA. Asterisks indicate significant differences (* $p < 0.05$; ** $p < 0.01$; *** $p < 0.001$). N.A. in transcript graphs (a) indicates that expression was not analyzed since the amount of RNA extracted from the sample was not sufficient to analyze all genes of interest.

3. Discussion

Surgical repair of the abdominal wall with the insertion of prosthetic materials has become a common procedure for the treatment of hernias or lesions of the muscular inner body walls. Recently, the same matrices have also been applied in breast reconstructive surgery [2]. Several materials are available to date, making the choice difficult. As several factors intervene to influence the outcome (the type of surgery needed, original lesion, the lifestyle of the patient, and comorbidities), it is very difficult to summarize indications even with extensive meta-analysis studies [4,13,14].

Biological matrices are derived from the extracellular matrix of a variety of tissues and species and undergo extensive processing to make them suitable for implantation; this processing can affect matrix properties and induce foreign body response (FBR) [6,15,16].

It has been proposed that biological matrices are more resistant than synthetic meshes to microbial infection, have the ability to provide a barrier to visceral adhesion formation, and to respond in a fashion similar to native tissue [7,8]. However, these desired features have not been investigated in detail.

In this work, we aimed to investigate the behavior of human fibroblasts, the most abundant cell type in connective tissues, when cultured *in vitro* in the presence of biological 3D matrices. Several aspects of the interaction of human primary fibroblasts from derma of healthy adult individuals with biological scaffolds *in vitro* were studied by means of cell counting, SEM, and gene expression analyses. We tested three types of biological mesh commonly used for hernia repair that differed in the tissue of origin and/or presence of crosslinking, together with a synthetic mesh, used for comparison. The physicochemical properties of the materials have been previously described by Deeken et al. [17]. Insertion of prosthetic materials can occur at different anatomical positions depending on the type of surgery. Thus, different fibroblast subtypes may be involved in the interaction. However, given the scarce knowledge about the different behavior of these cell subtypes, mainly obtained in model animals, the availability of cells, and the need to obtain several replicates, we focused our work on human dermal fibroblasts [18,19].

In our study, fibroblasts showed different ability to attach and grow on the different materials, with the following order: Biodesign > Permacol > Strattice > Prolene. Although on the Biodesign samples, the number of cells was initially higher, at 30 days, it was comparable to that of the other matrices. This number may represent the maximum number of cells that could grow on these matrices; however, we did not observe confluence on the other types of matrices. An alternative explanation is that on the Biodesign matrix, cells loosely interacting with the surface were lost during the processing of Biodesign samples. Indeed, at increasing cell density, fibroblasts formed a cell monolayer, and the interaction with this matrix appeared weakened (Figure 11). Cells firmly adhered and proliferated on Strattice and Permacol but showed a non-homogeneous distribution. Our morphological analysis under the scanning electron microscope seems to confirm that the strongly oriented collagen of the submucosal scaffold (Biodesign) may be the reason for a greater elongation and alignment of the fibroblasts if compared to the multi-directionally oriented collagen on dermal Permacol and Strattice scaffolds. The fact that collagen fibers' direction may influence cell growth has already been reported [20–23]. In addition, the differences in cell numbers that we observed between the two meshes derived from porcine derma may be due to the different procedures used for the preparation of matrices before commercialization.

The observation that human dermal fibroblasts bound less efficiently than rat kidney fibroblasts or mesenchymal stem cells (MSC) to Strattice has been reported previously [19]. In the same work, fibroblasts failed to coat Marlex, a small pore, monofilament, polypropylene mesh, confirming the results we obtained with Prolene, a similar material [19]. Also, *in vivo* in animal models, Strattice was described to undergo poor incorporation; however, no adhesion formation was observed [5].

Our study highlighted similarities and differences in the gene expression programs activated by fibroblasts grown on the different matrices. The first similarity was observed in the reduction of collagen transcripts in cells grown on all biological matrices compared to control cells in the investigated timeframe. However, the observation that at 30 days, the reduction in expression was less marked than at 10 days suggests that expression may increase later in time. Interestingly, collagen deposition seems to be a late event, also in an *in vivo* mouse model [24].

Fibroblasts grown on biological matrices showed a decreased expression of markers of fibrosis, such as Connective Tissue Growth Factor (CTGF), alpha-SMA, and collagen I, compared to control cells [3]. α -SMA—product of the *ACTA2* gene—is known to increase during tissue remodeling and fibrosis, when fibroblasts differentiate into myofibroblast, and its expression is associated with up-regulation of collagen I and fibronectin biosynthesis and down-regulation of matrix remodeling enzymes [25–28]. CTGF is involved in adhesion,

migration, and proliferation of fibroblasts, but also in myofibroblast differentiation and fibrotic disease [29,30]. Since myofibroblast differentiation occurs during the fibrotic processes and is strictly related to the amount of foreign body reaction (FBR) induced at the biomaterial/host-tissue interface, the lack of expression of these markers in cells grown on 3D matrices compared to control cells suggests that this type of differentiation does not occur in the timeframe we analyzed. It would have been interesting to compare the expression of the same genes in cells grown on the synthetic mesh; unfortunately, we did not retrieve sufficient cells for molecular analyses from this mesh. Prolene is a small pore polypropylene scaffold and, although this material is commonly used in surgery, it is increasingly recognized that it can increase recurrence rates and comorbidities, including fibrosis, compared to large pore meshes [31].

Our study also highlighted differences among matrices in the expression of specific genes. We found increased expression of MMP-1 in fibroblasts grown on all biological matrices both at the transcript and protein levels. Moreover, zymography showed that supernatants from fibroblasts grown on meshes are enriched in the active form of this collagenase. Also, MMP-2 was slightly increased at the protein level, as evident by ELISA and zymography. Although we found an increase in MMP-9 and MMP-13 at the transcript level, we did not find evidence of their activity in zymograms. Indeed, this is in keeping with the low starting level of these metalloproteinases when one considers the raw qPCR data in terms of cycle threshold (Supplementary Table S1). Published data confirm our findings, reporting that fibroblasts grown on 3D collagen express MMP-1 and MMP-2, but not MMP-9 [26]. High levels of MMP-2 expression and activity are known to promote fibroblast migration and increase angiogenesis during the proliferative phase of wound healing [32]. Since the expression of TIMP-1, targeting MMP-1, increased only slightly at 30 days in fibroblasts grown on all investigated 3D biological scaffolds, we hypothesized that matrix degradation exceeded collagen biosynthesis and degradation was not (yet) inhibited by TIMP production in the considered time frame. The activity of metalloproteinases could be involved in the degradation of the old collagen of the 3D matrices to be replaced with the newly synthesized matrix and to favor the colonization of fibroblasts.

Among the various cytokines regulating the expression of MMPs and TIMPs during wound healing [33,34], IL-6 is involved in fibroblast proliferation and fibroproliferative disorders [35]. Although cytokines are primarily produced by monocytes/macrophages at the wound site [36,37], there is evidence of an autocrine production by fibroblasts [38,39]. We found an increase in IL-6 protein in fibroblasts grown in the presence of all biological matrices, although the increase in the relative transcript was observed only in the Biodesign 3D scaffold after 30 days of culture.

Our data show that fibroblasts can grow on biological matrices used for surgical applications and adapt their transcriptional program to the presence of these materials. We found that they induce first matrix degrading enzymes, independently of the tissue of origin of the biomaterials or the presence of crosslinking; however, cells grown on Stratice expressed the highest levels of these enzymes. On the contrary, cells grown on Biodesign showed the highest levels of IL-6. Although it has been suggested that crosslinking may interfere with mesh incorporation *in vivo* [40–42], we did not find evidence of different cell growth or gene expression of the crosslinked matrix (Permacol) compared to the other materials *in vitro*. In order to mimic an *in vivo* interaction of fibroblasts with other cell types, such as macrophages, coculture experiments should also be performed.

The main limitation of this work is that it was an *in vitro* study. *In vivo*, the outcome of the insertion of prosthetic material is likely the result of the interaction of several cell types, including fibroblasts and monocytes/macrophages, which stimulate each other to produce and secrete cytokines and are capable to attract endothelial cells, stimulating angiogenesis and incorporation of meshes into host tissue [36,37]. Integration of data from *in vitro* and *in vivo* work (both in animal models and from human explants) will allow further understanding of the interaction between host cells and different types of matrix, to be able to choose the right material for each patient in clinical applications.

4. Materials and Methods

4.1. Cell Culture

Human dermal fibroblasts from healthy adult donors (aged 35–45) were obtained from the “Cell Line and DNA Biobank from Patients Affected by Genetic Diseases—NETWORK OF GENETIC BIOBANKS TELETHON” [43]. Fibroblasts were used for the experiments between passages 11 and 13. The experiments were performed using fibroblasts from two different donors.

Fibroblasts were grown in RPMI-1640 (Carlo Erba Reagents, Milan, Italy) supplemented with 10% Fetal Bovine Serum (FBS, Carlo Erba Reagents, Milan, Italy) and 2 mM L-Glutamine (Carlo Erba Reagents, Milan, Italy). Cultures were incubated at 37 °C in 95% humidity and 5% CO₂ atmosphere. At confluence, fibroblasts were detached from culture flasks by treatment with trypsin (Carlo Erba Reagents, Milan, Italy). Cells were thawed on an average of two weeks before each experiment to have sufficient numbers of cells. Cells were routinely checked for the presence of mycoplasma by using the nested PCR method described in Tang et al. [44].

4.2. Type and Preparation of Matrices

The matrices used in this study are described in Table 1 and were obtained from the manufacturing companies. The Prolene synthetic mesh was included for comparison.

The matrices were cut into small pieces (1 cm × 1 cm): Strattice and Permacol were washed with PBS (Phosphate Buffered Saline, Carlo Erba Reagents, Milan, Italy) for eight hours at room temperature with gentle shaking, changing the washing every 2 h, whereas Biodesign and Prolene were washed at room temperature for 25 min with gentle shaking, changing the washing every 5 min. The matrices were placed in 12 well tissue culture plates containing complete medium and were incubated for 12 h at 37 °C in 95% humidity and 5% CO₂ atmosphere.

Table 1. Description of matrices used in this study.

Trade Name	Manufacturer	Species	Tissue Type	Crosslinked	Sterilization
Strattice	LifeCell-Acelity	Porcine	Dermis	No	E-beam
Permacol	Covidien	Porcine	Dermis	Yes (hexamethylene diisocyanate)	Gamma irradiation
Surgisis-Biodesign	Cook-Medical	Porcine	Small intestine submucosa	No	Ethylene oxide
Prolene Polypropylene Mesh	Ethicon	Synthetic	Polypropylene high weight, monofilament	N.A. ^(a)	Ethylene oxide

^(a) N.A. Not applicable.

4.3. Experimental Setup

Twelve hours after preparation of the matrices, 5×10^4 fibroblasts were seeded on matrices' surface in each well and then incubated for two days at 37 °C in 95% humidity and 5% in a CO₂ atmosphere. Then, the matrices were transferred to a new tissue culture plate, and fibroblasts were allowed to grow for 10, 20, and 30 days.

Three days before the end of the treatment, the serum-containing culture medium was replaced with RPMI-1640 supplemented with 2 mM L-Glutamine and Lyset Kit 5% (Scavo Diagnostic International by Carlo Erba Reagents, Milan, Italy) using a ratio of 1:4 among the Lyset PL: AD reagents (PL: human platelet lysate from platelet-rich plasma; AD: human platelet-poor plasma), to have more controlled growth factor and cytokine composition.

For metalloproteinase zymography, the growth medium was replaced with serum-free medium (RPMI-1640 supplemented with 2 mM L-glutamine) two days before the end of treatment. For zymography experiments, the serum-free conditioned medium was collected.

The supernatants for ELISA and metalloproteinase zymography were collected at the end of the treatments and stored at -80°C . The matrices were used for RNA extraction, scanning electron microscopy, and cell counting.

The control condition was represented by fibroblasts grown in “2D” on plastics, with the same media described above. Since the cells on plastics proliferate faster and have to be passed while the cells on the biomaterials grow more slowly, we processed control cells when 80% confluent after the start of each experiment.

Three independent experiments were performed for scanning electron microscopy analysis and for cell counting; four independent experiments were performed for gene expression analyses/zymography.

4.4. Scanning Electron Microscopy (SEM)

Samples were washed in PBS and fixed for 1 h in Karnovsky fixative (2% paraformaldehyde and 2.5% glutaraldehyde in 0.1 M cacodylate buffer (pH 7.2)), washed in 0.1 M cacodylate buffer (pH 7.2) and subsequently postfixed for 2 h in 1% osmium tetroxide and potassium ferrocyanide in 0.1 M cacodylate buffer (pH 7.2). After a series of washes with PBS (pH 7.2), the samples were immersed for 1 h in osmium tetroxide (0.1% in PBS). After being dehydrated in an increasing series of ethanol (70%, 90%, and 100%), the samples were dried with hexamethyldisilazane at the critical point. Once mounted on stubs, the samples were coated in gold with a Sputter K250 (Emitech, Baltimore, MD, USA) and subsequently observed with a SEM-FEG XL-30 microscope (Philips, Eindhoven, The Netherlands).

4.5. Cell Counting

The number of cells grown on the different scaffolds was determined by two methods: the first, CellTiter-Glo kit (Promega, Milan, Italy), is based on ATP quantification and was performed following manufacturer instructions after direct lysis of cells on matrices. A calibration curve was prepared with known amounts of cells to estimate the number of cells retrieved from each matrix; the second method consisted of enzymatic detachment of cells from the matrices, followed by manual cell counting. Cell containing matrices were incubated for 25 min at 37°C with an enzymatic cocktail, composed of Collagenase from *Clostridium Histolyticum*, Type IA (Sigma-Aldrich, Milan, Italy), at a final concentration of 5 mg/mL, directly diluted in Accutase solution (Carlo Erba Reagents, Milan, Italy). Then 100 μL of trypsin was added for 5 min at 37°C . Cells were counted with a hemocytometer after adding a volume of trypan blue.

4.6. RNA Extraction and qPCR Analysis

3D matrices were manually scraped in 300 μL of TriReagent (Sigma-Aldrich, Milan, Italy) on ice to retrieve fibroblasts; then lysates were collected in tubes and stored at -80°C . Fibroblasts grown on tissue culture plates were used as the control condition. Total RNA was extracted using a Direct-zol RNA MiniPrep (Zymo Research, EuroClone, Milan, Italy) following manufacturer instructions. RNA samples were quantified with a NanoDrop 2000c (ThermoFisher, Life Technologies Italia, Milan, Italy) and run on an agarose gel. For real-time quantitative PCR (qPCR), cDNA was obtained from 750 ng of RNA by using the iScript cDNA synthesis kit (Biorad, Milan, Italy). Gene expression analyses were performed in triplicate using a CFX96 thermal cycler (Biorad, Milan, Italy) and the iTAQ Universal Sybr Green Supermix (Biorad, Milan, Italy). Relative mRNA quantification was obtained by applying the $2^{-\Delta\Delta\text{C}_q}$ method [45], using the geometric average of the C_q s of two reference genes, namely beta-2-Microglobulin and GAPDH, for normalization purposes. Melting curve analysis was performed to ensure that single amplicons were obtained for each target. Primers for the genes under investigation were designed to have at least one of the primers in the pair designed on an exon-exon junction or to encompass at least one intron. Primer sequences are reported in Supplementary Table S2.

4.7. Quantification of Secreted Proteins by ELISA

The concentrations of human MMP1, MMP2, and IL-6 in cell culture supernatants from fibroblasts grown on the different types of matrices were measured using Human MMP1 (ThermoFisher Scientific, Milan, Italy), Human MMP2 (Novex, Life Technologies Italia, Milan, Italy) and Human IL-6 (ThermoFisher Scientific, Milan, Italy) colorimetric ELISA kits, following manufacturer's instructions. The obtained ELISA measurements were normalized by cell number. The two ELISA kits for MMP-1 and MMP-2 recognize both the pro- and the active forms of each metalloproteinase.

4.8. Zymography Analysis

To evaluate the enzymatic activity of metalloproteinases, zymography was performed. Supernatants from cells cultured as described before preparation for electrophoresis by adding one volume of non-reducing sample buffer (250 mM Tris HCl pH 6.8, 40% glycerol, 8% SDS, 0.01% bromophenol blue) every three volumes of supernatant. The appropriate volumes of supernatant were calculated after normalization by cell number. Samples were loaded on eight percent polyacrylamide gels containing 5 mg/mL of gelatin from bovine skin (Sigma, Milan Italy) or 1 mg/mL of collagen type I from rat tail (Sigma, Milan, Italy). After electrophoresis, gels were washed for 1 h in 2.5% Triton X-100 at room temperature and then incubated at 37 °C in 10 mM CaCl₂, 150 mM NaCl and 50 mM Tris HCl pH 7.5 overnight for gelatinases and for 48 h for collagenases. At the end of incubation, gels were stained with 0.25% Coomassie brilliant blue G-250 in 50% methanol, 10% acetic acid, and then destained with a solution of 10% isopropanol and 10% acid acetic until metalloproteinase activity was detected as white bands in the gel.

4.9. Statistical Analysis

The numbers of cells grown on the different matrices were compared using analysis of variance (ANOVA) with *post-hoc* Bonferroni test (GraphPad Prism statistical software program, version 4.02, San Diego, CA, USA). Data from gene expression analysis and from quantification of secreted proteins from four independent experiments were compared using analysis of variance (ANOVA) with *post-hoc* Duncan's test (Statistica data analysis and visualization program, version 8.0, Hamburg, Germany). The differences in cell numbers grown on the different matrices at different times and the differences in protein secretion evaluated by ELISA were compared using analysis of variance (ANOVA) (GraphPad Prism statistical software program, version 4.02, San Diego, CA, USA).

5. Conclusions

The purpose of this study was to compare the growth of human primary dermal fibroblasts on 3D matrices commonly used for surgery and the activation of specific molecular pathways that may indicate the first processes occurring in the early stages of matrix implantation.

Our gene expression results suggest that biological matrices may be absorbed and substituted by endogenously produced extracellular matrix and that, in spite of an overall similar transcriptional program, there are some differences among the tested matrices that may influence the rate of implant engraftment and could even be exploited in particular instances.

Supplementary Materials: The following are available online at <https://www.mdpi.com/1422-0067/22/2/526/s1>. Figure S1. Morphological analysis of unseeded matrices and of fibroblasts grown on tested matrices for 10 or 30 days; Table S1. Average Cq and standard error for each metalloproteinase under investigation and for the reference genes used in this work; Table S2. Sequences of primers used for gene expression analysis in this study.

Author Contributions: Conceptualization, P.C.; methodology, S.G.; investigation, S.G., A.P., A.G., and T.C.; data curation, S.G., P.C., A.G., and T.C.; writing—original draft preparation, P.C.; writing—review and editing, P.C., S.G., G.C., and A.G.; supervision, P.C.; project administration, P.C.; funding

acquisition, P.C., A.G., and G.C. All authors have read and agreed to the published version of the manuscript.

Funding: This research was supported by Lifecell Corp. (now 3M), and co-funded by the University of Insubria and by Fondi di Ateneo per la Ricerca, University of Insubria to P.C. (CAM17FAR2017) and A.G. (DEE18FAR2018).

Institutional Review Board Statement: Not applicable.

Informed Consent Statement: Not applicable.

Data Availability Statement: The data presented in this study are available within the article and its supplementary material.

Acknowledgments: We thank Guido Cimoli for helpful discussion. S.G. is a PhD student of the “Biotechnology, Biosciences and Surgical Technology” PhD course at Università degli Studi dell’Insubria; A.P. is a PhD student of the “Life Science and Biotechnology” PhD course at Università degli Studi dell’Insubria. The “Cell Line and DNA Biobank from Patients Affected by Genetic Diseases” was a member of the Telethon Network of Genetic Biobanks (project no. GTB12001), funded by Telethon Italy, and provided the human primary dermal fibroblasts.

Conflicts of Interest: The authors declare that Campanelli G. received funding from Lifecell Corp. (now Acelity) to support this study. Part of the funding was used for a fellowship to Grossi S. to perform the work. The funders had no role in the design of the study; in the collection, analyses, or interpretation of data; in the writing of the manuscript, or in the decision to publish the results. The other authors (A.G., T.G., A.P., P.C.) declare no conflict of interest.

Abbreviations

2D	Two dimensional
3D	Three dimensional
α-SMA	Actin, alpha 2, smooth muscle protein
ACTA2	Actin, alpha 2, smooth muscle gene
ANOVA	Analysis of variance
B2M	Beta-2-microglobulin
COL1A1	CollCollagen type I alpha 1 chain
COL1A2	CollCollagen type I alpha 2 chain
COL3A1	Collagen type III alpha 1 chain
Cq	Cycle quantitative (PCR cycle number at which the amplification curve intersects the threshold line)
CTGF	Connective tissue growth factor
ECM	Extracellular matrix
ELISA	Enzyme-linked immunosorbent assay
FBR	Foreign body response
GAPDH	Glyceraldehyde-3-phosphate dehydrogenase
IL-6	Interleukin 6
MMP	Metalloproteinase
MSC	Mesenchymal stem cell
SEM	Scanning Electron Microscopy
TIMP	Metalloproteinase inhibitor

References

1. Ansaloni, L.; Catena, F.; Coccolini, F.; Gazzotti, F.; D’Alessandro, L.; Pinna, A.D. Inguinal hernia repair with porcine small intestine submucosa: 3-year follow-up results of a randomized controlled trial of Lichtenstein’s repair with polypropylene mesh versus Surgisis Inguinal Hernia Matrix. *Am. J. Surg.* **2009**, *198*, 303–312. [[CrossRef](#)] [[PubMed](#)]
2. Ellis, H.L.; Asaolu, O.; Nebo, V.; Kasem, A. Biological and synthetic mesh use in breast reconstructive surgery: A literature review. *World J. Surg. Oncol.* **2016**, *14*, 1–9.
3. Junge, K.; Binnebosel, M.; von Trotha, K.T.; Rosch, R.; Klinge, U.; Neumann, U.P.; Lynen Jansen, P. Mesh biocompatibility: Effects of cellular inflammation and tissue remodelling. *Langenbeck’s Arch. Surg.* **2012**, *397*, 255–270. [[CrossRef](#)] [[PubMed](#)]
4. FitzGerald, J.F.; Kumar, A.S. Biologic versus Synthetic Mesh Reinforcement: What are the Pros and Cons? *Clin. Colon Rectal Surg.* **2014**, *27*, 140–148.

5. Deerenberg, E.B.; Mulder, I.M.; Grotenhuis, N.; Ditzel, M.; Jeekel, J.; Lange, J.F. Experimental study on synthetic and biological mesh implantation in a contaminated environment. *Br. J. Surg.* **2012**, *99*, 1734–1741. [\[CrossRef\]](#)
6. Sandor, M.; Xu, H.; Connor, J.; Lombardi, J.; Harper, J.R.; Silverman, R.P.; McQuillan, D.J. Host response to implanted porcine-derived biologic materials in a primate model of abdominal wall repair. *Tissue Eng. Part A* **2008**, *14*, 2021–2031. [\[CrossRef\]](#)
7. Shankaran, V.; Weber, D.J.; Reed, R.L., 2nd; Luchette, F.A. A review of available prosthetics for ventral hernia repair. *Ann. Surg.* **2011**, *253*, 16–26. [\[CrossRef\]](#)
8. Cevasco, M.; Itani, K.M. Ventral hernia repair with synthetic, composite, and biologic mesh: Characteristics, indications, and infection profile. *Surg. Infect. (Larchmt)* **2012**, *13*, 209–215. [\[CrossRef\]](#)
9. El-Hayek, K.M.; Chand, B. Biologic prosthetic materials for hernia repairs. *J. Long Term Eff. Med. Implants* **2010**, *20*, 159–169. [\[CrossRef\]](#)
10. Sadava, E.E.; Krpata, D.M.; Gao, Y.; Rosen, M.J.; Novitsky, Y.W. Wound healing process and mediators: Implications for modulations for hernia repair and mesh integration. *J. Biomed. Mater. Res. A* **2014**, *102*, 295–302. [\[CrossRef\]](#)
11. Rastegarpour, A.; Cheung, M.; Vardhan, M.; Ibrahim, M.M.; Butler, C.E.; Levinson, H. Surgical mesh for ventral incisional hernia repairs: Understanding mesh design. *Plast Surg. (Oaku)* **2016**, *24*, 41–50. [\[CrossRef\]](#) [\[PubMed\]](#)
12. Baylon, K.; Rodriguez-Camarillo, P.; Elias-Zuniga, A.; Diaz-Elizondo, J.A.; Gilkerson, R.; Lozano, K. Past, Present and Future of Surgical Meshes: A Review. *Membranes* **2017**, *7*, 47. [\[CrossRef\]](#) [\[PubMed\]](#)
13. Ventral Hernia Working, G.; Breuing, K.; Butler, C.E.; Ferzoco, S.; Franz, M.; Hultman, C.S.; Kilbridge, J.F.; Rosen, M.; Silverman, R.P.; Vargo, D. Incisional ventral hernias: Review of the literature and recommendations regarding the grading and technique of repair. *Surgery* **2010**, *148*, 544–558.
14. Novitsky, Y.W.; Rosen, M.J. The biology of biologics: Basic science and clinical concepts. *Plast. Reconstr. Surg.* **2012**, *130* (Suppl. 2), 9S–17S. [\[CrossRef\]](#) [\[PubMed\]](#)
15. Nilsen, T.J.; Dasgupta, A.; Huang, Y.C.; Wilson, H.; Chnari, E. Do Processing Methods Make a Difference in Acellular Dermal Matrix Properties? *Aesthet. Surg. J.* **2016**, *36* (Suppl. 2), S7–S22. [\[CrossRef\]](#)
16. Sandor, M.; Leamy, P.; Assan, P.; Hoonjan, A.; Huang, L.T.; Edwards, M.; Zuo, W.; Li, H.; Xu, H. Relevant In Vitro Predictors of Human Acellular Dermal Matrix-Associated Inflammation and Capsule Formation in a Nonhuman Primate Subcutaneous Tissue Expander Model. *Eplasty* **2017**, *17*, e1.
17. Deeken, C.R.; Eliason, B.J.; Pichert, M.D.; Grant, S.A.; Frisella, M.M.; Matthews, B.D. Differentiation of biologic scaffold materials through physicochemical, thermal, and enzymatic degradation techniques. *Ann. Surg.* **2012**, *255*, 595–604. [\[CrossRef\]](#)
18. Dubay, D.A.; Wang, X.; Kirk, S.; Adamson, B.; Robson, M.C.; Franz, M.G. Fascial fibroblast kinetic activity is increased during abdominal wall repair compared to dermal fibroblasts. *Wound Repair Regen.* **2004**, *12*, 539–545. [\[CrossRef\]](#)
19. Gao, Y.; Liu, L.J.; Blatnik, J.A.; Krpata, D.M.; Anderson, J.M.; Criss, C.N.; Posielski, N.; Novitsky, Y.W. Methodology of fibroblast and mesenchymal stem cell coating of surgical meshes: A pilot analysis. *J. Biomed. Mater. Res. B Appl. Biomater.* **2014**, *102*, 797–805. [\[CrossRef\]](#)
20. Gigante, A.; Cesari, E.; Busilacchi, A.; Manzotti, S.; Kyriakidou, K.; Greco, F.; Di Primio, R.; Mattioli-Belmonte, M. Collagen I membranes for tendon repair: Effect of collagen fiber orientation on cell behavior. *J. Orthop. Res.* **2009**, *27*, 826–832. [\[CrossRef\]](#)
21. Zhong, S.; Teo, W.E.; Zhu, X.; Beuerman, R.W.; Ramakrishna, S.; Yung, L.Y. An aligned nanofibrous collagen scaffold by electrospinning and its effects on in vitro fibroblast culture. *J. Biomed. Mater. Res. A* **2006**, *79*, 456–463. [\[CrossRef\]](#) [\[PubMed\]](#)
22. Bashur, C.A.; Dahlgren, L.A.; Goldstein, A.S. Effect of fiber diameter and orientation on fibroblast morphology and proliferation on electrospun poly(D,L-lactic-co-glycolic acid) meshes. *Biomaterials* **2006**, *27*, 5681–5688. [\[CrossRef\]](#)
23. Delaine-Smith, R.M.; Green, N.H.; Matcher, S.J.; MacNeil, S.; Reilly, G.C. Monitoring fibrous scaffold guidance of three-dimensional collagen organisation using minimally-invasive second harmonic generation. *PLoS ONE* **2014**, *9*, e89761. [\[CrossRef\]](#)
24. Novitsky, Y.W.; Orenstein, S.B.; Kreutzer, D.L. Comparative analysis of histopathologic responses to implanted porcine biologic meshes. *Hernia* **2014**, *18*, 713–721. [\[CrossRef\]](#) [\[PubMed\]](#)
25. Lipson, K.E.; Wong, C.; Teng, Y.; Spong, S. CTGF is a central mediator of tissue remodeling and fibrosis and its inhibition can reverse the process of fibrosis. *Fibrogenesis Tissue Repair.* **2012**, *5* (Suppl. 1), S24. [\[CrossRef\]](#)
26. Helary, C.; Foucault-Bertaud, A.; Godeau, G.; Coulomb, B.; Guille, M.M. Fibroblast populated dense collagen matrices: Cell migration, cell density and metalloproteinases expression. *Biomaterials* **2005**, *26*, 1533–1543. [\[CrossRef\]](#) [\[PubMed\]](#)
27. Kramann, R.; DiRocco, D.P.; Humphreys, B.D. Understanding the origin, activation and regulation of matrix-producing myofibroblasts for treatment of fibrotic disease. *J. Pathol.* **2013**, *231*, 273–289. [\[CrossRef\]](#) [\[PubMed\]](#)
28. Yang, X.; Chen, B.; Liu, T.; Chen, X. Reversal of myofibroblast differentiation: A review. *Eur. J. Pharmacol.* **2014**, *734*, 83–90. [\[CrossRef\]](#)
29. Grotendorst, G.R.; Duncan, M.R. Individual domains of connective tissue growth factor regulate fibroblast proliferation and myofibroblast differentiation. *FASEB J.* **2005**, *19*, 729–738. [\[CrossRef\]](#)
30. Brigstock, D.R. Connective tissue growth factor (CCN2, CTGF) and organ fibrosis: Lessons from transgenic animals. *J. Cell Commun. Signal.* **2010**, *4*, 1–4. [\[CrossRef\]](#)
31. Brown, C.N.; Finch, J.G. Which mesh for hernia repair? *Ann. R. Coll. Surg. Engl.* **2010**, *92*, 272–278. [\[CrossRef\]](#) [\[PubMed\]](#)
32. Bornstein, P.; Sage, E.H. Matricellular proteins: Extracellular modulators of cell function. *Curr. Opin. Cell Biol.* **2002**, *14*, 608–616. [\[CrossRef\]](#)

33. Dasu, M.R.; Barrow, R.E.; Spies, M.; Herndon, D.N. Matrix metalloproteinase expression in cytokine stimulated human dermal fibroblasts. *Burns* **2003**, *29*, 527–531. [[CrossRef](#)]
34. Mauviel, A. Cytokine regulation of metalloproteinase gene expression. *J. Cell Biochem.* **1993**, *53*, 288–295. [[CrossRef](#)] [[PubMed](#)]
35. Wynn, T.A. Common and unique mechanisms regulate fibrosis in various fibroproliferative diseases. *J. Clin. Investig.* **2007**, *117*, 524–529. [[CrossRef](#)]
36. Orenstein, S.B.; Qiao, Y.; Kaur, M.; Klueh, U.; Kreutzer, D.L.; Novitsky, Y.W. Human monocyte activation by biologic and biodegradable meshes in vitro. *Surg. Endosc.* **2010**, *24*, 805–811. [[CrossRef](#)]
37. Orenstein, S.B.; Qiao, Y.; Klueh, U.; Kreutzer, D.L.; Novitsky, Y.W. Activation of human mononuclear cells by porcine biologic meshes in vitro. *Hernia* **2010**, *14*, 401–407. [[CrossRef](#)]
38. Fries, K.M.; Felch, M.E.; Phipps, R.P. Interleukin-6 is an autocrine growth factor for murine lung fibroblast subsets. *Am. J. Respir. Cell Mol. Biol.* **1994**, *11*, 552–560. [[CrossRef](#)]
39. Nguyen, H.N.; Noss, E.H.; Mizoguchi, F.; Huppertz, C.; Wei, K.S.; Watts, G.F.M.; Brenner, M.B. Autocrine Loop Involving IL-6 Family Member LIF, LIF Receptor, and STAT4 Drives Sustained Fibroblast Production of Inflammatory Mediators. *Immunity* **2017**, *46*, 220–232. [[CrossRef](#)]
40. Butler, C.E.; Burns, N.K.; Campbell, K.T.; Mathur, A.B.; Jaffari, M.V.; Rios, C.N. Comparison of cross-linked and non-cross-linked porcine acellular dermal matrices for ventral hernia repair. *J. Am. Coll. Surg.* **2010**, *211*, 368–376. [[CrossRef](#)]
41. Deeken, C.R.; Melman, L.; Jenkins, E.D.; Greco, S.C.; Frisella, M.M.; Matthews, B.D. Histologic and biomechanical evaluation of crosslinked and non-crosslinked biologic meshes in a porcine model of ventral incisional hernia repair. *J. Am. Coll. Surg.* **2011**, *212*, 880–888. [[CrossRef](#)] [[PubMed](#)]
42. De Silva, G.S.; Krpata, D.M.; Gao, Y.; Criss, C.N.; Anderson, J.M.; Soltanian, H.T.; Rosen, M.J.; Novitsky, Y.W. Lack of identifiable biologic behavior in a series of porcine mesh explants. *Surgery* **2014**, *156*, 183–189. [[CrossRef](#)] [[PubMed](#)]
43. Filocamo, M.M.R.; Corsolini, F.; Stroppiano, M.; Stroppiana, G.; Grossi, S.; Lualdi, S.; Tappino, B.; Lanza, E.; Galotto, S.; Biancheri, R. Cell Line and DNA Biobank From Patients Affected by Genetic Diseases. *Open J. Bioresour.* **2014**, *1*, e2.
44. Tang, J.; Hu, M.; Lee, S.; Roblin, R. A polymerase chain reaction based method for detecting Mycoplasma/Acholeplasma contaminants in cell culture. *J. Microbiol. Methods* **2000**, *39*, 121–126. [[CrossRef](#)]
45. Livak, K.J.; Schmittgen, T.D. Analysis of relative gene expression data using real-time quantitative PCR and the 2(-Delta Delta C(T)) Method. *Methods* **2001**, *25*, 402–408. [[CrossRef](#)]